State-of-the-Art of CO$_2$ Capture with Ionic Liquids

Mahinder Ramdin, Theo W. de Loos, and Thijs J.H. Vlugt*

Engineering Thermodynamics, Process & Energy Department, Faculty of Mechanical, Maritime and Materials Engineering, Delft University of Technology, Leeghwaterstraat 44, 2628 CA Delft, The Netherlands

ABSTRACT: Economical and environmental aspects are the main motivation for research on energy efficient processes and the search for environment friendly materials for CO$_2$ capture. Currently, CO$_2$ capture is dominated by amine-based (e.g., monoethanolamine) technologies, which are very energy intensive and less attractive from an environmental point of view due to emissions of the used volatile solvent components. Ionic liquids have been proposed as a promising alternative to the conventional volatile solvents, because of their low volatility and other interesting properties. This remarkable interest has led to a rapid growth of literature on this specific subject. The aim of the present review paper is to provide a detailed overview of the achievements and difficulties that has been encountered in finding a suitable ionic liquid for CO$_2$ capture from flue-gas streams. A major part of this review includes an overview of the experimental data of CO$_2$ solubility, selectivity, and diffusivity in different ionic liquids. The effect of anions, cations, and functional groups on the CO$_2$ solubility, biodegradability, and toxicity of the ionic liquids are highlighted. Recent developments on task-specific ionic liquids and supported ionic liquid membranes are also discussed. Scarcely available results of molecular simulations, which is a valuable tool in designing and evaluating ionic liquids, are also reviewed. The trends highlighted here can be used by solvent designers to navigate through the massive amount of theoretically possible ILs.

1. INTRODUCTION

The suspected correlation between the increased CO$_2$ concentration in the atmosphere and the green-house effect has initiated a worldwide debate aimed at emission reduction of CO$_2$ and other green-house gases.[1,2] CO$_2$ emissions have increased since the dawn of the industrial revolution. This resulted in an increase of CO$_2$ concentration in the atmosphere from about 280 ppm before the industrialization to 390 ppm nowadays.[3] The global CO$_2$ emission in 2008 was about 29.4 gigatons (Gt), which is an increase of around 40% relative to the 1990 emission of 20.9 Gt.[3] Currently the power sector is responsible for 41% of all the energy-related CO$_2$ emissions, followed by the transport sector (23%), industry sector (20%), buildings sector (10%), and others.[4] The high share of the CO$_2$ emission in the power sector is related to fuel combustion to generate electricity or heat. The share of coal in the total CO$_2$ emission from fuel combustion in 2008 was 43%, while the contribution of oil and gas was 37% and 20%, respectively.[3] Under the Baseline Scenario or Reference Scenario,[5] the CO$_2$ emission will continue to increase and will most likely double, relative to the 2007 emission of 28.8 Gt, by 2050.[4] Under this scenario the anticipated growth in future energy demand will be met using predominantly fossil fuels. This energy path is not consistent with the required deep cuts in global greenhouse-gas emissions by 2050 to limit the long-term global average temperature rise below 2 °C relative to preindustrial levels.[6] The 2 °C target, which is believed to be the point where dramatic climate change will set in,[7] was set during the UN conference on climate change in December 2009 in Copenhagen. In the long term, a transition in energy path, from fossil fuels to low-carbon-technologies, will be required to meet the 2 °C goal. McKinsey & Company investigated several readily available or developing low-carbon-technologies, which could be used to mitigate CO$_2$ emissions.[8−11] However, in the foreseeable future, fossil fuel, in particular coal,[12,13] will continue to be a substantial fraction of the energy portfolio.[3] In this regard CO$_2$ capture and storage (CCS) will be essential,[14] although it should be considered as a temporary solution to the problem. Both, the capture of CO$_2$ and the storage are technical challenging and many hurdles have to be overcome to commercialize these processes.[14−16]

The major barrier to commercialize the CO$_2$ capture and storage process at large scale is the energy/cost associated with the separation method. Currently available technology for CO$_2$ capture is based on amine-solvents, for example monoethanolamine (MEA).[17] The capture of CO$_2$ with amines involves a chemical reaction with a large enthalpy of reaction.[18] Consequently, a large amount of heat is required to release the captured CO$_2$ in the regeneration step. Retrofitting a CCS unit to an existing power plant, using conventional-amine solvents for CO$_2$ scrubbing, would lower the energy output of the plant by 25−40%.[14] Accordingly, the price of electricity would rise by 0.01−0.07 $/kWh relative to a plant without a CCS system.[1,19] The energy consumption for removing one ton of CO$_2$, by employing a 30 wt % MEA (aqueous) solution and assuming 90% CO$_2$ removal, is estimated to be in the range of 2.5−3.6 Gigajoule (GJ). The theoretical minimum work for CO$_2$ separation and compression to the required pressure of 150 bar is 0.42 GJ/ton CO$_2$, indicating the potential for process improvements.[17,20] About half of this energy is required in the stripper to regenerate the CO$_2$ and the other half is used to compress the CO$_2$ to about 150 bar for subsequent sequestration.[17] Currently, not a single large scale plant with
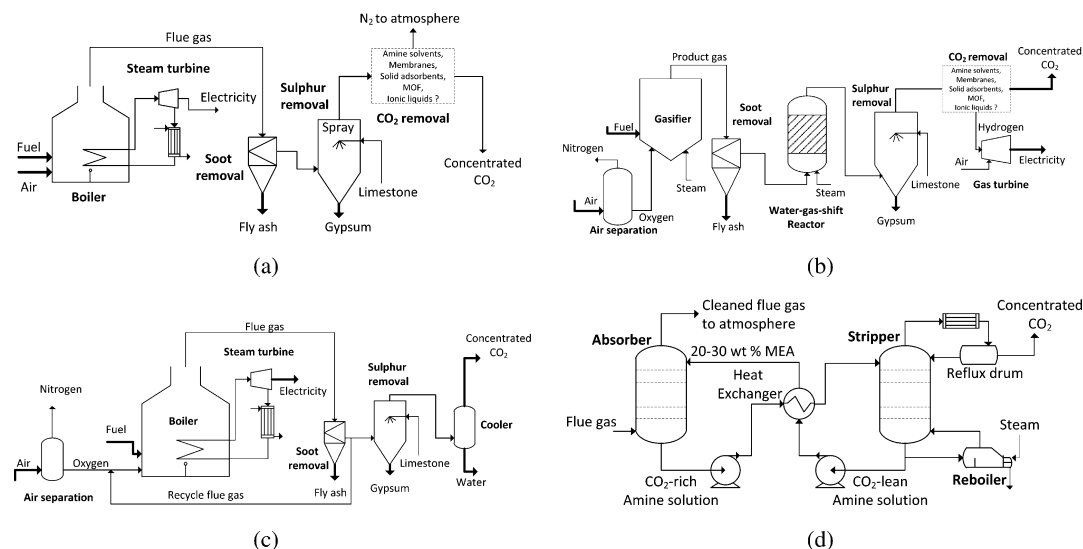
Figure 1. (a) Schematic representation of a simplified postcombustion CO_2 capture system.[60,283] In this process, the fuel is directly burned in air to produce large volumes of fluegas with low partial pressures of CO_2. The CO_2 can in principle be captured with amines, but this process turns out to be expensive.[26] (b) Schematic representation of a simplified precombustion CO_2 capture system.[61,283] In this process, the fuel is first gasified to produce syngas, which is converted to CO_2 and H_2 in the WGS reactor. Since this process operates at high pressures, the CO_2 can in principle be captured by several techniques. (c) Schematic representation of a simplified oxyfuel-combustion CO_2 capture system.[63,283] In this process, pure oxygen instead of air is used to burn the fuel, thereby eliminating nitrogen in the downstream separation. (d) Schematic representation of a simplified process for CO_2 absorption with amines.[17] CO_2 is captured in the absorber by a reaction with monoethanolamine (MEA) and subsequently released in the stripper by heating.

CCS is known to be operational. The primary reason for this is the high CO_2 removal cost ranging from 50 to 150 $/ton CO_2 removed, although recently much lower costs (30−35 $/ton CO_2) were reported.[21] Even a lower and debatable cost of 15 $/ton CO_2 was reported by Inventys,[22] but their technology is based on an adsorbent material instead of amines. However, the existing methodologies for CO_2 capture are energy intensive and far from cost-effective, hence unattractive for large scale applications.[1] Therefore, much research has been devoted to find or design new solvents/materials for CO_2 capture. This includes CO_2 separation by chemical/physical absorption, chemical/physical adsorption, membranes, solid adsorbents, and biomimetic approaches.[23−27] Recently D'Alessandro et al.[26] reviewed new and emerging materials for CO_2 capture, with particular attention for metal−organic frameworks (MOFs). A special class of absorption materials, namely ionic liquids (ILs), have been proposed as an alternative to the volatile, corrosive, and degradation sensitive amine-solvents.[28,29]

Ionic liquids are salts, which consist exclusively of ions, with a melting point lower than 100 °C.[30] The use of ionic liquids, although discovered a long time ago, was very limited until the late 1990s to a few examples in electrochemistry and organic chemistry. This changed unexpectedly as a result of an article published by Freemantle[31] in 1998, describing the potential applications of ionic liquids as novel solvents for green chemistry.[32−34] Since then, ionic liquids have been the interest of many researchers, resulting in an expansion of the application field. So far, (potential) applications of ionic liquids have been reported in analytical chemistry,[35] biochemistry,[30] catalysis,[36−38] electrochemistry,[39,40] separation technology,[41−44] fluid engineering,[45] and others.[46,47] ILs are nowadays applied at the industrial scale in the BASIL process of BASF for producing alkoxyphenylphosphines and the Degussa process for pigment paste production.[48] We note that the IL in the BASIL process does not serve as a solvent, but it is produced during the

reaction step. ILs owe their unexpected popularity to their remarkable properties, such as: (nearly) negligible volatility, high thermal stability, nonflammability, tunability, solvation properties, and high CO_2 solubility. The major driving force for research on ILs is their potential to replace traditional industrial solvents, which are often volatile organic compounds (VOCs). Substitution of the conventional volatile solvents by the relatively nonvolatile ionic liquids would prevent environmental pollution due to emission of VOCs into the atmosphere. Furthermore, the tunability property of ILs provide an extra degree of freedom for designing solvents with certain specific characteristics.[49]

This introduction provides an indication of the scale of the problem and the urgency to take action in order to prevent irreversible climate change. CCS is one of the remedies to the problem and in the following we will focus on the special application interest of ionic liquids as a CO_2 capture medium. Blanchard et al.[28] were the first to observe that significant amounts of CO_2 could be dissolved in imidazolium-based ionic liquids to facilitate an extraction of a dissolved product, without contaminating that product with the ionic liquid, since the ionic liquid was insoluble in CO_2. This study initiated an explosion of scientific research on CO_2 absorption with ionic liquids, leading to a rapid growth of the literature on this specific topic.[50] Therefore, the aim of the present paper is to give an extensive review of the achievements and recent developments in the search for a suitable ionic liquid for CO_2 capture from flue-gas streams and other point-sources. This paper provides a different perspective on CO_2 capture with ILs than those published in other recent reviews.[42,51−56] That is, we focus on the potential application of ILs for CO_2 capture at the postcombustion, precombustion, and natural gas sweetening process. More importantly, a comparison of the CO_2 capture performance (i.e., solubility, selectivity, viscosity, price, etc.) of ILs with the commercially available solvents is presented. The review is

started with an analysis of the relevant CO_2 capture processes (i.e., postcombustion, precombustion, oxyfuel combustion, and natural gas sweetening) and the conventional amine technology. Subsequently, a comprehensive overview of the main literature on CO_2 capture with ionic liquids is given. More specifically, attention is paid to the trends observed regarding CO_2 solubilities and selectivities in different ionic liquids, effect of anions, cations, and functional groups on physical properties, biodegradability, and toxicity of ionic liquids. The CO_2 capture performance of ILs is then compared with existing solvents (e.g., Selexol, Purisol, Sulfinol, etc.). The trends highlighted here may eventually help solvent designers to navigate through the massive number (about 10^{18}) of theoretically possible ternary IL systems.[49,57] Recent developments on task specific or functionalized ionic liquids and supported ionic liquid membranes are also discussed. Finally, the remaining challenges and future research possibilities are outlined.

2. CO₂ CAPTURE PROCESSES

The conditions for CO_2 capture, hence also the economics, are determined by the technology used for the production of electricity (or heat) from fossil fuels.[58] Today, a power company planning to build a new power station utilizing fossil fuels, can choose from two technologies, and a third one, which is in the development phase.[59] The characteristics of all the three processes (i.e., postcombustion, precombustion, and oxyfuel combustion) are different, yielding different conditions for CO_2 capture.

2.1. Postcombustion Capture. The first option is the postcombustion process,[60] which is widely used at traditional fossil-fuel-fired power stations to produce electricity. Under postcombustion conditions the fuel is burned fully in one step in air, see Figure 1a. The released heat is used to produce high-pressure steam, which drives a steam turbine to generate electricity. The flue-gas leaving the boiler contains substantial amounts of particulate matter, which is filtered out in the soot removal step. Subsequently, the sulfur in the flue-gas is scrubbed by a limestone slurry to produce gypsum. The cleaned flue-gas, which now contains 10−16% CO_2, would be released into the atmosphere in the absence of a CO_2 capture system. However, as explained in the Introduction, the role of CO_2 in the global warming requires it to be captured and stored safely underground for some time.

The following can be stated by analyzing the data shown in Table 1 for the postcombustion process: (1) the relevant separation is CO_2/N_2, hence any separation process should be CO_2 selective and (2) the process outputs large volumes of flue-gas with low CO_2 partial pressures, accordingly the separation process should be able to cope with these conditions. We will see later that a low CO_2 partial pressure, which is typical for postcombustion processes, is not very advantageous for (physical) CO_2 capture. However, the advantage of the postcombustion process is that the CCS unit can be retrofitted without major modifications to an existing power plant.

2.2. Precombustion Capture. The second option is the precombustion process,[61] which is associated with the integrated gasification combined cycle (IGCC) and is more complex as shown in Figure 1b. In this approach the fuel (coal, oil, etc.) is gasified, rather than burning it completely like in the postcombustion process, in the presence of pure oxygen and steam to produce syngas. The syngas, which is a mixture of carbon monoxide (CO) and hydrogen (H_2), is purified and fed

Table 1. Typical Conditions for Postcombustion[26,54] Capture, Precombustion[26,262] Capture and the Natural Gas Sweetening[51,62,263] Process

	postcombustion	precombustion[a]	natural gas sweetening
	Gas Composition (by mole)		
CO_2	10−15%	37.7%	0.1−8%
H_2O	5−10%	0.14%	
H_2		55.5%	
O_2	3−4%		
CO	20 ppm	1.7%	
N_2	70−75%	3.9%	0−0.2%
NO_x	<800 ppm		
SO_x	<500 ppm		
H_2S		0.4%	0−15%
CH_4			70−95%
C2+			0−15%
	Conditions		
temperature (°C)	40−75	40	30−40
pressure (bar)	1	30	5−120

[a]After the water−gas-shift reaction.

to the water−gas-shift (WGS) reactor. In this reactor, steam is added to convert the CO, according to the water−gas-shift reaction, to H_2 and CO_2. The gas can be desulphurized either before or after the WGS reactor, but preferentially before since any sulfur may be poisonous to the catalyst used in the WGS reactor.[62] At this stage the gas consists primarily of CO_2 and H_2. Subsequently, the CO_2 is captured and the H_2 is combusted in a gas turbine to produce electricity and heat. The heat produced during the combustion can be recovered by a heat recovery system (not shown in Figure 1b) to generate more electricity. The typical conditions, after the WGS reactor, for precombustion CO_2 capture are given in Table 1, from which we can deduce that the relevant separation is CO_2/H_2. Furthermore, the precombustion process yields a gas mixture with high CO_2 partial pressures, which is favorable for CO_2 separation.

2.3. Oxyfuel Combustion Capture. The third option is the oxyfuel combustion[63] process, which is a promising concept but still under development. A simplified schematic representation of this process is given in Figure 1c. In this approach concentrated oxygen, instead of air, is used to burn the fuel. The released heat is used to produce high-pressure steam, which turns a steam turbine to generate electricity. The flue-gas, which mainly consists of H_2O and CO_2, is stripped of the soot particles and partly recycled to the boiler to control the temperature. The remaining flue-gas stream is desulphurized and cooled down to condense the water. The result is a concentrated stream of CO_2, which is ready to be stored underground. The fundamental difference between this process and the other two processes is that no CO_2 capture is involved; instead N_2/O_2 is the relevant separation in this process. The concentrated CO_2 stream is a result of excluding nitrogen in the burning step.

Detailed economic evaluation of the three processes is provided by the US Department of Energy.[64−71] These cost estimation studies suggest that precombustion CO_2 capture is the least expensive option for CO_2 capture, but the investment for this process is higher than for the postcombustion and oxyfuel combustion process. In fact, precombustion and oxyfuel combustion technology can only be applied at new power

plants, since existing power plants operate and will continue to operate at least a decade according to the postcombustion scheme.[64] Currently, no commercial power plant (either post- or precombustion) with CCS is in operation, hence cost estimates are highly uncertain.[11] Nevertheless, the factors determining the cost for the different CO_2 capture processes can readily be identified. The most expensive component at postcombustion conditions in the CCS chain process is the CO_2 absorption/desorption, in particular the solvent regeneration step. In addition, the postcombustion capture process produces CO_2 at low pressures compared to sequestration requirements, adding significant expenses for pressurization. On the other hand, the advantage of the postcombustion process is that the CCS unit can be retrofitted directly, without major modifications, to an existing power plant. The precombustion process benefits from the high operating pressures, since (1) CO_2 is produced at high pressures reducing cost for pressurization, and (2) the higher pressures allow application of less energy intensive separation technologies. However, these cost savings may be offset as the capital cost might be higher due to the complexity of the process. The utilization of an expensive high pressure WGS reactor and a costly air separation unit may bring extra cost. The major disadvantage of the precombustion capture process is that it can be applied only at new power plants, since the majority of the existing power plants operate according to the postcombustion method. The oxyfuel combustion process eliminates the expensive CO_2 capture step, but on the other hand the process requires a costly air separation step. The boiler of the oxyfuel combustion process requires special construction materials to withstand the high temperatures, which is a consequence of using pure oxygen.[24] Other concern of the oxyfuel combustion process is the high SO_2 concentration in the flue gas causing tube corrosion.[72] It is evident that CCS will bring extra cost and that the cost will be governed by the process type utilized for power generation.

2.4. Natural Gas Sweetening. CO_2 capture is not only important from an environmental perspective, but is also of industrial relevance in the natural gas sweetening process. The global natural gas demand is expected to increase 1.4% per year in the coming two to three decades.[73] Hence it would be beneficial to find an efficient and cost-effective method for CO_2 removal from natural gas. Natural gas contains large amounts of methane (CH_4), but also all kind of impurities resulting in a classification as "sour" for high content of sour gases (e.g., H_2S and CO_2) or "sweet" for low content of H_2S and CO_2. The composition of natural gas is highly dependent on the location of the gas field, which is reflected in the large variation of the natural gas components shown in Table 1. The relevant separation in this process is CO_2/CH_4, but an additional separation may be required if other (e.g., H_2S) sour gases are involved. However, the acid gases in the natural gas should be removed at the well to avoid technological problems during gas transportation and to comply with environmental regulations.[51] Accordingly, the CO_2 should be removed to prevent dry ice or gas hydrate formation, which can clog the system during liquefaction of the natural gas. Furthermore, the corrosiveness of H_2S and CO_2 in the presence of water, the toxicity of H_2S, and the lack of heating value of CO_2 requires sweetening of the sour natural gas.[74] The most popular technology, comprising over 95% of the units in the field in the United States,[51] to capture H_2S and CO_2 is amine-based, although the high pressure at the gas well (see Table 1) allows the use of physical

absorbents, solid adsorbents, and membranes.[26] In fact, physical solvents like Rectisol, Purisol, and Selexol are preferred over chemical solvents for high pressure gas purification processes.[75]

2.5. Conventional Amine Technology. Many CO_2 capture technologies are under investigation, but presently amine scrubbing is probably the only feasible technology to capture CO_2 from a large scale fossil-fuel-fired power plant.[17] Amine scrubbing for CO_2 removal is a mature technology used in the ammonia process, steam reforming process, and the natural gas sweetening process.[18] Many alkanolamines like primary amines monoethanolamine (MEA) and diglycolamine (DEA), secondary amines like diethanolamine (DEA) and diisopropanolamine (DIPA), and tertiary amines like methyldiethanolamine (MDEA) and triethanolamine (TEA) and sterically hindered amines have been considered for CO_2 capture.[18] However, due to its high reactivity with CO_2, MEA is predominantly used for CO_2 capture. A typical process configuration for postcombustion CO_2 capture from flue-gas streams is shown in Figure 1d. The flue-gas, which is typically at 40−60 °C, is introduced at the bottom of an absorption tower, while a 20−30 wt % MEA solution is continuously added at the top. The CO_2 in the flue gas is selectively and chemically absorbed by a primary amine (e.g., MEA) through a zwitterion mechanism[18] to form carbamates (see Figure 2). Subsequently,
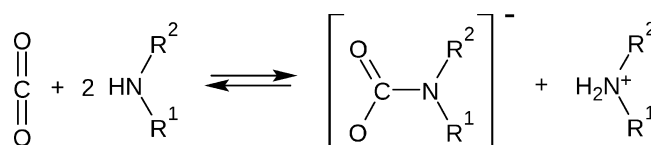

Figure 2. Absorption of CO_2 with primary amines. CO_2 reacts in a 1:2 stoichiometry with a primary amine forming a carbamate salt.

the CO_2-rich amine solution is drained off from the bottom of the absorber and introduced at the top of the stripper where the bounded CO_2 is released upon heating with steam. The regeneration of the amine solvent and concurrent liberation of the CO_2 takes place at elevated temperatures, typically at 100−140 °C, and at near atmospheric (1−2 bar) pressures. The regenerated amine solvent is recycled back to the absorption tower for continuing the cycle. The concentrated CO_2 stream leaving the stripper is ready to be stored underground after pressurization.

The major drawback of this process is the high energy requirement for solvent regeneration, which is a consequence of the high reactivity of MEA leading to a large enthalpy of formation associated with the carbamate production. Beside this energy penalty, MEA suffers a number of other drawbacks making it unattractive for large scale applications. These include the corrosiveness of MEA, this in fact is the reason for using dilute solutions, degradation of the solvent in the presence of oxygen, and the volatility of the solvent, which causes environmental pollution.[26] Furthermore, the theoretical maximum CO_2 loading of MEA for the carbamate formation scheme is approximately 0.5 mol CO_2 per mol of MEA, as can be deduced from Figure 2.[18] Clearly, MEA is not a very energy efficient and environment friendly solvent for CO_2 capture. Hence, much research focused on developing solvents with improved characteristics with respect to the following: energy requirements for solvent regeneration, CO_2 loading, kinetics, volatility, chemical degradation, and corrosivity.[76] Improved amines, such as the secondary amines (e.g., DEA) and tertiary

amines (e.g., MDEA) have been considered as an alternative for MEA. The reaction of CO_2 with secondary amines is also described by the zwitterion mechanism, but the enthalpy of reaction is lower due to the lower stability of the carbamate formed during the reaction.[26] Since tertiary amines do not have any hydrogen atom attached to the nitrogen atom, the carbamation reaction cannot take place. Instead, bicarbonate formation takes place according to a base-catalyzed hydration mechanism.[18] The enthalpy of reaction for the bicarbonate formation is lower than for the carbamate formation, resulting in a lower energy penalty for solvent regeneration. In addition, tertiary amines have a theoretical CO_2 loading capacity of 1 mol of CO_2 per mole of amine, although the reactivity of tertiary amines with respect to CO_2 is lower.[18] This is inherent to the thermodynamics of the reaction, since the enthalpy of reaction is related to the CO_2 capacity as $\ln K = -\Delta_r G^0 / RT$, where K is the equilibrium constant of the reaction, $\Delta_r G^0 = \Delta_r H^0 - T\Delta_r S^0$ is the standard Gibbs reaction energy, $\Delta_r H^0$ the standard enthalpy of reaction and $\Delta_r S^0$ the standard entropy of the reaction. Clearly, there is a trade-off between aiming a high CO_2 capacity at a certain temperature and wanting to keep the enthalpy of reaction low at the same time.[54]

Given the many disadvantages of the amine-process, it is highly desirable to develop solvents that perform substantially better than conventional amines with respect to the energy requirement for solvent regeneration, corrosivity, chemical degradation, thermal stability, and volatility. In the past decade, ionic liquids (ILs) have emerged as a promising alternative to the amines due to their remarkable properties, such as negligible volatility, high chemical/thermal stability, and tunability. The latter is probably the most important property of ionic liquids, since it allows design of task-specific ionic liquids (TSILs). In the following we analyze the data reported in the literature on CO_2 capture with ionic liquids.

3. CO₂ CAPTURE WITH IONIC LIQUIDS

The number of possible ILs is very large. A few examples of commonly used cations and anions of ILs are shown in Figure 3, where the R_i groups are often alkyl groups. Among these ILs, the imidazolium class is most widely investigated and reported in the literature. Initial research on CO_2 capture with ILs focused primarily on the phase behavior of CO_2 with different physical (nonfunctionalized) ionic liquids. As shown in Figure 4, the phase behavior of IL-CO_2 systems is remarkable compared to conventional organic solvents (e.g., n-hexane, toluene). First, a relatively large amount of CO_2 can be dissolved in a typical ionic liquid, like [emim][Tf₂N]. Second, conventional molecular solvent−CO_2 systems show a simple two-phase envelope with a mixture critical point at moderate pressures.[77] Clearly, this is not the case for a CO_2−IL system, instead CO_2 dissolves well at low pressures, but at higher mole fractions of CO_2 the bubble-point pressure sharply increases to very high pressures, without showing a critical point at moderate pressures. This unusual behavior is common for CO_2−IL systems and can be classified as type III fluid-phase behavior according the classification of van Konynenburg and Scott.[78,79] We note, however, that it is not fair to compare high molecular weight and almost nonvolatile ILs with low molecular weight volatile compounds. A more justifiable comparison of CO_2−IL systems would be that with high molecular weight liquid polymers. As shown in Figure 4, the PEG(600)−CO_2 system shows a behavior comparable to that of CO_2−IL systems. In the following a more systematic
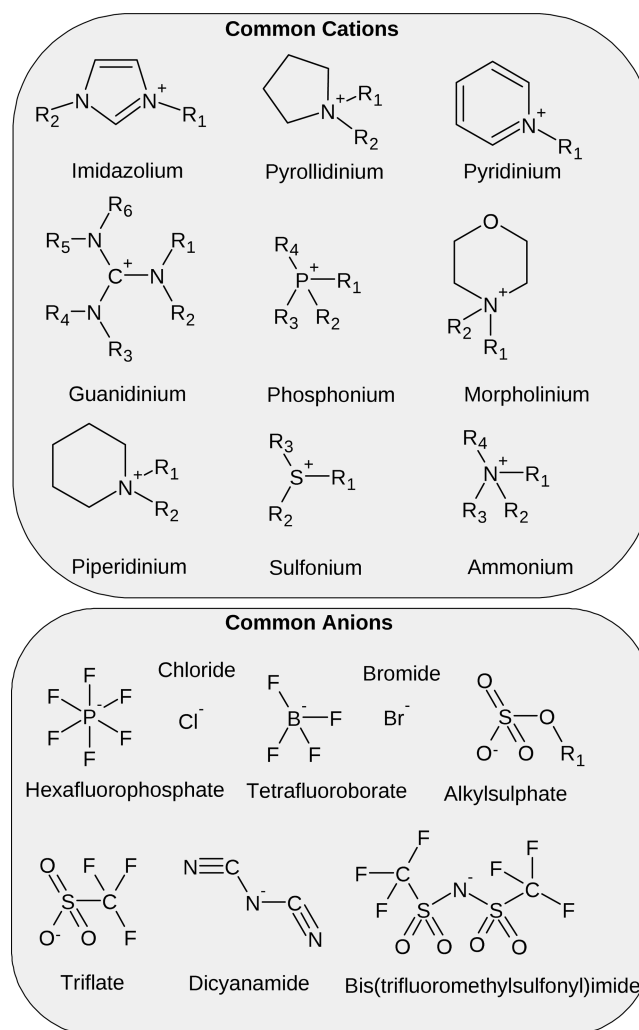
Figure 3. Commonly used anions and cations of ionic liquids.
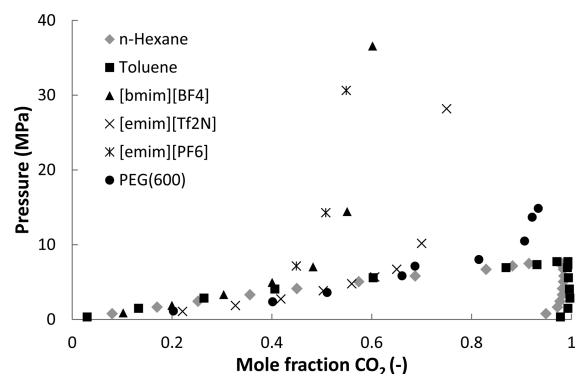
Figure 4. Comparison of the VLE phase behavior of CO_2−conventional solvents systems with CO_2−ILs systems. Conventional solvents show a critical point at moderate pressures, whereas ILs systems do not show this behavior. The behavior of CO_2−IL systems is comparable with high molecular weight liquid polymers, for example the PEG(600)−CO_2 system. Data at 313 K taken from refs 78, 284−288.

approach is used to show trends regarding CO_2 capture with ILs.

3.1. Physical Ionic Liquids. In this section we will only concentrate on CO_2 absorption by conventional ILs based on a physical mechanism (i.e., upon absorption of CO_2, no chemical

(a)

(b)

(c)

(d)
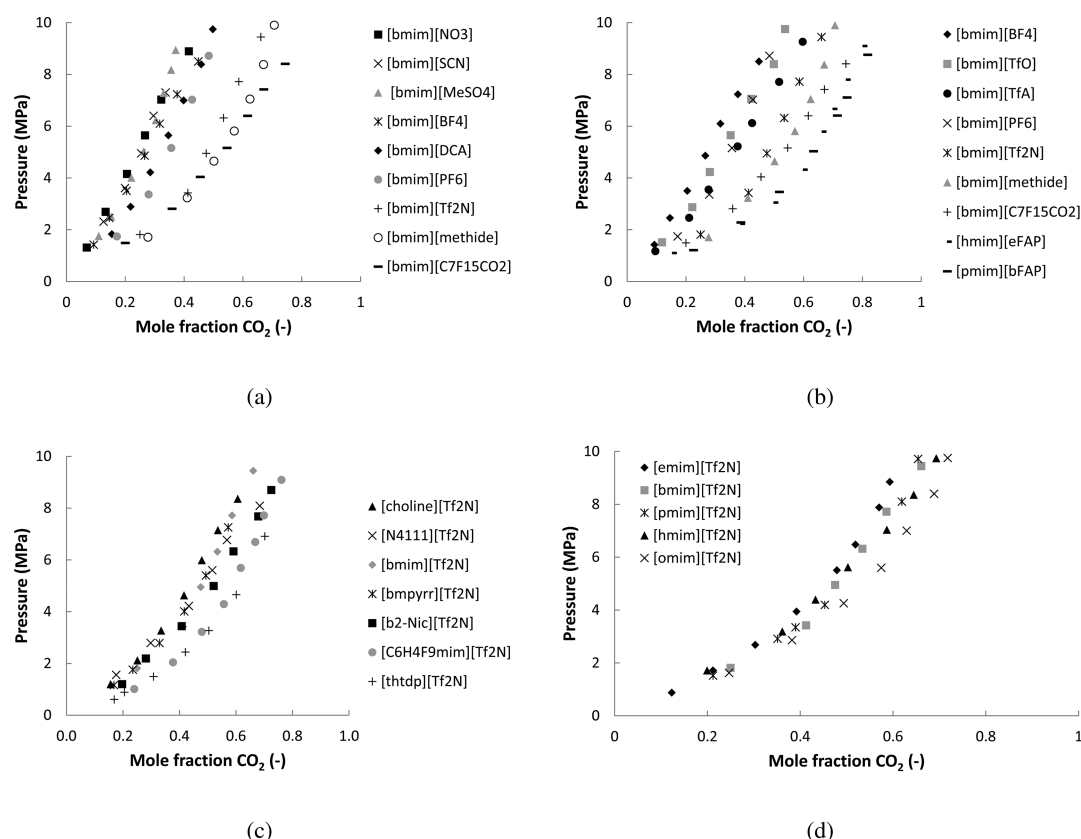
Figure 5. (a) Effect of anion on CO_2 solubility. Fluorinated anions show higher CO_2 solubilities than unfluorinated ones. Data at 333 K taken from refs 80, 289, and 290. (b) Effect of anion fluorination on CO_2 solubility. CO_2 solubility increases as the number of fluor groups increases in the anion. Data at 333 K taken from refs 80 and 289 (c) Effect of cation on CO_2 solubility. The cation seems to have a minor influence on the solubility of CO_2. Data at 333 K taken from refs 80, 111, 289, and 291. (d) Effect of alkyl chain length on CO_2 solubility. CO_2 solubility increases as the alkyl chain length becomes longer. Data at 333 K taken from refs 80, 287, and 292.

reaction takes place). CO_2 solubility, selectivity, ionic liquid viscosity, and volatility are considered.

3.1.1. CO$_2$ Solubility. The anion is believed to play a key role in the dissolution of CO_2, whereas the cation is supposed to have a secondary role.[80] This finding is supported by molecular simulation studies and experimental data.[81,82] To help understand the high solubility in imidazolium ILs, Cadena et al.[82] used molecular simulations. These authors found that the CO_2 primarily associates with the [PF6] anion, regardless of the cation. The in situ ATR-IR spectroscopy data of Kazarian et al.[83] earlier revealed the favorable interaction between the anions ([BF4] and [PF6]) and CO_2. The spectroscopic data suggested that the interaction is a Lewis acid−base type where the anion serve as a Lewis base, while CO_2 acts as a Lewis acid. Furthermore, the spectroscopic data provide strong evidence that the interaction between CO_2 and [BF4] anion should be stronger than for the [PF6] anion, since [BF4] is a stronger base. However, experimental solubility data show a higher CO_2 solubility in [bmim][PF6] rather than [bmim][BF4]. Thus, the solubility cannot solely be explained by anion−CO_2 interactions, and a free volume mechanism is also expected to play a significant role in dissolving CO_2.[83] A free volume mechanism where CO_2 molecules are hosted in the free spaces (cavities) of the liquid is not unlikely, since the liquid volumes of ILs do not change significantly upon dissolution of large amounts of CO_2.[77,80,82] In addition, Kanakubo et al.[84] performed X-ray diffraction measurements on the [bmim][PF6]−CO_2 system and showed that CO_2 preferentially organizes around the [PF6]

anion. The effect of the anion has been studied experimentally by pairing the [bmim] cation with several anions as shown in Figure 5a. This figure show data at 333 K with CO_2 solubilities increasing in order of the anions: [NO3] < [SCN] < [MeSO4] < [BF4] < [DCA] < [PF6] < [Tf2N] < [Methide] < [$C_7F_{15}CO_2$]. This trend was successfully reproduced by Maiti[85] and Sistla[86] using the COSMO-RS model (conductor-like screening model for real solvent) where guanidinium and phosphonium based ILs were supposed to be promising for higher CO_2 solubility than the corresponding imidazolium-ILs. Generally, fluor containing ILs have higher CO_2 solubilities compared to ILs without a fluor group. The effect of anion-fluorination is shown in Figure 5b for ILs with a common [bmim] cation. CO_2 solubility increases as the number of fluor groups in the anion increases. The solubility increases in the following anion order: [BF4] < [TfO] < [TfA] < [PF6] < [Tf2N] < [methide] < [$C_7F_{15}CO_2$] < [eFAP] < [bFAP]. Consistently, in a screening study Zhang et al.[87] used COSMO-RS to demonstrate that using a longer fluoroalkyl chain in the anion (e.g., [FAP] anion) corresponds to higher CO_2 solubilities. Recently, Palomar et al.[88] used the COSMO-RS methodology to achieve deeper insight into the dissolution behavior of CO_2 in ionic liquids. To this end, a wide number of ILs were screened and the Henry's constants of CO_2 were successfully related to the excess enthalpy of dissolution of CO_2 in ILs. This indicated that higher solubilities are associated with a higher exothermicity of the mixture. Further, the intermolecular interactions (electrostatic, hydrogen bonding,

and van der Waals) between the species in the fluid phase were computed. The contribution of each of these interactions to the solubility of CO_2 in ILs was determined, and the results indicate that the attractive van der Waals forces dominate the behavior of CO_2 dissolution in ILs. The electrostatic interactions had a secondary contribution to the excess enthalpy of dissolution, whereas the contribution of hydrogen bonds were found insignificant.[88] On the basis of this finding, Palomar et al. carried out a guided COSMO-RS screening to find ILs, which have increased van der Waals interactions with the CO_2. The screening resulted in new potential ILs with highly brominated anions (e.g., $[emim][PBr_6]$) with high CO_2 solubilities.

It is widely accepted that the anion dominates the dissolution of CO_2, although the cation is believed to play a secondary role. The small effect of the cation on the CO_2 solubility is clearly shown in Figure 5c. Cholinium, ammonium, imidazolium, pyridinium, pyrrolidinium, and phosphonium cations were paired with the $[Tf_2N]$ anion. Nevertheless, fluorination of the cation (e.g., $[C_6H_4F_9mim]$) can significantly improve the solubility, although to a lesser extent than anion-fluorination.[89] Moreover, using long alkyl chains on the phosphonium cation $[P66614]$ can also improve the solubility. Generally, the CO_2 solubility increases slightly by increasing the alkyl chain length as shown in Figure 5d. All the ionic liquids were paired with a common bis(trifluoromethylsulfonyl)amide $[Tf_2N]$ anion, while the alkyl chain length on the imidazolium cation was varied. Clearly, as the alkyl chain becomes longer the solubility increases in the following order: $[omim] > [hmim] > [pmim] > [bmim] > [emim]$. These trends have also been predicted using the COSMO approach.[85,86,88,90] It is known that the hydrogen attached to the C2 position (C2−H) on the imidazolium ring is acidic (i.e., it has a relatively large positive charge). Therefore, additional CO_2 may be dissolved at this C2 site via hydrogen bonds. The effect of this acidic site has been investigated by means of molecular simulations and experiments.[80,82] Molecular simulation shows that replacing the proton in the C2 position with a methyl group (C2-methyl) slightly decreases the CO_2 solubility.[82] Experiments support this finding, as the Henry's constant at 298 K for CO_2 in $[bmim][PF_6]$ and $[bmmim][PF_6]$ are 53.4 and 61.8 bar, indicating a lower solubility in the methyl-substituted $[bmmim]$ IL.[82]

Although molecular simulations have been used extensively to study the solvation behavior of CO_2 in ILs, computed solubility isotherms of CO_2 in ILs have been reported scarcely due to the increased computational effort.[91] For choosing an optimal IL for CO_2 capture from flue-gases, from a tremendous amount (around 10^{18}) of possible ILs, fast screening methods like COSMO are beneficial. However, several other methods using surface tension or viscosity as an input have been reported in the literature to predict gas solubilities in ILs.[92,92–94] A review of the different approaches that have been used to model the phase behavior of IL-gas systems is provided by Vega et al.[95] Camper et al.[94,96–100] demonstrated that regular solution theory (RST) is also able to predict solubility trends of various gases in ILs at low pressures. This is an interesting finding, since RST without taking into account the intermolecular interactions between the gas and the anion was used for describing solubility trends. Indeed, this contradicts the conventional wisdom that CO_2 solubility is dominated by CO_2−anion interactions. In RST, eq 1, the activity coefficient of a solute, γ_1, is related to its liquid molar

volume, V_1, and the difference in solubility parameters δ_1 and δ_2 of solute and solvent, respectively.

$$RT \ln \gamma_1 = V_1\Phi_2^2[\delta_1 - \delta_2]^2 \tag{1}$$

Shi and Maginn[101] showed that when the RST parameters are known, one can calculate the complete solubility isotherm for a gas. However, until recently the solubility parameter of ILs, δ_2, was unknown and was adjusted to fit experimental isotherms.[91] Recently, enthalpies of vaporization for many ILs were determined experimentally allowing the direct calculation of the solubility parameter by $\delta_2 = (\Delta_{vap}U_2/V_2)$. Using experimentally obtained solubility parameters, RST was found to significantly underpredict the solubility of CO_2 in $[hmim]-[Tf_2N]$. The poor performance of the RST when using actual, instead of correlated, solubility parameters to describe CO_2 solubility is not surprising. As shown in Figure 6, CO_2 solutions
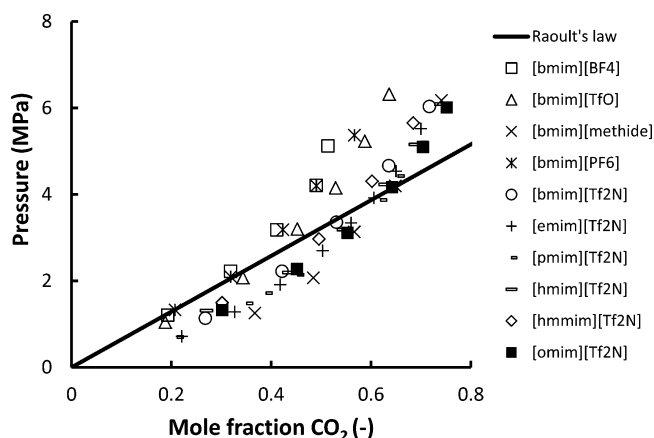
Figure 6. Comparison of the behavior of CO_2−ILs systems with Raoult's law predictions. Typically, CO_2−ILs systems show negative deviations to the ideality as represented by Raoult's law. Data at 298 K taken from refs 80 and 287.

in ILs at low pressure show negative deviations from ideality as represented by Raoult's law:

$$y_1P = x_1P_1^S \tag{2}$$

where P is the pressure, P_1^S is the vapor pressure of CO_2, x_1 is the mole fraction of CO_2 in the liquid phase, and y_1 is the mole fraction of CO_2 in the gas phase, which is equal to 1 assuming nonvolatility of ILs. As a consequence, the activity coefficient of CO_2 in ILs is lower than 1, while RST can only describe solutions with positive deviations from ideality. The performance of RST to predict solubilities should further be tested in the future using experimentally solubility parameters.

So far, CO_2 solubilities on a mole fraction basis were considered. Recently, Carvalho and Coutinho[102] claimed that physical CO_2 absorption in ILs is dominated by entropic effects, hence CO_2 solubilities when plotted as molality (e.g., mol/kg) versus pressure are solvent independent and fall on a common universal curve. Subsequently, they developed a universal correlation for the solubility of CO_2 in nonvolatile solvents with a validity for pressures up to 5 MPa, molalities up to 3 mol/kg, and temperatures ranging from room temperature to 363 K. This universal correlation is given by eq 3, where p is the pressure in MPa, m_i^0 is the molality in mol/kg, and T is the temperature in Kelvin.

$$p = m_i^0 e^{6.8591 - 2004.3/T} \tag{3}$$

Unfortunately, many ILs that do not obey the trend were excluded in the analysis.[54,102] The validity of the model, eq 3, proposed by Carvalho and Coutinho is explored by plotting a large number of ILs in the pressure-molality diagram shown in Figure 7. Indeed, the differences in CO_2 solubilities among

Figure 7. Solubility of carbon dioxide expressed as molality in different ionic liquids. Data show that many ILs do not fall on the universal curve proposed by Carvalho and Coutinho.[102] Data at 333 K taken from refs 77, 80, 111, 125, 164, 286, and 289–301.

many of the ILs are minimized. However, there are many ILs that significantly deviate from the curve proposed by Carvalho and Coutinho.[54,102] In the case of acetates (m-2-HEAA) and formates (m-2HEAF) the solubility is dominated by the formation of electron donor–acceptor (EDA) complexes and does not follow the universal curve, which was also noted by Carvalho and Coutinho. Furthermore, ILs with the following anions, regardless of the cation, also do not obey the curve: $[xSO_4]$, $[SCN]$, $[mp]$, $[doc]$, and $[NO_3]$. Even the simple IL $[bmim][BF4]$ and many of the $[PF6]$, $[DCA]$, and $[TfO]$ ILs do not follow the trend. It is likely that the model suggested by Carvalho and Coutinho[102] is a severe oversimplification. Nevertheless, these authors correctly noticed that there is a

strong influence of the IL molecular weight on the CO_2 solubility as can be seen in Figure 7. In the following, we will show that the CO_2 solubility increases with increasing IL molecular weight, but first we consider the CO_2 solubility as given in molarity (mol/m^3). The solubility data of CO_2, which are the same as in Figure 7, but now expressed in molarity are shown in Figure 8. We can see in Figure 8 that a pressure-

Figure 8. Solubility of carbon dioxide expressed as molarity (mol CO_2/m^3 solvent) in different ionic liquids. Solubility data at 333 K as used in Figure 7. Density data at 333 K taken from refs 133 and 302–310.

molarity plot for many ILs yields nearly straight lines up to ∼60 bar. The slope of these lines gives a first-order approximation of the (molarity-based) Henry's constants. These Henry's constants are plotted against the molecular weight of the IL in Figure 9a. Clearly, the Henry's constants (CO_2 solubility) show a decreasing (increasing) trend with an increasing IL molecular weight. The Henry's constants of CO_2 in the imidazolium-based ILs when plotted against the IL molecular weight seem to fall on a common curve, while this is apparently different for phosphonium-based ILs. However, considering the free-space mechanism it would be more interesting to analyze the CO_2 solubility with respect to the IL molar volume or IL free volume. In Figure 9b the Henry's constants are plotted as a function of the molar volume of the IL. The trend is similar as for molecular weight effects, i.e., the Henry's constant (CO_2 solubility) shows a decreasing (increasing) trend with an increasing IL molar volume. The free volumes of the ILs listed in the legend of Figure 8 have been estimated by

$$V_f = V_m - 1.3 V_{vdW} \tag{4}$$

where V_f is the free volume of the IL, V_m is the IL molar volume, and V_{vdW} is the van der Waals molar volume. Zhao et al.[103] provide a correlation based on Bondi principles[104] to estimate V_{vdW} ($Å^3$/molecule) rapidly with very good accuracy using only atomic and bond contributions:

$$V_{vdW} = \sum AAC - 5.92 N_B - 14.7 R_A - 3.8 N_{NR} \tag{5}$$

where AAC is the atomic contribution of all atoms, V_{vdW} is as given by Bondi[104], N_B is the number of total bonds, R_A is the number of aromatic rings, and R_{NR} is the number of nonaromatic rings. Zhao et al.[103] used eq 5 to calculate V_{vdW} of 677 organic compounds and compared their values with the
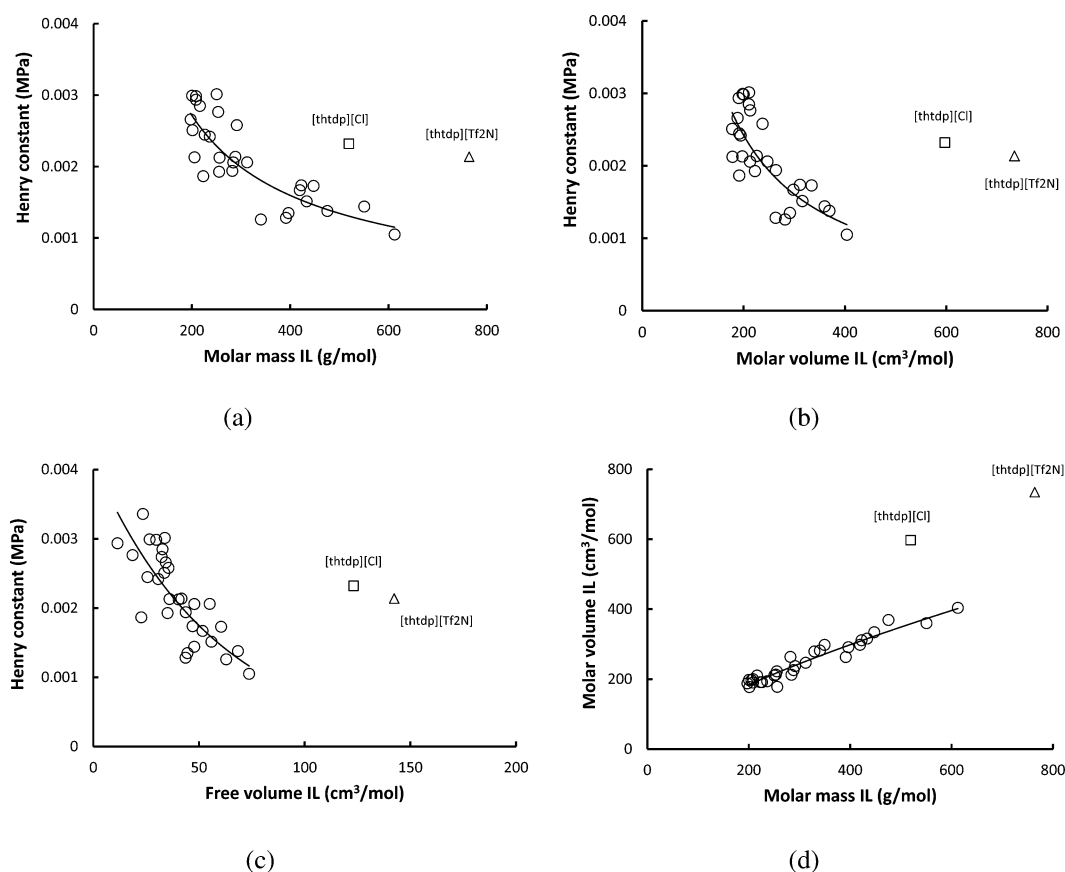
(a)

(b)

(c)

(d)

Figure 9. (a) Henry's constants (molarity based) plotted as a function of the molecular weight of the IL show that the Henry's constant (CO_2 solubility) is decreasing (increasing) with an increasing molecular weight. (b) Henry's constants (molarity based) plotted as a function of the molar volume of the IL show that the Henry's constant (CO_2 solubility) is decreasing (increasing) with an increasing molar volume. (c) Henry's constants (molarity based) plotted as a function of the free volume of the IL show that the Henry's constant (CO_2 solubility) is decreasing (increasing) with an increasing free volume. (d) Molecular weight plotted as a function of the IL molar volume show that the molar volume almost linearly increases with increasing IL molecular weight. Imidazolium-based ILs (circles), phosphonium-based ILs (square and triangle) and the lines are fit through the imidazolium-based data to guide the eye. All data are at 333 K.

values computed using the TSAR program (Oxford Molecular) having a regression coefficient value of 0.992 and a standard error of 8.6 Å^3/molecule. Using eqs 4 and 5 we have estimated the free volume of all ILs listed in the legend of Figure 8. Subsequently, we have correlated the Henry's constants (molarity based) with the free volume of the IL as shown in Figure 9c. Again, the Henry's constant (CO_2 solubility) shows a decreasing (increasing) trend with an increasing IL free volume. We note that in the calculation of the free volume based on eq 5, the imidazolium and the pyridine rings have been considered as aromatic, while the pyrrolidine ring has been taken as nonaromatic. Furthermore, the molar volume of ILs seems to be correlated with their molecular weight (see Figure 9d). The molar volume increases with an increasing IL molecular weight, although the trend seems to be different for imidazolium and phosphonium-based ILs. Recently, Shannon et al.[105] also showed that CO_2 solubility and selectivity in ILs are governed by the free volume of the IL. These authors used the COSMOtherm program to calculate the free volume of 165 existing and theoretical imidazolium-based ILs. Subsequently, they showed that the volume-normalized solubility of CO_2 is proportional to the free volume to the power −0.5, while the solubility of CH_4 and N_2 exhibited a linear dependence on the IL free volume.

In summary, CO_2 solubility increases with increasing IL molecular weight, molar volume, and free volume. All these results support the claim by Carvalho and Coutinho[102] that CO_2 solubility in ILs is dominated by entropic effects rather than solute−solvent interactions as claimed by many authors. It is clear that the solubility trends as a function of molality or molarity will be different than the trends established on mole fraction basis at the beginning of this chapter. The only trend that seems to survive (see Figure 8) is that the CO_2 solubility in fluor-containing ILs is higher than in nonfluorinated ILs. This suggests that in addition to the dominating free-space mechanism, solute−solvent interactions are also important. The most important message here is that CO_2 solubility should not be evaluated on mole fraction basis due to the strong molecular weight (molar volume) effect. In fact, from an application point of view it is more interesting to analyze the solubility per volume solvent (molarity) or on a molality basis.[51]

3.1.2. CO_2 Selectivity. In practice, separation processes involve mixtures of two or more components that have to be purified or separated, hence solubility data only is not enough to judge the separation performance of a solvent, but also selectivity is essential. Although dozens of CO_2 solubility data are avaible in the literature, selectivity data of CO_2 in ionic liquids are scarcely reported. Nevertheless, for CO_2 capture

from flue-gas and natural gas the following selectivities are mainly relevant: CO_2/N_2, CO_2/H_2, and CO_2/CH_4. Flue-gas or natural gas can contain a large number of impurities and selectivities like CO_2/H_2S, CO_2/SO_x, H_2S/CH_4, and CO_2/CO might also become important. Anderson et al.[106] measured the solubility of various gases in the IL [hmpy][Tf_2N] (see Figure 10). The solubility of the gases in [hmpy][Tf_2N] at 298 K
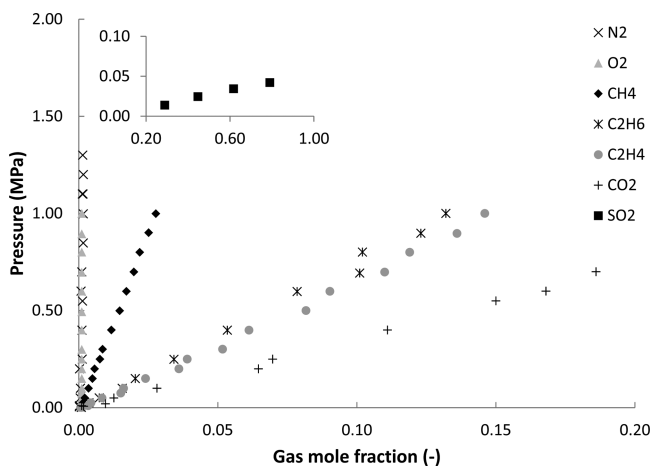

Figure 10. Solubility of gases in the ionic liquid [hmpy][Tf_2N]. Solubility of the gases show the following trend: $N_2 < O_2 < CH_4 < C_2H_6 < C_2H_4 < CO_2 < SO_2$. The inset shows the solubility behavior of SO_2 in [hmpy][Tf_2N]. Data at 298 K taken from refs 106 and 311.

decreases by the following order: $SO_2 > CO_2 > C_2H_4 > C_2H_6 > CH_4 > O_2 > N_2$. Similar gas solubility trends (i.e., $CO_2 > C_2H_4 > C_2H_6 > CH_4 > O_2$) were observed in the ILs [hmim][Tf_2N], [bmim][PF6], and [bmim][Tf_2N].[29,81,106] In general, N_2 and O_2 solubilities are much lower compared to CO_2 leading to a high CO_2/N_2 or CO_2/O_2 selectivity. The hydrocarbons show moderate solubilities, thereby reducing the CO_2/hydrocarbon selectivity. SO_2 is by far the most soluble component in [hmpy][Tf_2N], suggesting that it could compete with CO_2 in an absorption process. As usual, the solubility of CO_2, C_2H_4, and C_2H_6 decreases as the temperature increases, however the solubilities of CH_4 and O_2 were nearly temperature independent. Kumelan et al.[107] also observed the temperature independence of O_2 solubilities in [bmim][PF6].

Recently, Carvalho and Coutinho[108] measured CH_4 solubilities in imidazolium, phosphonium, and ammonium ILs. They also noticed that an increase in temperature had a small or even negligible impact on CH_4 solubility. The peculiarities of CH_4 + IL systems do not end here, Carvalho and Coutinho also observed a crossover in the $P - x$ diagram above which the temperature dependency is reversed such that the CH_4 solubility increases with increasing temperature. Furthermore, the solubility of CH_4 was shown to relate to the polarity of the IL and CO_2/CH_4 or H_2S/CH_4 selectivities were correlated using the Kamlet−Taft β parameter. The Kamlet−Taft parameters, α the hydrogen bond donor, β the hydrogen bond acceptor, and π the polarizability properties, are measures for the overall solvent polarity. The selectivities of sour gases/CH_4 were shown to increase with the β parameter, hence it could be used as a basis for designing ILs which maximize sour gases/CH_4 selectivities.

Hydrogen and carbon monoxide (CO) solubility was measured, respectively in [hmim][Tf_2N] and [bmim][PF6] by Kumelan et al.[109,110] Solubility of both gases in the ILs was

remarkably low compared to CO_2, which is indicative for high CO_2/H_2 and CO_2/CO selectivities in the corresponding ILs. The solubility of H_2 in [hmim][Tf_2N] and [bmpy][Tf_2N] was shown to increase with temperature.[111] This is in contrast with CO_2 + IL systems where the solubility decreases with temperature. CO solubility in [bmim][PF6] was not influenced upon increasing the temperature, while the CO solubility increased in [bmim][CH3SO_4] with increasing temperature.[112] Jacquemin et al.[113,114] measured low pressure solubilities of several gases in [bmim][BF4] and [bmim][PF6]. The solubility of CO_2 was the highest in both ILs, whereas the solubility of H_2 was the lowest. In addition, the hydrogen solubility was shown to increase with temperature at lower temperatures, but it started to decrease with increasing temperatures at higher temperatures. The solubility of the gases in [bmim][BF4] and [bmim][PF6] increases in the order: $H_2 < CO < N_2 < O_2 < Ar < CH_4 < C_2H_6 < CO_2$. The effect of the cation on the solubility of hydrogen was investigated by Jacquemin et al.[115] The [bmim], [emim], and [N4111] cation was paired with the [Tf_2N] anion and the subsequent solubility results show that the cation had a small effect on the H_2 solubility, although the solubility was higher in the ammonium [N4111] IL. For all the three systems, the hydrogen solubility decreased with temperature, this is opposite to what was found for [bmim][PF6], [hmim][Tf_2N], and [bmpy][Tf_2N] systems. Shiflett and Yokozeki[116] showed that much higher CO_2/H_2 selectivities (about 30−300) could be obtained with [bmim][PF6] compared to novel polymeric membranes which had selectivities ranging from 10 to 30 under typical operating conditions. The same authors developed an equation of state (EOS) for the $CO_2/H_2S/$[bmim][PF6] and $CO_2/H_2S/$[bmim][MeSO4] systems.[117,118] Subsequently they showed that competition between the two solutes exists, leading to a low (about 3.2 to 4) CO_2/H_2S selectivity in the [bmim][PF6] system. For the [bmim][MeSO4] system the selectivity was dependent on the CO_2/H_2S feed ratios; for large and intermediate feed ratios the selectivity was 10 to 13.[118] In particular, solubilities of diatomic gases (e.g., H_2, O_2, CO, N_2) measured in the same IL but by different authors show large discrepancies.[29,107,110,113,114,119] For example, the Henry's constant for O_2 in [bmim][PF6] at 283 K was reported by Anthony et al.[29] to be 650 ± 425 MPa, while Kumelan et al.[107] reported a value of 51.5 ± 0.6 MPa at 283 K. Nevertheless, the solubility trends of several gases observed in ILs are more or less similar. Simple gases often interact weakly with the IL ions, hence the polarizability of the gases is reflected in the solubility behavior, leading to the series $H_2 < CO < N_2 < O_2 < Ar < CH_4 < C_2H_6 < CO_2$. Molecules that possess an electric quadrupole moment (e.g., CO_2 and C_2H_4) show higher solubilities.[120] Accordingly, polar gases like SO_2, H_2S, and water vapor show very high solubilities.

Applying regular solution theory, Camper et al.[94,96−100] showed that the physical solubility of gases in ILs was well correlated with the liquid molar volume of the IL and that ideal selectivities for CO_2/N_2 and CO_2/CH_4 should increase as the molar volume of the IL decrease. Finotello et al.[100] measured CO_2, N_2, and CH_4 solubilities in pure [bmim][BF4] and [bmim][Tf_2N] and in mixtures of these ILs. They showed that CO_2/N_2 and CO_2/CH_4 ideal selectivity in [bmim][BF4] could be enhanced by adding 5 mol % [bmim][Tf_2N], which is consistent with RST as this IL mixture represented the lowest liquid molar volume. Bara et al.[121] measured the solubility and ideal selectivities of the gas pairs CO_2/N_2 and CO_2/CH_4 in
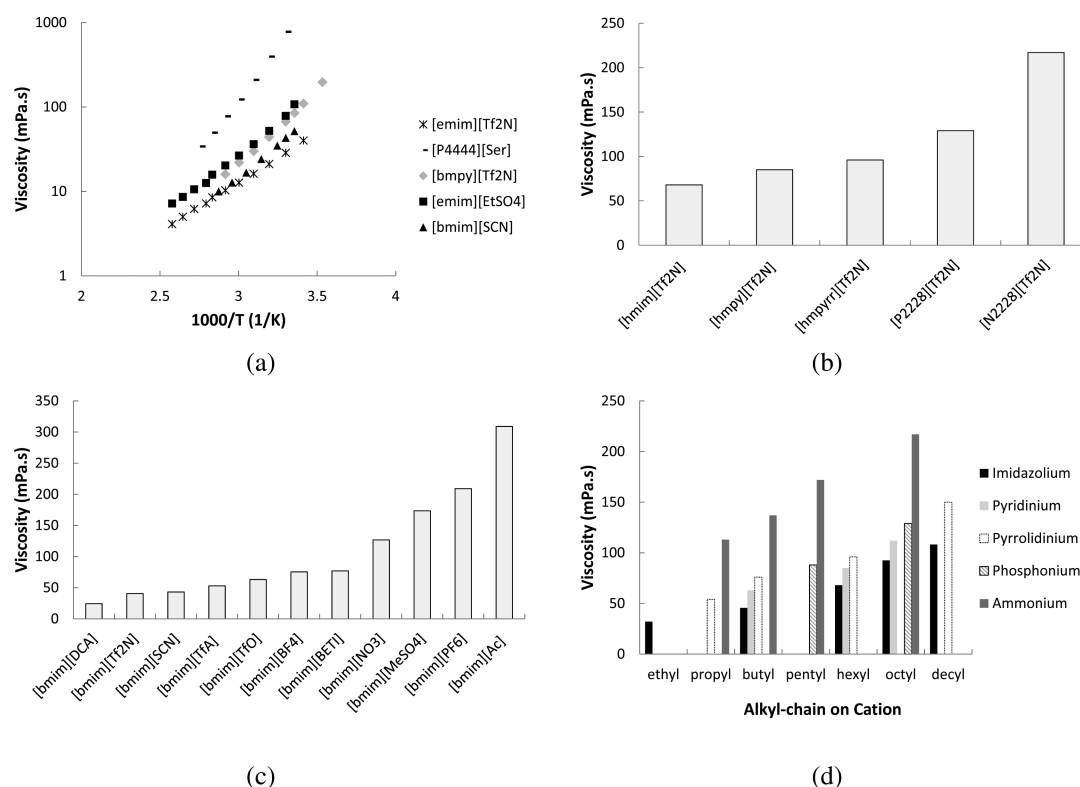
Figure 11. (a) Temperature dependence of the viscosity. The data significantly deviates from Arrhenius law and is usually described by the Vogel–Fulcher–Tammann rule.[133,303,312,313] (b) Effect of cation on viscosity for a common [Tf2N] anion. Viscosity shows the following trend: [imidazolium] < [pyridinium] < [pyrrolidinium] < [phosphonium] < [ammonium]. Data at 298 K taken from refs 313–315. (c) Effect of anion on viscosity for a common [bmim] cation. Data at 303 K taken from refs 133, 141, 303, 304, 307, 313, 316, and 317. (d) Effect of alkyl-chain length on viscosity for different ionic liquids with a common Tf2N anion. Viscosity increases with increasing alkyl chain length for all IL classes. Data at 298 K taken from refs 137, 313–315, 318, and 319.

imidazolium-based ILs functionalized with oligo(ethylene glycol). They showed that the CO_2 solubility in these oligo(ethylene glycol) functionalized ILs were similar to their corresponding alkyl analogues, but N_2 and CH_4 solubilities were lower corresponding to a higher ideal selectivity for the two gas pairs.[122] Similar results were reported by Carlisle et al.[122] for nitrile-functionalized ILs. The nitrile-functionalized ILs exhibited lower CO_2, N_2, and CH_4 solubilities, but showed improved CO_2/N_2 and CO_2/CH_4 selectivities compared to alkyl-substituted analogues. Mahurin et al.[123] measured CO_2/N_2 ideal selectivities in imidazolium, pyridinium, and pyrrolidinium ILs functionalized with a benzyl group. Improved CO_2/N_2 ideal selectivities, ranging from 22 to 33, were reported for these benzyl-functionalized ILs. It should be stressed here that mainly ideal selectivities (i.e., the ratio of pure gas solubilities) are reported in the literature. Unfortunately, real or actual selectivities in mixtures of gases cannot always be determined from pure gas solubilities with the assumption of ideal mixing. In general, measuring mixed-gas solubilities is significantly more difficult, therefore almost no mixture data can be found in the literature.[91] One of the first mixed gas solubilities was reported by Hert et al..[124] In this study, the authors reported an enhancement of the sparingly soluble gases O_2 and CH_4 in the IL [hmim][Tf2N] in the presence of CO_2. However, using molecular simulations Shi and Maginn[101] showed that there is no or very little enhancement of O_2 solubility in the presence of CO_2. Revised experiments on CO_2/O_2 support this finding, hence CO_2/O_2 selectivities can be expected to have near-ideal selectivities.[91] The literature on

mixed gas solubilities has mostly focused on the gas pairs CO_2/H_2S, CO_2/SO_2, and CO_2/H_2. The CO_2/H_2S and CO_2/SO_2 selectivities are extremely important in desulfurization processes and the natural gas sweetening process as natural gas can contain large amounts of sulfur compounds. CO_2/H_2S solubilities in ILs were investigated by Shiflett et al.[117,118] in the ILs [bmim][MeSO4] and [bmim][PF6], while Jalili et al. measured CO_2/H_2S solubilities in [omim][Tf2N]. CO_2/H_2S (gas phase) selectivity in [bmim][MeSO4] and [bmim][PF6] is somewhat dependent on the CO_2/H_2S feed ratio, but at 298.15 K it was ~10 and 1–4, respectively. Jalili et al.[125] reported a (gas phase) selectivity of ~3 at 303.15 K in the [omim][Tf2N] IL. Yokozeki and Shiflett[126,127] investigated experimentally the CO_2/SO_2 (gas phase) selectivity in the ILs [hmim][Tf2N] and [bmim][MeSO4], while Shi and Maginn[101] used molecular simulation for the $CO_2/SO_2/$[hmim]-[Tf2N] system. The CO_2/SO_2 (gas phase) selectivity in the ILs [hmim][Tf2N] and [bmim][SO4] was highly dependent on the gas feed ratio and IL addition, but for a CO_2/SO_2 ratio of 9/1 the selectivity was ~30 and 226–348, respectively. We note that H_2S and SO_2 are much more soluble than CO_2 and the selectivities reported here are gas phase selectivities (i.e., a high H_2S or SO_2 solubility in the liquid phase result in a high gas phase CO_2/sulfuric gas selectivity.) Beside CO_2/H_2S, also CO_2/CH_4 selectivities are important in the natural gas sweetening process; however, no data could be found for real CO_2/CH_4 selectivities. Nevertheless, the natural gas process operates at high pressures and ideal selectivity should not be expected for CO_2/CH_4 separation. As previously noted, in the

precombustion process the relevant separation/selectivity is CO_2/H_2. Mixed gas solubility of CO_2/H_2 mixtures has been investigated by Yokozeki and Shiflett,[116] Kumelan et al.,[128] and Shi et al.[129] Yokozeki and Shiflett reported a CO_2/H_2 selectivity of 30−300 in the IL [bmim][PF6], but the selectivity was shown to decrease with increasing temperature. Kumelan et al. investigated a mixture of $CO_2/H_2/$[hmim][Tf2N] and found that CO_2 acts as a cosolvent for hydrogen, thereby enhancing the solubility of the sparsely soluble hydrogen gas. Shi et al. found a CO_2/H_2 selectivity of ∼30 in the IL [hmim][Tf2N] at 313 K, but this number decreased to about 3 at 573 K. The CO_2 solubility decreases with increasing temperature, while this is the opposite for hydrogen resulting in a lower CO_2/H_2 selectivity at higher temperatures. The most relevant separation in the postcombustion process is the CO_2/N_2 separation, hence CO_2/N_2 selectivities are important in this process. Kim et al.[130] measured the mixed gas solubility of CO_2/N_2 mixtures in the IL [hmim][Tf2N]. Their results show that negligible amounts of N_2 were absorbed in the IL suggesting a high and ideal selectivity for this gas pair.

In summary, the most important separation in the postcombustion process is CO_2/N_2. Ideal CO_2/N_2 selectivity in ILs is expected to be high and close to real selectivity, since N_2 solubility in ILs is not influenced by the presence of the CO_2. In the precombustion process, assuming that the CO_2 is captured after the WGS reaction, the relevant separation is CO_2/H_2. Although ideal CO_2/H_2 selectivity in ILs are relatively high, real selectivity is expected to be lower than ideal selectivity especially at higher temperatures, since H_2 solubility in ILs shows an increasing trend with increasing temperature while this is the opposite for CO_2. In the natural gas sweetening process many impurities can be present, but the relevant separations considered here are CO_2/CH_4 and CO_2/H_2S. Ideal selectivity of CO_2/CH_4 in ILs is comparable to that in conventional physical solvents, however real CO_2/CH_4 selectivity in ILs is also expected to be lower than the ideal selectivity, since CH_4 solubility in many ILs also increases for increasing temperature while this is the opposite for CO_2. Ideal selectivity should not be expected for the gas pair CO_2/H_2S, since CO_2 solubility is significantly inhibited by the presence of H_2S. In fact, H_2S is much more soluble in ILs and both gases will compete in an absorption column. It is possible to remove both gases simultaneously, but this is not necessarily an advantage as an additional step may be required for separating CO_2 from H_2S.

3.1.3. Viscosity of Ionic Liquids. The shear viscosity, η, of an IL is one of the key material properties in process design, because high viscosities often form barriers for many applications and may lead to mass transfer limitations in chemical reactions.[120] Many ILs form highly viscous gel-like materials. Nevertheless, the tunability property of ILs can be invoked to design ILs with a broad range of viscosities. Figure 11a shows a plot of the shear viscosity η versus $1/T$ of some commonly used ILs. Simple liquids obey Arrhenius law, according to which the η versus $1/T$ plot yields a straight line. However, the data given in Figure 11a significantly deviate from Arrhenius law and are usually described by the Vogel–Fulcher–Tammann (VFT) equation:

$$\eta = A \exp(B/(T - T_0)) \tag{6}$$

where A, B, and T_0 are specific adjustable parameters.[120] Also the pressure dependence of the viscosity of ILs shows notable differences from the typical behavior of molecular sol-

vents.[131,132] It can readily be seen in Figure 11a that the IL viscosities are much higher than for conventional solvents like water, alcohols or acetonitrile. Therefore designing ILs with low viscosities by manipulating the nature of cations and anions has been the objective of many researchers. An analysis of the effect of the cation on the viscosity is given in Figure 11b. In this figure the viscosity of imidazolium, pyridinium, pyrrolidinum, phosphonium and ammonium ILs with a common [Tf$_2$N] anion at 298 K is given. The viscosity increases with the cation series: imidazolium [hmim] < pyridinium [hmpy] < pyrrolidinum [hmpyrr] < phosphonium [P2228] < ammonium [N2228]. It should be mentioned here that physical properties of ILs like density and viscosity are influenced by the amount of water and other impurities present in the IL.[133] To make a fair comparison in this section only viscosity data of dried ILs (i.e., water content lower than 1000 ppm) are considered. The effect of the anion on the viscosity at 303 K for ILs with a common [bmim] cation is given in Figure 11d. The viscosity increases with the anion order: [DCA] < [Tf$_2$N] < [SCN] < [TfA] < [TfO] < [BF4] < [BETI] < [NO$_3$] < [MeSO$_4$] < [PF6] < [Ac]. The dicyanamide anion [DCA] possess the lowest viscosity for the [bmim] cation. The relatively high viscosity of [bmim]-[PF6] is remarkable, since fluorinated ILs (e.g., [Tf$_2$N], [TfO] and [BF4]) generally show lower viscosities. The effect of the alkyl-chain length for several ILs is given in Figure 11d. The viscosity increases almost linearly with alkyl-chain length for all ILs. Gardas and Coutinho[134,135] developed a group contribution method to estimate thermophysical and transport properties (i.e., viscosity, electrical conductivity, thermal conductivity, refractive index, isobaric expansivity, and isothermal compressibility) of ILs. The group contribution approach estimated the viscosity of 29 ILs with a mean percent deviation of 7.7% and a maximum deviation of 28%. Molecular simulations have also been used for studying the dynamics of ILs. Recently, Maginn[91] gave an excellent state-of-the-art review on the dynamics of ILs and in general about molecular simulations of ILs. Although simulations generally capture the slow dynamics of IL systems the simulations in the past were performed on too short time scales to calculate reliable viscosities.[91,136] In chemical reactions, viscosity plays an important role, since in diffusion-controlled reactions the rate constant should be inversely proportional to the viscosity of the solvent.[120] For this reason many reactions are slower in ILs than in conventional solvents due to the high viscosity of ILs. The self-diffusion coefficients (D) of cations and anions at 298 K are of the order $D = 10^{-11}-10^{-10}$ m²/s, compared to $D = 10^{-10}-10^{-9}$ m²/s for simple molecular liquids.[91,120] The self-diffusion of a spherical particle with a radius r is often related to the viscosity, η, through the Stokes−Einstein relation, eq 7, where k_B is the Boltzmann constant.

$$D = \frac{k_B T}{6\pi\eta r} \tag{7}$$

The relation of CO_2 diffusivity normalized with temperature and solvent viscosity is shown in Figure 12. The figure contains data of several imidazolium, ammonium, phosphonium, and pyridinium ILs as well as alcoholic and hydrocarbonous solvents. Despite the complex structure of ILs the CO_2 diffusivity dependency on solvent viscosity appears to be universal, with self-diffusivities proportional to solvents viscosity to the power −0.43. Similarly, Moganty and Baltus[137] found a power of −0.45 by taking fewer data points of ILs into
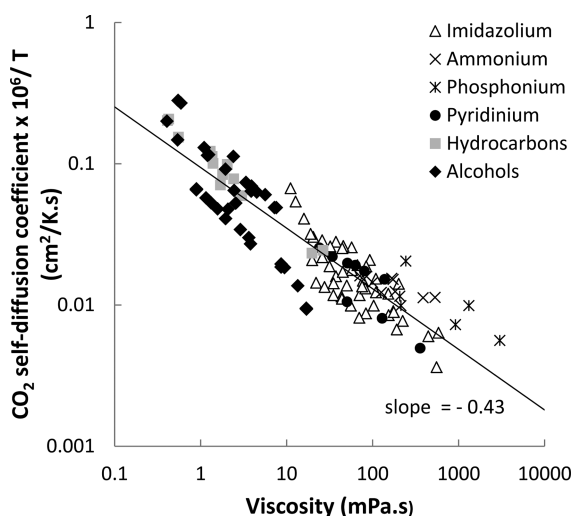
Figure 12. Viscosity/diffusivity relationship for ionic liquids and conventional solvents. Self-diffusivities of CO_2 in different solvents appears to be proportional to solvents viscosity to the power −0.43. Ionic liquids data taken from refs 137, 141−144, and 320 Data of alcohols and hydrocarbonous solvents taken from refs 138, 140, and 321−323.

account. It is surprising to note that a power of around −0.45 was found for CO_2 diffusion in organic solvents and dilute liquids.[138−140] The data for diffusion of gases in ILs reported so far indicate a fractional Stokes−Einstein behavior having the form given by

$$D \propto (T/\eta)^m \qquad (8)$$

The exponent m in eq 8 is generally lower than 1 ($m < 1$) and has been determined for imidazolium, ammonium, and phosphonium ILs. Morgan et al.[141] used a lag-time technique to measure gas diffusivities in imidazolium based ILs. They found $m = 0.6$ for imidazolium ILs. Furthermore, they provided a correlation based on IL viscosity and solute molar volume for the diffusivity of gases in imidazolium ILs. However, Hou and Baltus[142] used a different correlation for CO_2 diffusivity in imidazolium ILs taking IL viscosity, molar mass, density, and temperature into account. Diffusion of gases in phosphonium ILs was investigated by Ferguson and Scovazzo.[143] They found that the diffusivity was inversely related to the phosphonium IL viscosity with a power of 0.35 ($m = 0.35$). The diffusivity of gases in phosphonium ILs was correlated with the solvent viscosity, solvent, and solute molar volumes. Diffusivities of gases in ammonium ILs were measured by Condemarin and Scovazzo,[144] and they found a viscosity dependence with a power of 0.5 ($m = 0.5$). In this study the authors correlated the diffusion of gases in ammonium ILs with IL viscosity, molar volume of solvent and solute. Clearly, the power dependency of diffusivity is different for different classes of ionic liquids. The diffusivity of gases in ILs are less dependent on the viscosity ($0.3 < m < 0.7$) than predicted by Stokes−Einstein equation ($m = 1$). This is probably not very surprising, since the Stokes−Einstein equation generally represents the case where a large solute molecule is diffusing in a solvent of relatively small molecules.[141] Nevertheless, the self-diffusion coefficients of CO_2 at room temperature in all the ILs are $\sim 1 \times 10^{-10}$ m^2/s, which is an order of magnitude lower than for conventional solvents. Molecular simulations have also been used to calculate diffusivities, however the simulation runs in many of these

computational studies in the past were too short (i.e., ps scale) to calculate reasonably transport properties.[91,120,136,145] More recent studies with much longer simulation times (i.e., several to hundreds of ns) have overcome this problem and reliable transport properties could be calculated.[91,136,146]

3.1.4. Volatility of Ionic Liquids. The discussion here will be limited to aprotic ionic liquids, since protic ILs contain an acidic proton on the cation, which can be abstracted by the basic anion. This acid−base reaction leads to the formation of neutral molecular species that can readily evaporate, hence protic ILs are volatile by their nature.[147] Since its origins ionic liquids were considered substances with zero vapor pressure, but this general belief changed abruptly after the publication by Earle et al.[148] In this study the authors showed that several commonly used aprotic ionic liquids, pure and mixed, could be distilled at 300 °C and high vacuum without significant decomposition. For example the IL [hmim][Tf$_2$N] could be distilled at 170 °C and 0.07 mbar. Since the breakthrough publication by Earle et al. several studies have been reported concerning the nature of the vapor phase, vapor pressure (P_v), enthalpy of vaporization ($\Delta_{vap}H$), boiling point (P_b) and boiling temperature (T_b) of ILs. Review on these topics are provided by Ludwig and Kragl[149] and Esperanca et al.[147] Both reviews address the difficulty in experimentally determining the liquid−vapor equilibrium (VLE) properties (e.g., $\Delta_{vap}H$, P_v) for ILs. This is mainly due to the competition between evaporation and decomposition mechanisms at sufficiently high temperatures complicating the experimental interpretation. A detailed study on the nature of the vapor phase and enthalpy of vaporization was first given by Armstrong et al.[150] The ionic liquid was evaporated under ultrahigh vacuum and the vapor phase was analyzed by line of sight mass spectroscopy (LOSMS). The vapor phase was shown to consist of neutral ion pairs, where the enthalpy of vaporization was primarily dependent on the Coulombic interactions between the gas-phase and the liquid-phase ion pair.[150] Similar results on the nature of the vapor phase were found by Leal et al.[151] using Fourier transform ion cyclotron resonance mass spectrometry (FTICR−MS) at reduced-pressure distillation conditions. The FTICR−MS results indicated that at low pressures and at temperatures above 474 K the vapor phase consists of neutral ion pairs, without free ions, and larger clusters. By contrast, the vapor phase of protic ILs was shown to consist of isolated neutral molecules, supporting the proton transfer mechanism. More recently, Rai and Maginn[152] investigated the nature of the vapor phase by means of molecular simulations. Their simulation results support the experimental finding that the vapor phase predominantly consists of isolated ion pairs. However, the molecular simulations also indicate that a substantial fraction of the ions is present in larger aggregates, and this fraction increases as the temperature and pressure increases. The enthalpy of vaporization, $\Delta_{vap}H$, has been measured by several techniques: the Knudsen method, surface tension, microcalorimetry, temperature-programmed-desorption, transpiration and molecular dynamics (MD) simulation.[147,153] Unfortunately, the different techniques do not yield uniform enthalpies of vaporizations for a given IL, for example the measured values of $\Delta_{vap}H$ for [omim][Tf$_2$N] range from 150 to 192 kJ/mol.[149] Nonetheless, reliable $\Delta_{vap}H$ values range from 120 to 200 kJ/mol rather than the very high values up to 300 kJ/mol reported by Rebelo et al.[154] Recently, Fumino et al.[155] used far-infrared measurements to measure the enthalpy of vaporization of several imidazolium ILs. The values reported were in the range

8161

dx.doi.org/10.1021/ie3003705 | *Ind. Eng. Chem. Res.* 2012, 51, 8149−8177

of 128−165 kJ/mol. Deyko et al.[156] used LOSMS for the measurement of 12 ILs and provided a simple theory for estimating the enthalpy of vaporization as a sum of a Coulombic contribution and two van der Waals contributions resulting from the anion and the cation. Verevkin[157] developed a simple group contribution approach to accurately estimate the enthalpy of vaporization of several imidazolium and pyrrolidinium based ILs. Furthermore, the experimental data compiled by Esperanca et al.[147] indicate that Trouton's rule ($\Delta_{vap}H_{Tb}/T_b$ = constant) is not obeyed by $[C_n mim][Tf_2N]$ IL family. The $\Delta_{vap}H_{Tb}$ values showed an increasing and decreasing trend with a maximum at n = 4. This is opposite to what is found by molecular simulation for $[C_n mim][BF4]$ series where it was shown that $\Delta_{vap}H_{Tb}$ decreases with increasing chain length showing a Trouton-like correlation with a Trouton's constant of approximately 65 kJ/mol.[152] The vapor pressure of ILs in the homologues series of $[C_n mim][Tf_2N]$ was measured by Zaitsau et al. using a Knudsen effusion method.[158] They obtained vapor pressures between 10^{-1} and 10^{-3} Pa for temperatures ranging from 450 to 550 K. Recently, Rocha et al.[159] presented high-accuracy vapor pressure data of nine imidazolium-based ILs. These authors provided for the first time a quantitative evidence for the structural percolation phenomenon in ILs and its relation with the thermodynamic properties of ILs. Furthermore, the high-accuracy vapor pressure data of all the ILs at 450 K were ~0.02 Pa. Since these pressures are so low and even lower at standard experimental conditions, it is not very surprising that it took some time to notice the volatility of ionic liquids. However, the proven (negligible) volatility of ionic liquids will not damage the reputation, which is largely built on their nonvolatility property, as green solvents.[160]

3.2. Functionalized Ionic Liquids. Large scale application of physical ILs for CO_2 capture from flue-gas is mainly hindered by the low CO_2 absorption capacity at postcombustion conditions. The partial pressure of CO_2 at postcombustion conditions (see Table 1) is rather low, hence CO_2 solubility is lower than 5 mol % even for the best physical ILs. To overcome this problem researchers appealed to the amine chemistry by arguing that including an amine moiety to conventional ILs (amine-functionalized ILs) could greatly improve CO_2 absorption capacity. The progress in this branch of research is reported in this section.

3.2.1. Cation Functionaliztion. The concept of ionic liquid functionalization or task-specific ionic liquid (TSIL) was first introduced by Bates et al.[161,162] In this study the authors functionalized the imidazolium cation with a primary amine moiety. This new TSIL was shown to react in a 2:1 stoichiometry with CO_2 according to Figure 13. We note that this stoichiometry is similar to the theoretical maximum molar uptake of CO_2 by conventional amines under the carbamate formation scheme.

Figure 13. Reaction between cation functionalized ionic liquid and CO_2. The IL react in a 2:1 stoichiometry with CO_2 forming a carbamate salt.[161].

Evidence for carbamate formation as proposed in Figure 13 was given by FT-IR and NMR spectra analysis of the CO_2-treated and CO_2-untreated ionic liquids. Furthermore, the authors reported that the reaction was reversible and the CO_2 could be released upon heating (80−100 °C) for several hours under vacuum. Although the authors observed a relatively high viscosity of the synthesized ionic liquid, they did not notice the dramatic viscosity increase after reacting the CO_2 with the TSIL. Galán Sánchez et al.[163,164] further verified this concept by functionalizing the [bmim] cation by a primary and tertiary amine. These functionalized cations were paired with [BF4] and [DCA] anions. The CO_2 solubility in the physical nonfunctionalized ILs, [bmim][BF4] and [bmim][DCA], does not vary significantly. Functionalization of the [bmim] cation with an amino group [Ambim] improved the CO_2 absorption, relative to the nonfunctionalized counterparts, by a factor 13 and 4, respectively, for [Ambim][BF4] and [Ambim][DCA] at 0.1 MPa and 303 K. Clearly, the CO_2 solubility can be enhanced by including amine groups in the cation and by choosing a proper anion. Furthermore, the isotherms of CO_2-functionalized ILs show a trend which is typical for chemical absorption. At low pressures the solubility increases sharply, while a steady increase in solubility is observed at higher pressures due to contribution of the physical mechanism. Although a similar trend was observed for the tertiary-amine-functionalized IL [3Amim][BF4]−CO_2 system the solubility was significantly lower compared to the primary-amine-functionalized ILs. This is likely due to the lower reactivity of tertiary amines toward CO_2.[18] The ILs did not show reduced absorption capacity after regenerating it at 353 K in vacuum. However, the viscosity problem after reaction with CO_2 was again noted. To overcome the viscosity problem of the amine-functionalized ILs to some extent, Camper et al.[165] proposed the use of (nonfunctionalized) RTIL-amine solutions. They showed that a RTIL solution containing 50 mol % MEA is capable of rapid and reversible capture of CO_2 approaching a stoichiometry of 1 mol of CO_2 per 2 mols of MEA. Since the viscosity of the used IL was much lower than the amine-functionalized IL by Bates et al., the absorption rate in the IL-MEA solution was much faster. Nevertheless, the lowest viscosity of an IL measured up to now is ~20 mPa·s, which is still much higher than for aqueous MEA solutions (e.g., the viscosity of 30 wt % MEA solution at 25 °C is 2.2 mPa·s).

To help understand the high viscosities in neat cation-amine-functionalized IL, Yu et al.[166] used molecular simulations. They found that amino addition does not significantly affect the organization of the anions around the imidazolium ring, instead the anions strongly organize around the -NH_2 forming strong hydrogen bonds. The calculated ionic self-diffusion coefficients of the functionalized ILs were roughly 2 orders of magnitude lower than of the nonfunctionalized counterparts, consistent with the observed high viscosities in the experiments. A mechanistic explanation for the dramatic viscosity increase upon reaction of CO_2 with the amine-functionalized ionic liquid was given by Gutowski and Maginn[167] using molecular simulations. They performed a detailed hydrogen bond analysis and found evidence for the formation of strong, dense hydrogen-bonded networks, primarily between the zwitterion and dication species formed during the reaction.

3.2.2. Anion Functionalization. It is obvious that CO_2 uptake by ILs with amine-functionalized cations is much greater (at precombustion conditions) than by physical absorption. However, the 1:2 reaction stoichiometry for

cation-functionalized ILs is atom inefficient and the question remains whether a more favorable stoichiometry can be achieved. To answer this question Gurkan et al.[168] used ab initio calculations to investigate the relationship between the position of the amine functional group and the reaction stoichiometry. They showed that tethering the amine to the cation favored the formation of the carbamate leading to 1:2 stoichiometry, while tethering the amine to the anion favored 1:1 reaction stoichiometry. Accordingly, they synthesized two amino acid-based ILs, trihexyl(tetradecyl)phosphonium prolinate [P66614][Pro] and trihexyl(tetradecyl)phosphonium methionate [P66614][Met], which were experimentally shown to react with CO_2 in a 1:1 stoichiometry. Figure 14
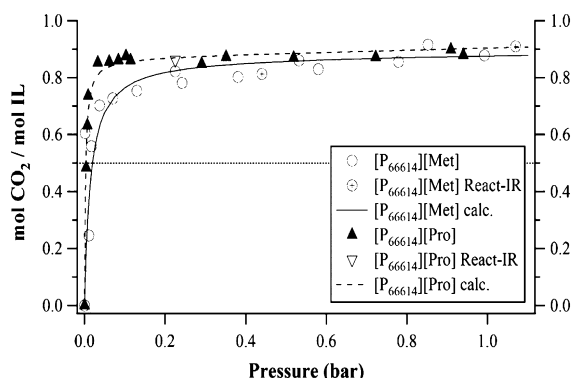
Figure 14. Experimental CO_2 absorption isotherm by anion-functionalized ILs [P66614][Pro] and [P66614][Met] at 22 °C. Note that the reaction stoichiometry of these ILs with CO_2 approaches 1:1, which is better than the 2:1 stoichiometry for conventional amines and CO_2. Reprinted from ref 168. Copyright 2010 American Chemical Society.

shows clearly a CO_2 uptake greater than one mole of CO_2 per two moles of IL which approaches the 1:1 stoichiometry. The isotherms can be subdivided in two distinct parts: a sharp increase at low pressures due to chemical absorption and a marginal increase in capacity at higher pressures which is typical for physical absorption. Nonetheless, it was shown that the vast majority of the uptake was due to chemical absorption. Furthermore, the 1:1 stoichiometry was confirmed by FTIR spectroscopy.[168] Inherent to these amine-functionalized ILs is the increase in the enthalpy of reaction and the increase in viscosity. The enthalpy of reaction of CO_2 with [P66614][Pro] and [P66614][Met] was measured at 25 °C with calorimetry to be −80 and −64 kJ/mol, respectively. These values are intermediate compared to physical absorption (−10 to −20 kJ/mol) and chemical absorption with conventional amines (−85 to −100 kJ/mol). Of course the increased reaction enthalpy will bring extra expenses in the regeneration step. Similar to the case of cation-functionalized ILs, the viscosity increases further upon reaction with CO_2. The occurrence of the latter phenomena was recently demonstrated for amino-acid based ionic liquids.[169] In this study the trihexyl(tetradecyl)-phosphonium [P66614] cation was paired with several deprotonated amino acid anions, like glycinate, isoleucinate, etc. The viscosity of the isoleucinate IL was shown to increase 240-fold, relative to the neat IL. Such high viscosities will preclude the application of these viscous, gel-like, ionic liquids in an industrial absorber-stripper configuration. The energy requirement for pumping the viscous IL will increase, but also the absorption kinetics will deteriorate as diffusion might be

slow in these viscous ILs. The slow diffusion will cause mass transfer limitations, requiring more (equivalent) trays in a typical absorption column, thereby increasing the capital cost.

Carboxylate functionalized anions, such as acetate, also deserve special attention. Chinn et al.[170] investigated the [bmim][acetate] IL diluted in a 14 wt % water solution and showed that CO_2 absorption in this IL exhibits an absorption behavior, which is typical for a chemical complexation process. The volumetric absorption capacity of this acetate-based IL (∼25 m³/m³) is intermediate between amines (∼65 m³/m³ for 30 wt % aqueous MEA solution) and physical ILs (∼3 m³/m³). The enthalpy of reaction of CO_2 in the acetate IL is −40 kJ/mol, which is also intermediate compared to MEA (−85 kJ/mol) and physical ILs (−15 kJ/mol). Therefore, the regeneration step requires a much lower energy input than the MEA process. Chinn et al.[170] put forward a mechanism where the acetate group interacts with the water and the CO_2 is captured as a bicarbonate group. The CO_2+[bmim][acetate] system has also been studied experimentally by Maginn et al.,[171] but they offered a different mechanism involving a proton extraction by the acetate anion from the C2-position of the imidazolium ring leading to acetic acid in the process. In a next step, the CO_2 reacts with the carbene to form a bicarbonate. Shiflett et al.[172] performed a detailed experimental study on the CO_2+[bmim][acetate] system in the presence or absence of water. These authors used spectroscopic analyses to show that the acetic acid formation mechanism put forward by Maginn et al. is not very likely. However, the authors did smell some acetic acid during the experiments, which suggests that at least a limited amount of acetic acid is produced. They classified the phase behavior of CO_2+[bmim][acetate] system as an extremely rare case with strong intermolecular interactions and complex formation. An economic evaluation of the process using [bmim][acetate] for CO_2 capture carried out by Shiflett et al.[173] showed that the IL-process could reduce the energy losses by 16% compared to the MEA process. Furthermore, they estimated a 11% lower investment for the IL-process and 12% reduction in equipment footprint relative to the MEA process. Shiflett and Yokozeki[174] investigated CO_2 solubility in the ILs [emim][acetate], [emim][trifluoroacetate], and mixtures of both ILs. The [emim][acetate] IL absorbed the CO_2 chemically, while the [emim][trifluoroacetate] IL showed physical absorption behavior. The mixture of both ILs showed a combination of a physical and a chemical absorption behavior. Carvalho et al.[175] studied the specific interactions of CO_2 with imidazolium-based [bmim] ILs containing the [acetate] and [trifluoroacetate] anion. Their experimental data showed that CO_2 solubility in [bmim][acetate] unlike in [bmim]-[trifluoroacetate] is spontaneous because of the differences in enthalpies of solvation. Furthermore, these authors used ab initio calculations and high resolution spectroscopy to provide evidence for an acid/base type of solvation mechanism in the acetate IL. Recently, Gurau et al.[176] demonstrated the chemisorption of CO_2 in 1,3-dialkylimidazolium acetate ILs using NMR spectroscopy and X-ray diffraction analysis. These authors explored the reactivity of CO_2 with [emim][acetate] by bubbling CO_2 through the acetate IL at atmospheric and ambient temperature conditions. Using NMR spectroscopy after 24 h bubbling, the formation of 1-ethyl-3-methylimidazolium-2-carboxylate was observed. In addition, X-ray diffraction analysis of single crystals clearly showed that imidazolium carboxylate and acetic acid are formed in the absence of water. Water was shown to inhibit the interaction of acetate with the

proton at the C2 position of the imidazolium ring, thereby inhibiting the CO_2 reaction. Almost simultaneously, Besnard et al.[177] also studied the [bmim][acetate]+CO_2 system using Raman, infrared spectroscopy, DFT calculations, and NMR spectroscopy. They also showed that CO_2 reacts with [bmim][acetate] to form an imidazolium carboxylate and acetic acid originating from the deprotonation of the C2 of the imidazolium ring.

Much recently, Gurkan et al.[178] used a computational approach to design a new class of ILs, namely aprotic heterocyclic anions (AHAs). The authors computed the structure and energetics of pyrrolide, an AHA, and CO_2 reaction product using molecular electronic structure calculations at the G3 level. The pyrrolide was computed to directly combine with CO_2 to form a carbamate product with a computed enthalpy of reaction of −109 kJ/mol. Subsequently, they showed that the reaction enthalpy could be tuned depending on the position of substitution on the pyrrolide ring. Further, MD simulations were used to probe the viscosity of the pyrrolide-based IL with CO_2. For this purpose 2-cyanopyrrolide anions (AHA) were paired with tetrabutylphosphonium [tbp] cations. The MD simulations suggest that the viscosity will not suffer the large viscosity increase upon reaction with CO_2. This result stands in stark contrast with previously reported results for amine-functionalized TSILs where the viscosity increases dramatically upon complexation with CO_2. In addition, experiments with trihexyl(tetradecyl)-phosphonium 2-cyanopyrrolide [thtdp][2-CNpyr] confirmed the findings of the simulations. The [thtdp][2-CNpyr] IL was shown to react in a 1:1 stoichiometry with CO_2 forming carbamate, which was identified using in situ infrared spectrometry. The viscosity was also measured and indeed the viscosity of the reacted and unreacted IL remained nearly the same. Differential calorimetry was used to measure the enthalpy of reaction with a value of −53 kJ/mol, which was in good agreement with the G3-computed value of −49 kJ/mol. Furthermore, these authors state that the approach is not limited to pyrrolides only but imidazolides and pyrazolides may also show similar chemistry. For proving this they synthesized a 3-(trifluoromethyl)pyrazolide [3-CF_3pyra] IL containing the [thtdp] cation. Indeed, CO_2 uptake of this IL was similar to the [2-CNpyr]-IL showing a stoichiometry close to 1:1. Again the viscosity increase was not significant, while the calorimetrically measured enthalpy of reaction for [3-CF_3pyra] was −46 kJ/mol. Hence, AHA-ILs provide a platform with the possibility to tune the reaction enthalpy, to enhance reaction stoichiometry relative to conventional amines, and to circumvent the viscosity increase when reacting with CO_2. Unfortunately the viscosity problem remains also for AHA-ILs, since the neat or CO_2 reacted AHA-ILs given by Gurkan et al.[178] had viscosities at room temperature higher than 100 cP. Such a high viscosity may be still a barrier for using AHAs in industrial CO_2 capture processes. Nonetheless, there is still some room to improve the viscosity and enthalpy of reaction of AHAs by including proper functional groups.

Wang et al.[179−182] also reported equimolar CO_2 absorption in IL-superbase mixtures. Superbases are neutral organic bases, which possess very high proton affinities enabling their protonated conjugate acids to withstand deprotonation by the hydroxide ion.[180] Hence, superbases play an important role as proton acceptors, thereby providing the opportunity to capture CO_2. Wang et al.[180] investigated the CO_2 absorption performance of the IL-superbase system containing two ILs

1-(2-hydroxyethyl)-3-methylimidazolium bis-(trifluoromethylsulfonyl)imide [Im21OH][Tf2N] and 2-hydroxyethyl(dimethyl)-isopropylammonium bis-(trifluoromethylsulfonyl)imide [Nip,211OH][Tf2N] and four superbases 1,8-diazabicyclo-[5.4.0]undec-7-ene (DBU), 1,3,4,6,7,8-hexahydro-1-methyl-2H-pyrimido[1,2-a]pyrimidine (MTBD), 2-tert-butylamino-2-diethylamino-1,3-dimethylper-hydro-1,3,2-diazaphosphorine (BEMP), and 1-ethyl-2,2,4,4,4-pentakis(dimethylamino)-$2\lambda^5,4\lambda^5$5-catenadi(phosphazene) (EtP2(dma)). The performance of the [Im21OH][Tf2N]-DBU system was the best at achieving a molar ratio of CO_2 to DBU slightly more than 1, indicating a combination of physical and chemical absorption. NMR results showed that CO_2 reacted with DBU to form an amidinium alkylcarbonate salt. Furthermore, the absorbed CO_2 could be released easily by heating, and minor loss of activity was observed during several absorption−desorption cycles. The authors reported similar results using imidazolium-based ILs containing different types of anions and the bases DBU, MTBD, EtP2, and tetramethyl guanidine (TMG). Recently, Wang et al.[179] synthesized superbase-derived protic ionic liquids (PILs) for CO_2 capture. They combined the superbases MTBD or P2Et with six weak proton donors (i.e., partially fluorinated alcohols (TFE, TFPA, HFPD), imidazole, pyrrolidone, and phenol) to obtain the superbase-derived PILs. These superbase-derived PILs showed excellent CO_2 capture properties, for example the [MTBDH$^+$]-[TFE$^-$] PIL absorbed 1.13 mol of CO_2 per mol of PIL. Since the viscosity of [MTBDH$^+$][TFE$^-$] was relatively low (8.63 cP at 23 °C), the absorption of CO_2 in [MTBDH$^+$][TFE$^-$] was very fast. Furthermore, the CO_2 could be released completely by bubbling nitrogen at 80 °C and the PILs showed only a slight capacity loss after several absorption−desorption cycles. The same group reported equimolar CO_2 capture by tuning the basicity of ILs. These basic ILs were synthesized by deprotonating several weak proton donors (i.e., trizole, tetrazole, imidazole, pyrazole, oxazolidinone, phenol, indole, and bentrizole) with trihexyltetradecylphosphonium hydroxide [thtdp][OH]. ILs containing the [thtdp] cation and the [pyrazole], [imidazole], [indole], [trizole], or [oxazolidinone] cation showed an absorption capacity close to 1 mol CO_2 per mol of basic IL. Moreover, the absorption capacity and the enthalpy of reaction was shown to increase with an increasing pK_a value of the ILs. Although the CO_2 could be released easily, the viscosity of the basic ILs after reacting with CO_2 was very high (>550 cP), which will cause serious problems in a typical absorption−desorption process.

3.3. Reversible Ionic Liquids. The relatively new approach to capture CO_2 with reversible ionic liquids (RILs) was introduced by Jessop et al.[183,184] Jessop et al. showed that RILs could be formed from a nonionic liquid (an alcohol and an amine base) by exposing it to CO_2 forming a salt (ionic liquid), which can revert back to its nonionic initial state by exposing it to nitrogen or other inert gas.[183] These kind of solvents are also referred to as switchable solvents, since the polarity of the solvent can be tuned upon reaction with CO_2.[185] Heldebrant et al.[184] investigated the reaction of 1,8-diazabicyclo[5.4.0]undec-7-ene (DBU) with carbon dioxide in the absence and presence of water. Their spectroscopic data showed that an IL [DBUH$^+$][HCO$_3^-$] is formed when DBU (amidine) is exposed to CO_2 in the presence of water, while there is no reaction in the absence of water. Phan et al.[186] showed that a guanidine/alcohol mixture also exhibits a similar chemistry as an amidine/water or amidine/alcohol mixture when exposing it to CO_2,

8164

dx.doi.org/10.1021/ie3003705 | Ind. Eng. Chem. Res. 2012, 51, 8149−8177

Table 2. Comparison of the Properties[a] of Commercially Used Solvents and Ionic Liquids for CO_2 Capture. Many Other Commercial Solvents Exist, Only the Ones Commonly Used Are Listed.[q]

	Selexol	fluor solvent	Purisol	Rectisol	Sulfinol	Econamine FG	ionic liquids
chemical	DMPEG	PC	NMP	MeOH	DIPA+sulfolane	MEA[j]	salts
licensor	UOP	Fluor	Lurgi	Linde+Lurgi	Shell	Fluor	n/a
type absorption	physical	physical	physical	physical	chem.[e]/phys.[f]	chemical	physical
solvent cost ($/kg)[b]	2.5	1.5−2	4	0.7	2.5/4	1.5−2	<40[m]
viscosity (mPa.s)	5.8	3	1.65	0.6	186[g]/10	18.98[k]	20−1000
density (kg/m^3)	1030	1195	1027	785	1004/1261	1017	800−1500
molar mass (g/mol)	280	102	99	32	133.19/120.17	61.09	200−750
vapor pressure (mmHg)	0.00073	0.085	0.4	125	0.035/0.02	0.36	0.000001
freezing point (°C)	−28	−48	−24	−92	44/26	10.5	−140 to 180
boiling point (°C)	275	240	202	65	249/285	171	>250
max. operating temp. (°C)	175	65	202	65	150	150	depend on stability
operating pressure	high	high	high	high	low	low	high
$\Delta_{abs}H$ (kJ/mol CO_2)	−14.3	−15.9	−16.4	−13	−73.7[h]	−85	−10 to −20
CO_2 solubility (m^3/m^3)	3.63	3.4	3.57	14.4[d]	30−40[i]	50−85[l]	>2.51
CO_2/CH_4 selectivity[c]	15	26	14	20[d]	n/a	n/a	8−35
H_2S/CO_2 selectivity[c]	8.8	3.3	10.2	7[d]	1−2[i]	1−2[l]	2−10
CO_2/H_2 selectivity[c]	77	126	178	185[d]	n/a	n/a	50−150
CO_2/N_2 selectivity[c]	50	117	50	83[d]	n/a	n/a	30−100
$\Delta_{vap}H$ (kJ/mol)	76.16[n]	60.2	54.5[o]	35.27	57.4/66.8	49.8	>120
H_2O miscibility	yes	partial	yes	yes	yes	yes	variable[p]

[a]Properties at 25 °C and 1 bar, unless otherwise stated. [b]Indicative prices ($/2007) taken from www.icis.com or from supplier info. [c]Ideal selectivity, real H_2S/CO_2 selectivity will differ significantly from ideal selectivity. [d]Solubility, selectivity data at −25 °C. [e]Pure compound property of DIPA / [f]Pure compound property of Sulfolane. [g]Property at 45.5 °C taken from Henni et al.[264] [h]Enthalpy of reaction of CO_2 in diisopropanolamine. [i]Property in a mixture of 40 wt % DIPA + 40 wt % Sulfolane + 20 wt % water. [j]Properties of pure MEA are reported, unless otherwise stated. [k]Viscosity of 30 wt % aqueous MEA solution is 2.2 mPa·s at 25 °C. [l]Solubility, selectivity in a solution of 30 wt % MEA. [m]Estimation of BASF (30 euro/kg) for ton scale production of ionic liquids. [n]Property of tetra-ethylene glycol dimethyl ether. [o]Property at 20 °C. [p]Ranging from completely miscible to immiscible. [q]Majority of the data taken from refs 265−269. Other data taken from refs 99, 100, 111, 116−118, 128, and 270−282.

thereby forming a carbonate salt. The solution could be reversed to its nonionic state by bubbling nitrogen or mild heating. Heldebrant et al.[187] performed a detailed study on organic liquid CO_2 capture using DBU, TMG, Barton's base, and Hunig's base mixed with water or an alcohol. These authors showed that CO_2 reversibly and chemically bind in a mixture of alcohols and amidine/guanidine bases to form a liquid alkylcarbonate. The CO_2 capacity of these RILs was up to 19% by weight, which is comparable to that of MEA. CO_2 was shown to absorb selectively in the presence of N_2 and the RILs did not show any loss of activity or selectivity after five cycles. The enthalpy of reaction of CO_2 in the Barton's base is comparable with MEA, while it was significantly higher for the TMG/alcohol and DBU/alcohol mixtures. However, the authors estimated that 50% less energy would be required in the regeneration step for the RILs compared to the MEA process, since the anticipated specific heat of RILs is three times lower than water. Unfortunately, in the presence of water undesired bicarbonates were formed, which will cause problems when considering that fluegas can contain substantial amounts of water. Blasucci et al.[188] developed a one-component RIL derived from siloxylated amines, which formed a carbamate salt upon reaction with CO_2. Blasucci et al.[189] investigated four silylated amines and their corresponding RILs in combination with CO_2 absorption. They showed that the silyl amines were stable also in the presence of water, while the siloxylated amines were susceptible to degradation. Furthermore, they showed these RILs obeyed both physical and chemical absorption mechanisms to have an absorption capacity of 13−20 mol CO_2/kg amine at 35 °C and 62.5 bar. For further information on this interesting topic, the reader is referred to the reviews by Blasucci,[188] Jessop,[190] and Shannon.[191]

3.4. CO_2 Capture Performance: ILs versus Commercial Solvents. The application potential of ILs for CO_2 capture depends on their performance with respect to already commercialized solvents. The measures that can be used to gauge a solvents' performance are, for example, absorption capacity, gas selectivity, viscosity, stability, solvents' cost, and most importantly the overall process cost. Table 2 provides an overview of the performance of ILs for CO_2 capture with respect to six commercially applied solvents. The Selexol, Fluor Solvent, Purisol, and Rectisol processes utilize a physical solvent, while the Sulfinol process uses a mixed solvent, either DIPA or MDEA with Sulfolane. The standard Econamine process of Fluor uses 30 wt % MEA, which runs on a chemical reaction.[192] However, Fluor has recently improved the Econamine process allowing a higher MEA concentration.[192] All these physical or chemical solvents are applied industrially in the natural gas sweetening process. Tennyson and Schaaf[75] provide useful guidelines for solvent selection depending on acid gas conditions (e.g., partial pressure of acid gas, impurities, and product specification). Ionic liquids exhibiting only physical absorption have been considered in Table 2. Upon comparison of the data presented in Table 2 it becomes clear that ILs are much more expensive than conventional solvents. Current (labscale) prices of ILs are ~1000 $/kg, but economy of scale should apply and according to BASF the price for a large scale process will drop to <40 $/kg. The cost of ILs, even at this price level, would still be a factor of 10 to 20 higher than conventional solvents. This means that a successful application of ILs would rely on other properties of ILs. This property is certainly not the viscosity, since the viscosity of ILs is also significantly higher than of conventional solvents. We note that the viscosity of pure DIPA and MEA are also very high, but

8165

dx.doi.org/10.1021/ie3003705 | Ind. Eng. Chem. Res. 2012, 51, 8149−8177

these solvents are always used in diluted form with viscosities not much higher than that of water. A property, which is inherently related to and in favor of ILs is the vapor pressure. Indeed, the vapor pressure of ILs is much lower than that of the currently used solvents. However, the Selexol process also uses a solvent with a very low vapor pressure, but with a much lower viscosity compared to ILs. The volatility of a number of amines, including MEA, has been reported by Nguyen et al.[193,194] However, volatility is not the only cause for the solvent losses in a CO_2 capture process, but also losses due to thermal and chemical degradation should be considered. Rochelle et al.[195,196] estimated the total MEA loss at stripper conditions to be 80−540 g/ton CO_2 captured, where the lower and upper limit correspond to a stripper operating temperature of ∼110 and ∼130 °C, respectively. In terms of process cost, this loss would result in a solvent replacement cost of $0.19-$1.31/ton of CO_2 removed assuming a price of $1.10/lb of MEA. Reddy et al.[197] estimated the solvent replacement cost of Fluor's Econamine FG Plus process to be $2.30/ton of CO_2 removed. A property not considered in Table 2 is the corrosivity and degradation sensitivity of the solvents. Although MEA is known to be corrosive and sensitive to chemical degradation, these properties have been scarcely investigated and reported for ILs. However, some of the commonly used ILs are also known to be corrosive especially at higher temperatures and for copper alloys, but carbon steel shows very low corrosion rates.[198−206] Surprising to note is that some ILs have been considered as anticorrosion agents.[207,208] Nonetheless, a systematic analysis of the corrosion and degradation behavior of ILs is still lacking, but these issues should be considered in future research. Considering the price/performance ratio of ILs and conventional solvents for CO_2 capture it seems that we will not gain much utilizing physical ILs. We could take advantage of the tunability property of ILs, which can be used to design ILs with an improved selectivity of a gas pair over conventional solvents. Furthermore, ILs can be designed to operate in a range where conventional (physical) solvents cannot be applied. For example, at postcombustion conditions where the CO_2 partial pressure is very low, none of the physical solvents including ILs can be applied. Nevertheless, in this case an amine functionalized IL with a better energy efficiency and reaction stiochiometry than the Sulfinol or MEA process could be used. In this regard, it is very promising and challenging to design ILs with a lower enthalpy of reaction than conventional amines. At precombustion and natural gas sweetening conditions where the CO_2 partial pressure can be quite high (see Table 1), one can optionally choose for a physical IL solvent. However, the price/performance ratio of existing ILs is still insufficient to compete with existing commercial solvents (e.g., Selexol).

In the following we will discuss an another approach for gas separation, namely supported ionic liquid membranes (SILMs), which is a promising alternative for low pressure applications.

4. SUPPORTED IONIC LIQUID MEMBRANES (SILMS)

A relatively new research field is the application of ILs as a solvent in supported liquid membranes (SLMs) technology. Usually, SLMs consist of two phases, a supporting porous (or nonporous) membrane and a liquid solvent phase, which resides in the pores (or are being held between two nonporous membrane sheets). Solute molecules diffuse/dissolve into the membrane facilitating a reaction or separation in the liquid phase and finally desorb at the opposite side of the

membrane.[209] One of the disadvantages of conventional SLMs is the loss of solvent due to evaporation of the stabilized liquid phase.[210−212] This problem can be circumvented by using ILs as the liquid phase and taking advantage of their unique properties such as, relatively low volatility, high chemical and thermal stability.[213] The potential of supported ionic liquid membranes (SILMs) for gas separation has been studied by several researchers.[210,214−219] Reviews of SILMs for gas separation are given by Bara et al.[220] and by Noble and Gin.[213] The performance of SILMs is generally evaluated through a "Robeson plot" together with polymeric membranes data. An example of a Robeson plot, which shows a trade-off between permeability and selectivity for CO_2/N_2 separation by polymers, is given in Figure 15. Interesting to see in Figure 15 is
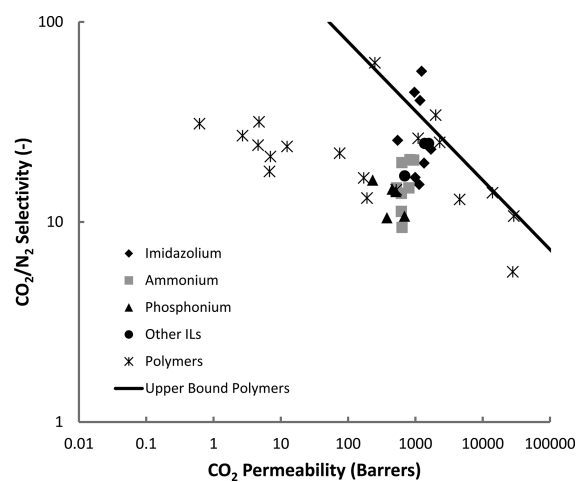
Figure 15. Robeson plot showing the performance of polymeric membranes and supported IL membranes (SILMs) for CO_2/N_2 separation. Some of the SILMs cross the "upper bound"[324] limit of polymeric membranes. SILMs data at 303 K taken from Scovazzo[221] and data of polymers taken from Robeson[324] and Stern.[325]

that some SILMs cross the upper bound limit set for polymeric membranes. This means that SILMs can be designed with a permeability and selectivity superior to traditional polymeric membranes.

The transport mechanism of gases through membranes is extremely important and for SILM it is assumed that a solution-diffusion mechanism governs this transport.[221] Therefore, the ideal permeability (P_i) of a gas through a SILM can be expressed as a product of the solubility coefficient (in moles per volume per partial pressure) and the diffusion coefficient:

$$P_i = S_i D_i \tag{9}$$

Ideal selectivity (α_{ij}) is then calculated by taking the ratio of the ideal gas permeabilities for a given gas pair:

$$\alpha_{ij} = \frac{P_i}{P_j} = \frac{S_i}{S_j}\frac{D_i}{D_j} \tag{10}$$

Several correlations for predicting gas solubilities[92,98,222] and diffusivities[141,143,144] in ILs have been proposed. Recently, Scovazzo[221] reviewed the progress in the SILM field and presented upper limits and benchmarks for guiding future research. Scovazzo provides a correlation, depending only on the molar volume of the IL, for the selectivity of the gas pairs CO_2/N_2 and CO_2/CH_4. A correlation, only depending on the IL viscosity, for CO_2 permeability through SILMs is also

provided by Scovazzo. The (ideal) selectivity correlation by Camper[97] and the universal correlation by Scovazzo[221] both predict an increasing selectivity with decreasing IL molar volume for the gas pairs CO_2/N_2 and CO_2/CH_4. Ideal CO_2/N_2 selectivity in SILMs has been reported by Scovazzo et al.,[209] Bara et al.,[223] Neves et al.,[218] and Cserjesi et al.[224] Scovazzo investigated SILMs based on [emim][Tf2N], [emim]-[CF3SO3], [emim][dca] and [thtdp][Cl] reporting CO_2 permeabilities in the range of 350−1000 barrers (1 barrer = 10^{-10} cm³ (STP) cm/cm² s cmHg) and ideal CO_2/N_2 selectivities of 15−61. Bara et al. measured the solubility of CO_2, N_2, O_2 and CH_4 in fluoroalkyl-functionalized imidazolium-based SILMs. They reported CO_2 permeabilities of 210−320, while the ideal selectivity of CO_2/N_2 and CO_2/CH_4 was 16−27 and 13−19, respectively. Neves et al. studied the ideal and mixed gas solubility of several gases in imidazolium-based ILs using two membrane supports with different hydrophobicity. They reported mixed-gas CO_2/N_2 and CO_2/CH_4 selectivities, which was not much different than the ideal selectivities, ranging from 20 to 32 and 98−200, respectively. Furthermore, they showed that the hydrophobic supports were more stable than the hydrophilic ones. Cserjesi et al. investigated the solubility of several gases in SILMs using different type of ILs. Ideal selectivities of the gas pairs CO_2/N_2, CO_2/H_2, and CO_2/CH_4 ranged from 10 to 52, 5−13, and 5−23, respectively. Mixed gas solubilities of the gas pairs CO_2/N_2 and CO_2/CH_4 in several SILMs were reported by Scovazzo et al.[210] The highest mixed-gas selectivity for CO_2/N_2 and CO_2/CH_4 was 21.2 and 27 for [emim][Tf2N] and [emim][BF4] based SILMs, respectively. Furthermore, the mixed-gas selectivities were approximately equal to the ideal selectivities for the corresponding gas pairs. Mixed gas solubility of the gas pair CO_2/H_2 was measured by Myers et al.[216] using an amine-functionalized IL in a cross-linked Nylon 66 support. They reported selectivities greater than 15 and CO_2 permeabilities ranging from 100 to 1000 barrers. Ideal CO_2/CH_4 selectivity has also been studied by Iarikov et al.[219] and Yoo et al.,[217] while Hanioka et al.[215] measured mixed-gas solubilities. Iarikov et al. studied SILMs based on ammonium, imidazolium, pyridinium, pyrrolidinium and phosphonium ILs obtaining an ideal selectivity of 5−30. Yoo et al. obtained an ideal CO_2/CH_4 selectivity of 26 using imidazolium-based ILs in a Nafion membrane. Hanioka et al. used an amine-functionalized IL membrane obtaining high CO_2/CH_4 selectivity and a high membrane stability. On the basis of a limited amount of data, Scovazzo[221] concluded that solubility selectivity dominates the selectivity in SILMs, whereas diffusion determines the selectivity in polymers. Since, diffusion selectivity plays a minor role, mixed gas solubilities in SILMs are expected to be approximately equal to ideal selectivities.[210] For more information on SILMs, the reader is referred to the excellent reviews by Scovazzo[221] and Lazano.[225]

5. BIODEGRADABILITY AND TOXICITY OF IONIC LIQUIDS

Ionic liquids are often referred to as "green" and environmentally benign. This classification was initially justified on the ground of their low vapor pressure, nonflammability, and reusability. However, important issues within the context of green chemistry[226,227] (e.g., biodegradability and toxicity) were initially neglected.[228] The importance of biodegradability and toxicity should not be underestimated, since these parameters are relevant in the authorization process of any substance.[229]

Persistent and toxic ionic liquids, due to their potential hazard to environment and humans, may fail the authorization process or their use will be restricted to only a few applications.[230] Anticipating the large scale application of ionic liquids, disposal of exhausted nonbiodegradable ionic liquids may also become an issue.[231] Therefore, a thorough assessment of the potential risks of ILs is essential before commercializing the IL processes. Since recently much more attention has been paid to these issues, as a result the IL literature for biodegradability and toxicity has grown considerably. Here, we analyze data from existing literature and aim to provide rules of thumbs or generalizations, which might be relevant for designing inherently safer ionic liquids.

In the next section we will discuss the biodegradability and toxicity of ILs. As the research field is expanding and IL processes are close to reaching the market, it is important to analyze the environmental fate of IL. An IL may come in contact with several streams, in which they might be soluble (for example water) thereby having a chance to end in the environment via the effluent streams of a process. Environmental issues of ILs have been characterized as a major barrier to commercialize IL processes, therefore these topics will be discussed next.[232]

5.1. Biodegradability of Ionic Liquids. It is well-known that biodegradability is affected not only by a compounds structure, but also by the environmental conditions. However, safe design of a product should start at the earliest phase in the long process of commercializing a new chemical. The earliest phase in product/process design is often the design of the molecule itself, hence the principles of safe design should preferentially be applied at the molecular level.[233] The emphasis, here, is the effect of molecular structure (i.e., anion, cation, functional groups) on the biodegradability of ionic liquids. Before starting with the analysis of the reported data, it is informative to mention the rules of thumbs given by Boethling et al.[233] for the biodegradability of small molecules.

5.1.1. Rules of Thumb. These rules of thumb are not specifically for ionic liquids, but originate from decades of research mainly in the detergent and pesticide industry. However, initial research suggests that designing ILs according to some of these rules of thumb may also improve the biodegradability of ionic liquids.[231,234] According to Boethling et al. the following molecular features generally result in poor biodegradation and should be avoided when possible: halogens (e.g., chlorine and fluorine), extensive chain branching (e.g., quaternary C), tertiary amine, nitro, nitroso, azo, arylamino groups, polycyclic residues (e.g., polycyclic aromatic hydrocarbons), heterocyclic residues (e.g., imidazole), and aliphatic ether bonds.

The following molecular features generally improve biodegradation: esters, amides, hydroxyl, aldehyde, carboxylic acid groups, probably ketone, unsubstituted linear alkyl chains (≥4 carbons), and phenyl rings. The rules of thumb given here should not be used as universal generalizations, since exceptions exist for these rules of thumb.[233] Nevertheless, it can serve as a good starting point in the design of biodegradable ILs.

5.1.2. Biodegradation Studies of Ionic Liquids. Biodegradability of substances are generally assessed according to the guidelines laid down by the Organization for Economic Co-operation and Development (OECD).[235] Several standard methods compliant with the OECD guidelines exist: Die-Away test (OECD 301 A), Modified Sturm test (OECD 301 B),

Closed Bottle test (OECD 301 D), CO_2 Headspace test (ISO 14593), OECD 309 and ASTM D 5988 test. Each method employs a different principle, whereby depending on the chosen method one of the following is monitored as a measure for biodegradability: the dissolved organic carbon (DOC), CO_2 production, and O_2 uptake. However, care should be taken in the selection, since the suitability of each method for assessing biodegradation depends on several physical properties of the compound in question (i.e., water solubility, volatility, and the tendency to adsorb on solid phases). Detailed information on the measuring principle of each method, a selection criterion and a review on the biodegradation of ILs is given by Coleman and Gathergood.[235] The group of Scammells[231,234,236] was the first to report the poor biodegradability of commonly used imidazolium ILs. Garcia et al.[236] used the Closed Bottle test to evaluate the biodegradability of [bmim][X] ILs, where X = Br, BF4, PF6, TF$_2$N, DCA, and octylsulphate. All the ILs, except for the octylsulphate IL, underwent a biodegradation less than 5% while the octylsulphate IL had a modest biodegradability of 25%. Clearly, these ILs cannot be classified as "readily biodegradable", which is an arbitrary classification for substances that undergo more than 60% biodegradation within a specified test period (normally 28 days).[236] In a subsequent study, Gathergood et al.[231] applied some of the rules of thumb given by Boethling et el.[233] to improve biodegradation of the above-mentioned ILs. Accordingly, they incorporated an ester or an amide group in the alkyl side chain of the imidazolium cation. The ester-functionalized ILs were shown to significantly improve biodegradation, while the effect of the amide-functionalization was negligible. Furthermore, biodegradability was shown to increase with alkyl-chain length of the ester-functionalized cation. Introduction of a methyl group at the C2-position of the imidazolium ring was shown to have negligible effect on biodegradability compared to the C2-unsubstituted ILs. Although biodegradability of the ester-functionalized ILs was higher than the nonfunctionalized ILs, only a combination of [mim-ester] cation and [octylsulphate] anion resulted in biodegradabilities higher than 60%. These ester-functionalized imidazolium cations with the [octylsulphate] anion formed the first readily biodegradable ILs.[237] Morrissey et al.[238] measured the biodegradability of a large number of imidazolium-based ILs containing an ester and/or ether group in the alkyl side chain, using the "CO_2 Headspace" test. Ester-functionalized ILs were shown to have a higher degree of degradation, while including ether groups into the side chain did not have a detrimental effect on the biodegradation of the ILs. Morrissey et al. paired the ester/ether-functionalized cations with several commonly used anions (i.e., Br, BF$_4$, PF$_6$, Tf$_2$N, DCA, and octylsulphate); however, only ILs containing the [octylsulphate] anion passed the readily biodegradable test. Clearly, the [octylsulphate] anion has an important role in determining the high biodegradation of ILs.[238,239] Moreover, the data reported by Morrissey et al.[238] and Docherty et al.[240] show close agreement with Boethling's rules of thumb where biodegradability increases as the alkyl chain length (≥4 carbons) increases.

Biodegradability of pyridinium-based ILs has been measured by several authors.[240,244] Docherty et al.[240] used the "Die-Away" test to investigate the biodegradability of six imidazolium and pyridinium ILs ([bmim], [hmim], [omim], [bmpy], [hmpy], and [ompy]), all containing the [bromide] anion as the counterion. None of the imidazolium ILs could be classified readily biodegradable, while the pyridinium IL with the longest alkyl chain [ompy] passed the test. The data showed further that the pyridinium ILs had higher biodegradabilities than the imidazolium analogues and that the biodegradability improved with increasing alkyl length. Harjani et al.[242] evaluated the biodegradability of several (ester-functionalized) pyridinium ILs using the "CO_2 Headspace" test. The (ester-functionalized) pyridinium cations were paired with a range of anions (i.e., Br, PF$_6$, octylsulphate, bis(trifluoromethylsulfonyl)imide and iodide). Pyridinium ILs bearing an ester side chain moiety was shown to have high levels of biodegradation and could be classified as "readily biodegradable". In contrast, pyridinium ILs with alkyl side chains without an ester functionality did not pass the biodegradability test. In this case, the biodegradability did also not improve as the alkyl chain length was increased, contradicting Boethling's rules of thumb. Further, the effect of the anion on the biodegradability was shown to be insignificant.[241,242] Ford et al.[243] studied the biodegradability (CO_2 headspace test) of pyridinium and thiazolium ILs containing one of the following functionalities: hydroxyethyl side chain, methyl or ethyl ether side chain, acetal, and carbamate. Pyridinium ILs, regardless of the anion, containing the hydroxyethyl functionality showed higher levels of biodegradation and passed the readily biodegradable test. In contrast, thiazolium ILs containing the hydroxyethyl functionality showed surprisingly low biodegradation. Pyridinium ILs bearing an ether, acetal, or carbamate functionality showed significantly lower biodegradation. Biodegradation studies of ammonium and phosphonium ILs are relatively scarce so far. Yu et al.[245] and Pavlovica et al.[246] reported that cholinium (i.e., 2-hydroxyethylammonium) ILs containing napthenic acid or lactate anion were highly biodegradable. Atefi et al.[247] used the CO_2 headspace test to evaluate biodegradation of phosphonium-based ILs. The phosphonium cation was functionalized with an ester, ether, alcohol, or alkane moiety and paired with halide, triflimide, or octylsulphate anions. As expected, ILs containing the octylsulphate anion showed an increased biodegradation, but in all cases the biodegradability was lower than 30%. It is surprising to note that ester-functionalization of phosphonium, in contrast to imidazolium and pyridinium, ILs failed to promote biodegradation.

In summary, pyridinium and cholinium ILs are more biodegradable than imidazolium and phosphonium ILs. Biodegradation can be improved by including ester-functionalities in the imidazolium and pyridinium cations, while the phosphonium cation is an exception to this rule of thumb. A longer alkyl chain seems to promote biodegradation in many cases, however exceptions exist also for this rule of thumb. The anion seems to play a minor role in biodegradation, although the octylsulphate anion generally yields higher biodegradation. Overall, the rules of thumb given by Boethling et al.[233] should not be used as universal generalizations, but can serve as guidelines for designing biodegradable ILs.

5.2. Toxicity of Ionic Liquids. Toxicological studies are essential in determining the impact of ILs on the environment and humans. Generally, toxicity of ILs is evaluated according to standard methods (i.e., OECD, ISO, or ASTM), where a test model (e.g., microorganisms) is exposed to the IL and the response of it is a measure of toxicity, often expressed as a LC_{50}, EC_{50}, or IC_{50} value. Many studies appeared in the past few years addressing the toxic nature of some commonly used ILs. Compilation of raw data on the toxicity of ILs can be found in several recent reviews and the references cited therein.[248−252]

However, the emphasis here is to show toxicity trends with respect to anions, cations, and functional groups of ILs.

The cation is believed to play a key role in determining the toxicity of an IL, while the anion has a minor influence.[230,253] Wells and Coombe[244] studied the ecotoxicity of quaternary-ammonium, imidazolium, quaternary-phosphonium, and pyridinium ILs toward two aquatic test models. All the investigated ILs were shown to have EC_{50} based toxicities much greater ($\sim 10^4 - 10^6$ for the worse cases) than conventional solvents like methanol and acetonitrile. Further, toxicity was shown to increase as the alkyl chain length on the imidazolium cation was increased for an IL containing the [chloride] anion.[244,254] This trend has consistently been reported for ammonium,[255] morpholinium,[255] phosphonium,[244] pyridinium,[256,257] and pyrrolidinium[257] ILs. Stolte et al.[258] studied the aquatic toxicity of a large number of ILs with a different headgroup. These authors found a correlation between the lipophilicity of ILs and (eco)toxicity, where the toxicity increases as the lipophilicity (i.e hydrophobicity) becomes higher.[259] This may explain the increased toxicity of ILs containing a large alkyl chain (i.e., increased lipophilicity). Furthermore, the toxicity not only increases with an increasing alkyl chain length also the number of alkyl chains on the cation increases the toxicity.[251] The latter explains the higher toxicity of quaternary-ammonium and quaternary-phosphonium ILs compared to imidazolium and pyridinium analogues. Couling et al.[253] developed a quantitative structure−property relationship (QSPR) for assessing and predicting the toxicity of a range of ILs. The QSPR-model predicted the following toxicity trend with cation: ammonium < pyridinium < imidazolium < triazolium < tetrazolium. Unfortunately, this trend is not universal since many ammonium and pyridinium ILs are shown to be more toxic than imidazolium ones.[255,258,260]

Although the anion is believed to play a secondary role in the toxicity of ILs, it can significantly increase or reduce toxicities. Toxicity data for aquatic organisms compiled by Frade et al.[251] show the following anion trend: [Br] < [DCA] < [Cl] < [BF$_4$] < [PF$_6$] < [Tf$_2$N]. Especially the fluorinated anions (e.g., BF$_4$ and Tf$_2$N) are highly toxic and forms a serious risk for the environment.[230,259,261]

In summary, the toxicity data reported in the literature should be treated with some caution. Different test models have been used in the separate studies to evaluate toxicity, which complicate data interpretation since different test models can respond differently to the same IL. This is also the reason why data extrapolation from one test model to another should be avoided.[252] So far, the only consistently reported trend is that toxicity increases with alkyl chain length and with the number of alkyl chains on the cation. Further, the [morpholinium] cation and the [DCA] anion seem to be good candidates for reducing toxic effects.[251,260] In the future more unified and systematic approaches should be used to evaluate toxicity of ILs.

6. CONCLUSIONS AND FUTURE DIRECTIONS

Efficient removal of the greenhouse gas carbon dioxide (CO_2) from fluegas turns out to be extremely challenging from an economic and technical point of view. The energy penalty, hence also the cost, for CO_2 removal from fluegas/natural gas is extremely high, thus, unattractive for large scale applications. Many new processes/materials, in particular ionic liquids (ILs) due to their unique properties, have been proposed to overcome this problem. In this review we have analyzed the literature data of the past decade on CO_2 capture with ILs and aimed to present trends regarding CO_2 solubilities and selectivities in different ILs, effect of anions, cations, and functional groups on physical properties, volatility, biodegradability and toxicity of ionic liquids. In addition, recent developments on functionalized ILs and supported IL membranes have also been addressed. Among the many solubility trends reported here, the main finding is that the CO_2 solubility in conventional ILs based on a physical mechanism is still too low at postcombustion capture conditions to compete with the amine process. Furthermore, the Henry's constant (CO_2 solubility) tends to decrease (increase) with an increasing IL molecular weight, molar volume, and free volume. Therefore, the CO_2 solubility in ILs should be compared on a molality (mol/kg) or molarity (mol/m^3) basis, instead of mole fraction basis. CO_2 absorption capacity has successfully been improved by functionalizing conventional ILs with an amine moiety, thereby allowing the CO_2 to react chemically with the amine. In this way even a better (1:1) reaction stoichiometry, compared to conventional CO_2−amine chemistry, could be achieved when the amine was functionalized to the anion of the IL. Not only solubility, but also selectivity is of great importance in industrial separation processes. Selectivity analysis shows that CO_2 is generally much more soluble than other simple gases (e.g., H$_2$, N$_2$, O$_2$); however SO$_2$ and H$_2$S are by far the most soluble gases in ILs. This means that the selectivity will be high for CO_2/simple-gas systems, while the selectivity will likely drop for CO_2/sour-gas systems. Regular solution theory predicts that CO_2/N$_2$ and CO_2/CH$_4$ selectivity can be improved by using ILs with a low molar volume. A common problem to all functionalized or nonfunctionalized ILs is their high viscosity, which forms a great barrier for industrial application. Trends are shown in this paper, which can be used to design low viscosity ILs. Biodegradability and toxicity data analysis show that many commonly used ILs are nonbiodegradable and highly toxic. Rules of thumb from the detergent industry have been used to improve biodegradation; however, only some of the rules of thumb apply also to ILs. Within the limited amount of toxicity data some trends are apparent, which could be used to design inherently safer ILs. As a final note, we want to address the following barriers,[232] which should be resolved in the future to commercialize IL processes: (1) Lack of physicochemical and thermodynamic data. Although some physical properties of ILs have been reported recently, there is need for more data on density, viscosity, surface tension, diffusion coefficients, specific heat, chemical/thermal stability, heat of fusion, water solubility, corrosivity, etc. These properties of ILs have scarcely been reported in the literature and accurate property predicting tools are still lacking. (2) Lack of lifetime and recyclability studies. Analysis of long-term chemical and thermal stability of ILs is required under severe conditions to prevent degradation during absorption/desorption cycles. (3) Lack of scale-up studies. Lab-scale processes need to be scaled up to a pilot plant scale to assess the feasibility of ILs on industrial scale. Industry almost always demands demonstration on pilot scale before commercialization. (4) Lack of engineering studies. Manufacturing and process costs of ILs can only be reduced/optimized by systematic process engineering studies. These studies are lacking, mostly due to the absence of physicochemical properties of ionic liquids. (5) Lack of safety, health, and environmental studies. Biodegradability and toxicity of candidate ILs should be assessed thoroughly to prevent

environmental pollution. (6) High price of ILs. The current lab-scale price of ILs is extremely high (~1000 $/kg), which is 100−1000 times more expensive than conventional solvents. The price will drop for a large scale production of ILs, but a price level typical for conventional solvents should not be expected since ILs are complex molecules, requiring advanced synthesis and purification steps. To conclude, a lot of research is going on to improve CO_2 absorption capacities by taking advantage of the tunability property of ILs. Nevertheless, many barriers need to be overcome before ILs can be applied at a commercial scale.

■ AUTHOR INFORMATION

Corresponding Author
*E-mail: t.j.h.vlugt@tudelft.nl.

Notes
The authors declare no competing financial interest.

■ REFERENCES

(1) Working Group III of the IPCC. *IPCC Special Report on Carbon Dioxide Capture and Storage*; Intergovernmental Panel on Climate Change: Geneva, Switzerland, 2005.

(2) IPCC. *Climate Change 2007: Synthesis Report*; Intergovernmental Panel on Climate Change: Geneva, Switzerland, 2007.

(3) *CO₂ Emissions from Fuel Combustion Highlights*; International Energy Agency: Paris, 2010

(4) *Energy Technology Perspectives*; International Energy Agency: Paris, 2010

(5) *World Energy Outlook*; International Energy Agency: Paris, 2009

(6) Meinshausen, M.; Meinshausen, N.; Hare, W.; Raper, S. C. B.; Frieler, K.; Knutti, R.; Frame, D. J.; Allen, M. R. Greenhouse-gas emission targets for limiting global warming to 2 °C. *Nature* **2009**, *458*, 1158−1162.

(7) Solomon, S. Irreversible climate change due to carbon dioxide emissions. *Proc. Natl. Acad. Sci. U.S.A.* **2010**, *106*, 1704−1709.

(8) *Pathways to a Low-Carbon Economy. Version 2 of the Global Greenhouse Gas Abatement Cost Curve*; McKinsey & Company: Atlanta, GA, 2009.

(9) *Reducing U.S. Greenhouse Gas Emissions: How Much at What Cost?*; McKinsey & Company: Atlanta, GA, 2007.

(10) *a Cost Curve for Greenhouse Gas Reduction*; McKinsey & Company: Atlanta, GA, 2007.

(11) *Carbon Capture & Storage: Assessing the Economics*; McKinsey & Company: Atlanta, GA, 2008.

(12) *The Future of Coal*; Massachusetts Institute of Technology: Cambridge, MA, 2007.

(13) *Coal Use in the New Economies of China, India and South Africa*; IEA Clean Coal Centre: London, 2010.

(14) Haszeldine, R. S. Carbon capture and storage: How green can black be? *Science* **2009**, *325*, 1647−1651.

(15) Socolow, R. H. Can we bury global warming? *Sci. Am.* **2005**, *July*, 49−55.

(16) Gough, C. State of the art in carbon dioxide capture and storage in the UK: An experts' review. *Int. J. Greenhouse Gas Control* **2008**, *2*, 155−168.

(17) Rochelle, G. T. Amine scrubbing for CO_2 capture. *Science* **2009**, *325*, 1652−1654.

(18) Vaidya, P. D.; Kenig, E. Y. CO_2-alkanolamine reaction kinetics: A review of recent studies. *Chem. Eng. Technol.* **2007**, *30*, 1467−1474.

(19) *Carbon Dioxide Capture from Existing Coal-Fired Power Plants*; DOE-NETL: Pittsburgh, PA, 2007.

(20) *Research and Development Goals for CO₂ Capture Technology*; DOE-NETL: Pittsburgh, PA, 2011.

(21) Tollefson, J. Low cost carbon capture project sparks interest. *Nature* **2011**, *469*, 276−277.

(22) Inventys, CO_2 capture for $15 per tonne. *Carbon Capture J.* **2011**, Jan−Feb, 6−7.

(23) Herzog, H.; Meldon, J.; Hatton, A. *Advanced Post-Combustion CO₂ Capture*; Massachusetts Institute of Technology: Cambridge, MA, 2009.

(24) Figueroa, J. D.; Fout, T.; Plasynski, S.; McIlvried, H.; Srivastava, R. D. Advances in CO_2 capture technology. The U.S. Department of Energy's Carbon Sequestration Program. *Int. J. Greenhouse Gas Control* **2008**, *2*, 9−20.

(25) Jones, C. W. CO_2 Capture from dilute gases as a component of modern global carbon management. *Annu. Rev. Chem. Biomol. Eng.* **2011**, *2*, 31−52.

(26) D'Alessandro, D. M.; Smit, B.; Long, J. R. Carbon dioxide capture: Prospects for new materials. *Angew. Chem., Int. Ed.* **2010**, *49*, 6058−6082.

(27) MacDowell, N.; Florin, N.; Buchard, A.; Hallett, J.; Galindo, A.; Jackson, G.; Adjiman, C. S.; Williams, C.; Shah, N.; Fennell, P. An overview of CO_2 capture technologies. *Energy Environ. Sci.* **2010**, *3*, 1645−1669.

(28) Blanchard, L. A.; Hancu, D.; Beckman, E. J.; Brennecke, J. F. Green processing using ionic liquids and CO_2. *Nature* **1999**, *399*, 28−29.

(29) Anthony, J. L.; Maginn, E. J.; Brennecke, J. F. Solubilities and thermodynamic properties of gases in the ionic liquid 1-*n*-butyl-3-methylimidazolium hexafluorophosphate. *J. Phys. Chem. B* **2002**, *106*, 7315−7320.

(30) Freemantle, M. *An Introduction to Ionic Liquids*; RSC Publishing, London, 2010.

(31) Freemantle, M. Designer Solvents: Ionic liquids may boost clean technology development. *Chem. Eng. News* **1998**, *76*, 32−37.

(32) Seddon, K. R. Ionic liquids for clean technology. *J. Chem. Tech. Biotechnol.* **1997**, *68*, 351−356.

(33) Earle, M. J.; Seddon, K. R. Ionic liquids. Green solvents for the future. *Pure Appl. Chem.* **2000**, *72*, 1391−1398.

(34) Brennecke, J. F.; Maginn, E. J. Ionic liquids: Innovative fluids for chemical processing. *AIChE J.* **2001**, *47*, 2384−2389.

(35) Berthod, A.; Ruiz-Angel, M. J.; Carda-Broch, S. Ionic liquids in separation techniques. *J. Chromatogr. A* **2008**, *1184*, 6−18.

(36) Sheldon, R. Catalytic reactions in ionic liquids. *Chem. Commun.* **2001**, *23*, 2399−2407.

(37) Zhao, D.; Wu, M.; Kou, Y.; Min, E. Ionic liquids: Applications in catalysis. *Catal. Today* **2002**, *74*, 157−189.

(38) Parvulescu, V. I.; Hardacre, C. Catalysis in ionic liquids. *Chem. Rev.* **2007**, *107*, 2615−2665.

(39) Buzzeo, M. C.; Evans, R. G.; Compton, R. G. Non-haloaluminate room-temperature ionic liquids in electrochemistry-A review. *Chem. Phys. Chem.* **2004**, *5*, 1106−1120.

(40) MacFarlane, D. R.; Forsyth, M.; Howlett, P. C.; Pringle, J. M.; Sun, J.; Annat, G.; Neil, W.; Izgorodina, E. Ionic liquids in electrochemical devices and processes: Managing interfacial electro-chemistry. *Acc. Chem. Res.* **2007**, *40*, 1165−1173.

(41) Blanchard, L. A.; Brennecke, J. F. Recovery of organic products from ionic liquids using supercritical carbon dioxide. *Ind. Eng. Chem. Res.* **2001**, *40*, 287−292.

(42) Han, X.; Armstrong, D. W. Ionic liquids in separations. *Acc. Chem. Res.* **2007**, *40*, 1079−1086.

(43) Huddleston, J. G.; Willauer, H. D.; Swatloski, R. P.; Visser, A. E.; Rogers, R. D. Room temperature ionic liquids as novel media for "clean" liquid−liquid extraction. *Chem. Commun.* **1998**, 1765−1766.

(44) Buzzeo, M. C.; Evans, R. G.; Compton, R. G. Examination of the potential of ionic liquids for gas separations. *Sep. Sci. Technol.* **2005**, *40*, 525−541.

(45) Zhao, H. Innovative applications of ionic liquids as "green" engineering liquids. *Chem. Eng. Commun.* **2006**, *193*, 1660−1677.

(46) Zhu, S.; Wu, Y.; Chen, Q.; Yu, Z.; Wang, C.; Jin, S.; Ding, Y.; Wu, G. Dissolution of cellulose with ionic liquids and its application: A mini-review. *Green Chem.* **2006**, *8*, 325−327.

(47) Rogers, R. D. Reflections on ionic liquids. *Nature* **2007**, *447*, 917−918.

(48) Wasserscheid, P.; Welton, T. *Ionic Liquids in Synthesis*; Wiley-VCH, New York, 2008; Vol. 2.

(49) Rogers, R. D.; Seddon, K. Ionic Liquids—Solvents of the future? *Science* **2003**, *302*, 792−793.

(50) Seddon, K. R. Ionic Liquids: A taste of the future. *Nature* **2003**, *2*, 363−365.

(51) Karadas, F.; Atilhan, M.; Aparicio, S. Review on the use of ionic liquids (ILs) as alternative fluids for CO_2 capture and natural gas sweetening. *Energy Fuels* **2010**, *24*, 5817−5828.

(52) Huang, J.; Rüther, T. Why are ionic liquids attractive for CO2 absorption? An overview. *Aust. J. Chem.* **2009**, *62*, 298−308.

(53) Hasib-ur-Rahman, M.; Siaj, M.; Larachi, F. Ionic liquids for CO_2 capture—Development and progress. *Chem. Eng. Proc.* **2010**, *49*, 313−322.

(54) Brennecke, J. F.; Gurkan, B. E. Ionic liquids for CO_2 capture and emission reduction. *J. Phys. Chem. Lett.* **2010**, *1*, 3459−3464.

(55) Maginn, E. J. What to do with CO_2. *J. Phys. Chem. Lett.* **2010**, *1*, 3478−3479.

(56) Bara, J. E.; Camper, D. E.; Gin, D. L.; Noble, R. D. Room-temperature ionic liquids and composite materials: Platform technologies for CO_2 capture. *Acc. Chem. Res.* **2010**, *43*, 152−159.

(57) Plechkova, N. V.; Seddon, K. R. Applications of ionic liquids in the chemical industry. *Chem. Soc. Rev.* **2008**, *37*, 123−150.

(58) Feron, P. H. M.; Hendriks, C. A. CO_2 capture process principles and costs. *Oil Gas Sci. Technol.* **2005**, *60*, 451−459.

(59) Biello, D. Can captured carbon save coal? *Sci. Am. Earth 3.0* **2009**, June, 52−59.

(60) Bailey, D. W.; Feron, P. H. M. Post-combustion decarbonisation processes. *Oil Gas Sci. Technol.* **2005**, *60*, 461−474.

(61) Eide, L. I.; Bailey, D. W. Precombustion decarbonisation processes. *Oil Gas Sci. Technol.* **2005**, *60*, 475−484.

(62) Moulijn, J. A.; Makkee, M.; van Diepen, A. *Chemical Process Technology*; Wiley, New York, 2001.

(63) Anheden, M.; Yan, J.; De Smedt, G. Denitrogenation (or oxyfuel concepts). *Oil Gas Sci. Technol.* **2005**, *60*, 485−495.

(64) *Cost and Performance Baseline for Fossil Energy Plants, Volume 1: Bituminous Coal and Natural Gas to Electricity*; DOE-NETL: Pittsburgh, PA, 2010.

(65) *Coal-Fired Power Plants in the United States: Examination of the Costs of Retrofitting with CO_2 Capture Technology*, revision 3; DOE-NETL: Pittsburgh, PA, 2011.

(66) *Cost and Performance Baseline for Fossil Energy Plants, Volume 3 Executive Summary: Low Rank Coal and Natural Gas to Electricity*; DOE-NETL: Pittsburgh, PA, 2011.

(67) *Cost and Performance Baseline of PC and IGCC Plants for a Range of Carbon Dioxide Capture*; DOE-NETL: Pittsburgh, PA, 2011.

(68) *Cost and Performance Baseline for Fossil Energy Plants, Volume 3a: Low Rank Coal to Electricity: IGCC Cases*; DOE-NETL: Pittsburgh, PA, 2011.

(69) *Cost and Performance Baseline for Fossil Energy Plants, Volume 3a: Low Rank Coal to Electricity: Combustion Cases*; DOE-NETL: Pittsburgh, PA, 2011.

(70) *Advancing Oxycombustion Technology for Bituminous Coal Power Plants: An R&D Guide*; DOE-NETL: Pittsburgh, PA, 2012.

(71) *Current and Future Technologies for Power Generation with Post-Combustion Carbon Capture*; DOE-NETL: Pittsburgh, PA, 2012.

(72) *Oxyfuel Combustion of Pulverised Coal*; IEA Clean Coal Centre: London, 2010.

(73) *World Energy Outlook*; International Energy Agency: Paris, 2010.

(74) *Gas Sweetening*; Dow Chemical Company: Midland, MI, 1998

(75) Tennyson, R. N.; Schaaf, R. P. Guidelines can help choose proper process for gas-treating plants. *Oil and Gas J.* **1977**, *75*, 78−80, 85.

(76) *Post-Combustion Carbon Capture from Coal Fired Plants—Solvent Scrubbing*; IEA Clean Coal Centre: London, 2007

(77) Blanchard, L. A.; Gu, Z.; Brennecke, J. F. High-Pressure Phase Behavior of Ionic Liquid/CO_2 Systems. *J. Phys. Chem. B* **2001**, *105*, 2437−2444.

(78) Kroon, M. C.; Shariati, A.; Costantini, M.; van Spronsen, J.; Witkamp, G.; Sheldon, R. A.; Peters, C. J. High-pressure phase behavior of systems with ionic liquids: Part V. The binary system carbon dioxide + 1-butyl-3-methylimidazolium tetrafluoroborate. *J. Chem. Eng. Data* **2005**, *50*, 173−176.

(79) Konynenburg, P. H. V.; Scott, R. L. Critical lines and phase equilibria in binary van der Waals mixtures. *Phil. Trans. R. Soc. A* **1980**, *298*, 495−540.

(80) Aki, S. N. V. K.; Mellein, B. R.; Saurer, E. M.; Brennecke, J. F. High-pressure phase behavior of carbon dioxide with imidazolium-based ionic liquids. *J. Phys. Chem. B* **2004**, *108*, 20355−20365.

(81) Anthony, J. L.; Anderson, J. L.; Maginn, E. J.; Brennecke, J. F. Anion effects on gas solubility in ionic liquids. *J. Phys. Chem. B* **2005**, *109*, 6366−6374.

(82) Cadena, C.; Anthony, J. L.; Shah, J. K.; Morrow, T. I.; Brennecke, J. F.; Maginn, E. J. Why is CO_2 so soluble in imidazolium-based ionic liquids? *J. Am. Chem. Soc.* **2004**, *126*, 5300−5308.

(83) Kazarian, S. G.; Briscoe, B. J.; Welton, T. Combining ionic liquids and supercritical fluids: In situ ATR-IR study of CO_2 dissolved in two ionic liquids at high pressures. *Chem. Commun.* **2000**, 2047−2048.

(84) Kanakubo, M.; Umecky, T.; Hiejima, Y.; Aizawa, T.; Nanjo, H.; Kameda, Y. Solution structures of 1-butyl-3-methylimidazolium hexafluorophosphate ionic liquid saturated with CO_2: Experimental evidence of specific anion−CO_2 interaction. *J. Phys. Chem. B Lett.* **2005**, 13847−13850.

(85) Maiti, A. Theoretical screening of ionic liquid solvents for carbon capture. *ChemSusChem* **2009**, *2*, 628−631.

(86) Sistla, Y. S.; Khanna, A. Validation and prediction of the temperature-dependent Henry's constant for CO_2−ionic liquid systems using the conductor-like screening model for realistic solvation (COSMO-RS). *J. Chem. Eng. Data* **2011**, *56*, 4045−4060.

(87) Zhang, X.; Liu, Z.; Wang, W. Screening of ionic liquids to capture CO_2 by COSMO-RS and experiments. *AIChE* **2008**, *54*, 2717−2728.

(88) Palomar, J.; Gonzalez-Miquel, M.; Polo, A.; Rodriguez, F. Understanding the physical absorption of CO_2 in ionic liquids using the COSMO-RS method. *Ind. Eng. Chem. Res.* **2011**, *50*, 3452−3463.

(89) Almantariotis, D.; Gefflaut, T.; Padua, A. A. H.; Coxam, J. Y.; Costa Gomes, M. F. Effect of fluorination and size of the alkyl side-chain on the solubility of carbon dioxide in 1-alkyl-3-methylimidazolium bis(trifluoromethylsulfonyl)amide ionic liquids. *J. Phys. Chem. B* **2010**, *114*, 3608−3617.

(90) Shimoyama, Y.; Ito, A. Predictions of cation and anion effects on solubilities, selectivities and permeabilities for CO2 in ionic liquid using COSMO based activity coefficient model. *Fluid Phase Equilib.* **2010**, *297*, 178−182.

(91) Maginn, E. J. Molecular simulation of ionic liquids: current status and future opportunities. *J. Phys.: Condens. Matter* **2009**, *21*, 1−17.

(92) Kilaru, P. K.; Condemarin, R. A.; Scovazzo, P. Correlations of low-pressure carbon dioxide and hydrocarbon solubilities in imidazolium-, phosphonium-, and ammonium-based room-temperature ionic liquids. Part 1. using surface tension. *Ind. Eng. Chem. Res.* **2008**, *47*, 900−909.

(93) Blath, J.; Christ, M.; Deubler, N.; Hirth, T.; Schiestel, T. Gas solubilities in room temperature ionic liquids−correlation between RTIL-molar mass and Henry's law constant. *Chem. Eng. J.* **2011**, *172*, 167−176.

(94) Camper, D.; Scovazzo, P.; Koval, C.; Noble, R. Gas solubilities in room-temperature ionic liquids. *Ind. Eng. Chem. Res.* **2004**, *43*, 3049−3054.

(95) Vega, L. F.; Vilaseca, O.; Llovell, F.; Andreu, J. S. Modeling ionic liquids and the solubility of gases in them: Recent advances and perspectives. *Fluid Phase Equilib.* **2010**, *294*, 15−30.

(96) Camper, D.; Koval, C.; Noble, R. Low pressure hydrocarbon solubility in room temperature ionic liquids containing imidazolium rings interpreted using regular solution theory. *Ind. Eng. Chem. Res.* **2005**, *44*, 1928−1933.

(97) Camper, D.; Bara, J.; Koval, C.; Noble, R. Bulk-fluid solubility and membrane feasibility of RMIM-based room-temperature ionic liquids. *Ind. Eng. Chem. Res.* **2006**, *45*, 6279−6283.

(98) Scovazzo, P.; Camper, D.; Kieft, J.; Poshusta, J.; Koval, C.; Noble, R. Regular Solution theory and CO_2 gas solubility in room-temperature ionic liquids. *Ind. Eng. Chem. Res.* **2004**, *43*, 6855−6860.

(99) Finotello, A.; Bara, J. E.; Narayan, S.; Camper, D.; Noble, R. D. Ideal gas solubilities and solubility selectivities in a binary mixture of room-temperature ionic liquids. *J. Phys. Chem. B* **2008**, *112*, 2335−2339.

(100) Finotello, A.; Bara, J. E.; Camper, D.; Noble, R. D. Room-temperature ionic liquids: temperature dependence of gas solubility selectivity. *Ind. Eng. Chem. Res.* **2008**, *47*, 3453−3459.

(101) Shi, W.; Maginn, E. J. Molecular simulation and regular solution theory modeling of pure and mixed gas absorption in the ionic liquid 1-*n*-hexyl-3-methylimidazolium bis-(trifluoromethylsulfonyl)amide ([hmim][Tf2N]). *J. Phys. Chem. B* **2008**, *112*, 16710−1670.

(102) Carvalho, P. J.; Coutinho, J. A. P. On the nonideality of CO_2 solutions in ionic liquids and other low volatile solvents. *J. Phys. Chem. Lett.* **2010**, *1*, 774−780.

(103) Zhao, Y. H.; Abraham, M. H.; Zissimos, A. M. Fast calculation of van der Waals volume as a sum of atomic and bond contributions and its application to drug compounds. *J. Org. Chem.* **2003**, *68*, 7368−7373.

(104) Bondi, A. van der Waals volumes and radii. *J. Phys. Chem.* **1964**, *68*, 441−451.

(105) Shannon, M. S.; Tedstone, J. M.; Danielsen, S. P. O.; Hindman, M. S.; Irvin, A. C.; Bara, J. E. Free volume as the basis of gas solubility and selectivity in imidazolium-based ionic liquids. *Ind. Eng. Chem. Res.* **2012**, *51*, 5565−5576.

(106) Anderson, J. L.; Dixon, J. K.; Brennecke, J. F. Solubility of CO_2, CH_2, C_2H_6, C_2H_4, O_2 and N_2 in 1-hexyl-3-methylpyridinium bis(trifluoromethylsulfonyl)imide: Comparison to other ionic liquids. *Acc. Chem. Res.* **2007**, *40*, 1208−1216.

(107) Kumelan, J.; Perez-Salado Kamps, A.; Urukova, I.; Tuma, D.; Maurer, G. Solubility of oxygen in the ionic liquid [bmim][PF_6]: Experimental and molecular simulation results. *J. Chem. Thermodyn.* **2005**, *37*, 595−602.

(108) Carvalho, P. J.; Coutinho, J. A. P. The polarity effect upon the methane solubility in ionic liquids: A contribution for the design of ionic liquids for enhanced CO_2/CH_4 and H_2S/CH_4 selectivities. *Energy Environ. Sci.* **2011**, *4*, 4614−4619.

(109) Kumelan, J.; Perez-Salado Kamps, A.; Tuma, D.; Maurer, G. Solubility of H_2 in the ionic liquid [hmim][Tf_2N]. *J. Chem. Eng. Data* **2006**, *51*, 1364−1367.

(110) Kumelan, J.; Perez-Salado Kamps, A.; Tuma, D.; Maurer, G. Solubility of CO in the ionic liquid [bmim][PF_6]. *Fluid Phase Equilib.* **2005**, *228−229*, 207−211.

(111) Kumelan, J.; Tuma, D.; Perez-Salado Kamps, A.; Maurer, G. Solubility of the single gases carbon dioxide and hydrogen in the ionic liquid [bmpy][Tf2N]. *J. Chem. Eng. Data* **2010**, *55*, 165−172.

(112) Kumelan, J.; Perez-Salado Kamps, A.; Tuma, D.; Maurer, G. Solubility of the single gases H_2 and CO in the ionic liquid [bmim][CH_3SO_4]. *Fluid Phase Equilib.* **2007**, *260*, 3−8.

(113) Jacquemin, J.; Costa Gomes, M. F.; Husson, P.; Majer, V. Solubility of carbon dioxide, ethane, methane, oxygen, nitrogen, hydrogen, argon, and carbon monoxide in 1-butyl-3-methylimidazolium tetrafluoroborate between temperatures 283 and 343 K and at pressures close to atmospheric. *J. Chem. Thermodyn.* **2006**, *38*, 490−502.

(114) Jacquemin, J.; Husson, P.; Majer, V.; Costa Gomes, M. F. Low-pressure solubilities and thermodynamics of solvation of eight gases in 1-butyl-3-methylimidazolium hexafluorophosphate. *Fluid Phase Equilib.* **2006**, *240*, 87−95.

(115) Jacquemin, J.; Husson, P.; Majer, V.; Costa Gomes, M. F. Influence of the cation on the Solubility of CO_2 and H_2 in ionic liquids based on the bis(trifluoromethylsulfonyl)imide anion. *J. Solution Chem.* **2007**, *36*, 967−979.

(116) Yokozeki, A.; Shiflett, M. B. Hydrogen purification using room-temperature ionic liquids. *Appl. Energy* **2007**, *84*, 351−361.

(117) Shiflett, M. B.; Yokozeki, A. Separation of CO_2 and H_2S using room-temperature ionic liquid [bmim][PF6]. *Fluid Phase Equilib.* **2010**, *294*, 105−113.

(118) Shiflett, M. B.; Niehaus, A. M. S.; Yokozeki, A. Separation of CO_2 and H_2S using room-temperature ionic liquid [bmim][$MeSO_4$]. *J. Chem. Eng. Data* **2010**, *55*, 4785−4793.

(119) Costa Gomes, M. F. Low-pressure solubility and thermodynamics of solvation of carbon dioxide, ethane, and hydrogen in 1-hexyl-3-methylimidazolium bis(trifluoromethylsulfonyl)amide between temperatures of 283 and 343 K. *J. Chem. Eng. Data* **2007**, *52*, 472−475.

(120) Weingärtner, H. Understanding ionic liquids at the molecular level: facts, problems, and controversies. *Angew. Chem., Int. Ed.* **2008**, *47*, 654−670.

(121) Bara, J. E.; Gabriel, C. J.; Lessmann, S.; Carlisle, T. K.; Finotello, A.; Gin, D. L.; Noble, R. D. Enhanced CO_2 separation selectivity in oligo(ethylene glycol) functionalized room-temperature ionic liquids. *Ind. Eng. Chem. Res.* **2007**, *46*, 5380−5386.

(122) Carlisle, T. K.; Bara, J. E.; Gabriel, C. J.; Noble, R. D.; Gin, D. L. Interpretation of CO_2 solubility and selectivity in nitrile-functionalized room-temperature ionic liquids using a group contribution approach. *Ind. Eng. Chem. Res.* **2008**, *47*, 7005−7012.

(123) Mahurin, S. M.; Dai, T.; Yeary, J. S.; Luo, H.; Dai, S. Benzyl-functionalized room temperature ionic liquids for CO_2/N_2 separation. *Ind. Eng. Chem. Res.* **2011**, *50*, 14061−14069.

(124) Hert, D. G.; Anderson, J. L.; Aki, S. N. V. K.; Brennecke, J. F. Enhancement of oxygen and methane solubility in 1-hexyl-3-methylimidazolium bis(trifluoromethylsulfonyl) imide using carbon dioxide. *Chem. Commun.* **2005**, 2603−2605.

(125) Jalili, A. H.; Mehdizadeh, A.; Shokouhi, M.; Sakhaeinia, H.; Taghikhani, V. Solubility of CO2 in 1-(2-hydroxyethyl)-3-methylimidazolium ionic liquids with different anions. *J. Chem. Thermodynamics* **2010**, *42*, 787−791.

(126) Shiflett, M. B.; Yokozeki, A. Separation of carbon dioxide and sulfur dioxide using room-temperature ionic liquid [bmim][MeSO4]. *Energy Fuels* **2010**, *24*, 1001−1008.

(127) Yokozeki, A.; Shiflett, M. B. Separation of carbon dioxide and sulfur dioxide gases using room-temperature ionic liquid [hmim]-[Tf_2N]. *Energy Fuels* **2009**, *23*, 4701−4708.

(128) Kumelan, J.; Tuma, D.; Maurer, G. Simultaneous solubility of carbon dioxide and hydrogen in the ionic liquid [hmim][Tf2N]: Experimental results and correlation. *Fluid Phase Equilib.* **2011**, *311*, 9−16.

(129) Shi, W.; Sorescu, D. C.; Luebke, D. R.; Keller, M. J.; Wickramanayake, S. Molecular simulations and experimental studies of solubility and diffusivity for pure and mixed gases of H_2, CO_2, and Ar absorbed in the ionic liquid 1-n-hexyl-3-methylimidazolium bis-(Trifluoromethylsulfonyl)amide ([hmim][Tf2N]). *J. Phys. Chem. B* **2010**, *114*, 6531−6541.

(130) Kim, Y. S.; Jang, J.; Lim, B. D.; Kang, J. W.; Lee, C. S. Solubility of mixed gases containing carbon dioxide in ionic liquids: Measurements and predictions. *Fluid Phase Equilib.* **2007**, *256*, 70−74.

(131) Harris, K. R.; Kanakubo, M.; Woolf, L. A. Temperature and pressure dependence of the viscosity of the ionic liquids 1-methyl-3-octylimidazolium hexafluorophosphate and 1-methyl-3-octylimidazolium tetrafluoroborate. *J. Chem. Eng. Data* **2006**, *51*, 1161−1167.

(132) Harris, K. R.; Kanakubo, M.; Woolf, L. A. Temperature and pressure dependence of the viscosity of the ionic liquid 1-butyl-3-methylimidazolium tetrafluoroborate: Viscosity and density relationships in ionic liquids. *J. Chem. Eng. Data* **2007**, *52*, 2425−2430.

(133) Jacquemin, J.; Husson, P.; Padua, A. A. H.; Majer, V. Density and viscosity of several pure and water-saturated ionic liquids. *Green Chem.* **2006**, *8*, 172−180.

(134) Gardas, R. L.; Coutinho, J. A. P. A group contribution method for viscosity estimation of ionic liquids. *Fluid Phase Equilib.* **2008**, *266*, 195−201.

(135) Gardas, R. L.; Coutinho, J. A. P. Group contribution methods for the prediction of thermophysical and transport properties of ionic liquids. *AIChE J.* **2009**, *55*, 1274−1290.

(136) Maginn, E. J. Atomistic simulation of the thermodynamic and transport properties of ionic liquids. *Acc. Chem. Res.* **2007**, *40*, 1200−1207.

(137) Moganty, S. S.; Baltus, R. E. Diffusivity of carbon dioxide in room-temperature ionic liquids. *Ind. Eng. Chem. Res.* **2010**, *49*, 9370−9376.

(138) Davies, G. A.; Ponter, A. B.; Craine, K. The diffusion of carbon dioxide in organic liquids. *Can. J. Chem. Eng.* **1967**, *45*, 372−376.

(139) Hayduk, W.; Cheng, S. C. Review of relation between diffusivity and solvent viscosity in dilute liquid solutions. *Chem. Eng. Sci.* **1971**, *26*, 635−646.

(140) McManamey, W. J.; Woollen, J. M. The diffusivity of carbon dioxide in some organic liquids at 25° and 5O°C. *AIChE J.* **1973**, *19*, 667−669.

(141) Morgan, D.; Ferguson, L.; Scovazzo, P. Diffusivities of gases in room-temperature ionic liquids: Data and correlations obtained using a lag-time technique. *Ind. Eng. Chem. Res.* **2005**, *44*, 4815−4823.

(142) Hou, Y.; Baltus, R. E. Experimental measurement of the solubility and diffusivity of CO2 in room-temperature ionic liquids using a transient thin-liquid-film method. *Ind. Eng. Chem. Res.* **2007**, *46*, 8166−8175.

(143) Ferguson, L.; Scovazzo, P. Solubility, diffusivity, and permeability of gases in phosphonium-based room temperature ionic liquids: Data and correlations. *Ind. Eng. Chem. Res.* **2007**, *46*, 1369−1374.

(144) Condemarin, R.; Scovazzo, P. Gas permeabilities, solubilities, diffusivities, and diffusivity correlations for ammonium-based room temperature ionic liquids with comparison to imidazolium and phosphonium RTIL data. *Chem. Eng. J.* **2009**, *147*, 51−57.

(145) Morrow, T. I.; Maginn, E. J. Molecular dynamics study of the ionic liquid 1-n-butyl-3-methylimidazolium hexafluorophosphate. *J. Phys. Chem. B* **2002**, *106*, 12807−12813.

(146) Liu, X.; Vlugt, T. J. H.; Bardow, A. Maxwell-Stefan diffusivities in binary mixtures of ionic liquids with dimethyl sulfoxide (DMSO) and H2O. *J. Phys. Chem. B* **2011**, *115*, 8506−8517.

(147) Esperanca, J. M. S. S.; Canongia Lopes, J. N.; Tariq, M.; Santos, L. M. N. B. F.; Magee, J. W.; Rebelo, L. P. N. Volatility of aprotic ionic liquids−A review. *J. Chem. Eng. Data* **2010**, *55*, 3−12.

(148) Earle, M. J.; Esperanca, J. M. S. S.; Gilea, M. A.; Canongia Lopes, J. N.; Rebelo, L. P. N.; Magee, J. W.; Seddon, K. R.; Widegren, J. A. The distillation and volatility of ionic liquids. *Nature* **2006**, *439*, 831−834.

(149) Ludwig, R.; Kragl, U. Do we understand the volatility of ionic liquids? *Angew. Chem., Int. Ed.* **2007**, *46*, 6582−6584.

(150) Armstrong, J. P.; Hurst, C.; Jones, R. G.; Licence, P.; Lovelock, K. R. J.; Satterley, C. J.; Villar-Garcia, I. J. Vapourisation of ionic liquids. *Phys. Chem. Chem. Phys.* **2007**, *9*, 982−990.

(151) Leal, J. P.; Esperanca, J. M. S. S.; Minas da Piedade, M. E.; Canongia Lopes, J. N.; Rebelo, L. P. N.; Seddon, K. R. The nature of ionic liquids in the gas phase. *J. Phys. Chem. A* **2007**, *111*, 6176−6182.

(152) Rai, N.; Maginn, E. J. Vapor−liquid coexistence and critical behavior of ionic liquids via molecular simulations. *J. Phys. Chem. Lett.* **2011**, *2*, 1439−1443.

(153) Köddermann, T.; Paschek, D.; Ludwig, R. Ionic liquids: Dissecting the enthalpies of vaporization. *ChemPhysChem* **2008**, *9*, 549−555.

(154) Rebelo, L. O. N.; Canongia Lopes, J. N.; Esperanca, J. M. S. S.; Filipe, E. On the critical temperature, normal boiling point, and vapor pressure of ionic liquids. *J. Phys. Chem. B Lett.* **2005**, *109*, 6040−6043.

(155) Fumino, K.; Wulf, A.; Verevkin, S. P.; Heintz, A.; Ludwig, R. Estimating enthalpies of vaporization of imidazolium-based ionic liquids from far-infrared measurements. *ChemPhysChem* **2010**, *11*, 1623−1626.

(156) Deyko, A.; Lovelock, K. R. J.; Corfield, J.; Taylor, A. W.; Gooden, P. N.; Villar-Garcia, I. J.; Licence, P.; Jones, R. G.; Krasovskiy, V. G.; Chernikova, E. A.; Kustov, L. M. Measuring and predicting $\Delta_{vap}H_{298}$ values of ionic liquids. *Phys. Chem. Chem. Phys.* **2009**, *11*, 8544−8555.

(157) Verevkin, S. P. Predicting enthalpy of vaporization of ionic liquids: A simple rule for a complex property. *Angew. Chem.* **2008**, *120*, 5149−5152.

(158) Zaitsau, D. H.; Kabo, G. J.; Strechan, A. A.; Paulechka, Y. U.; Tschersich, A.; Verevkin, S. P.; Heintz, A. Experimental vapor pressures of 1-alkyl-3-methylimidazolium bis(trifluoromethylsulfonyl)-imides and a correlation scheme for estimation of vaporization enthalpies of ionic liquids. *J. Phys. Chem. A* **2006**, *110*, 7303−7306.

(159) Rocha, M. A. A.; Lima, C. F. R. A. C.; Gomes, L. R.; Schröder, B.; Coutinho, J. A. P.; Marrucho, I. M.; Esperanca, J. M. S. S.; Rebelo, L. P. N.; Shimizu, K.; Canongia Lopes, J. N.; Santos, L. M. N. B. F. High-accuracy vapor pressure data of the extended $[C_nC_1im][Ntf_2]$ ionic liquid series: trend changes and structural shifts. *J. Phys. Chem.* **2011**, *115*, 10919−10926.

(160) Wasserscheid, P. Volatile times for ionic liquids. *Nature* **2006**, *439*, 797.

(161) Bates, E. D.; Mayton, R. D.; Ntai, I.; Davis, J. H. CO2 capture by a task-specific ionic liquid. *J. Am. Chem. Soc.* **2002**, *124*, 926−927.

(162) Davis, J. H., Jr Task-specific ionic liquids. *Chem. Lett.* **2004**, *33*, 1072−1077.

(163) Galan Sanchez, L.; Meindersma, G. W.; de Haan, A. B. Solvent properties of functionalized ionic liquids for CO2 absorption. *IChemE* **2007**, *85*, 31−39.

(164) Galán Sánchez, L. M. Ph.D. Thesis, *Eindhoven University of Technology*, 2008.

(165) Camper, D.; Bara, J.; Gin, D. L.; Noble, R. Room-temperature ionic liquid-amine solutions: Tunable solvents for efficient and reversible capture of CO2. *Ind. Eng. Chem. Res.* **2008**, *47*, 8496−8498.

(166) Yu, G.; Zhang, S.; Zhou, G.; Liu, X.; Chen, X. Structure, interaction and property of amino-functionalized imidazolium ILs by molecular dynamics simulation and ab initio calculation. *Applied Energy* **2007**, *53*, 3210−3221.

(167) Gutowski, K. E.; Maginn, E. J. Amine-functionalized task-specific ionic liquids: A mechanistic explanation for the dramatic increase in viscosity upon complexation with co2 from molecular simulation. *J. Am. Chem. Soc.* **2008**, *130*, 14690−14704.

(168) Gurkan, B. E.; de la Fuente, J.; Mindrup, E. M.; Ficke, L. E.; Goodrich, B. F.; Price, E. A.; Schneider, W. F.; Brennecke, J. F. Equimolar CO2 absorption by anion-functionalized ionic liquids. *J. Am. Chem. Soc.* **2010**, *132*, 2116−2117.

(169) Goodrich, B. F.; de la Fuente, J. C.; Gurkan, B. E.; Zadigian, D. J.; Price, E. A.; Huang, Y.; Brennecke, J. F. Experimental measurements of amine-functionalized anion-tethered ionic liquids with carbon dioxide. *Ind. Eng. Chem. Res.* **2011**, *50*, 111−118.

(170) Chinn, D.; Vu, D. Q.; Driver, M. S.; Boudreau, L. C. *CO2 removal from gas using ionic liquid absorbents*. US Pat 7527775, May 5, 2009.

(171) Maginn, E. J. Quarterly Technical Report to the U.S. Department of Energy, *Design and Evaluation of Ionic Liquids as Novel CO2 Absorbents*, May 31, 2005.

(172) Shiflett, M. B.; Kasprzak, D. J.; Junk, C. P.; Yokozeki, A. Phase behavior of carbon dioxide + [bmim][Ac] mixtures. *J. Chem. Thermodyn.* **2008**, *40*, 25−31.

(173) Shiflett, M. B.; Drew, D. W.; Cantini, R. A.; Yokozeki, A. Carbon dioxide capture using ionic liquid 1-butyl-3-methylimidazolium acetate. *Energy Fuels* **2010**, *24*, 5781−5789.

(174) Shiflett, M. B.; Yokozeki, A. Phase Behavior of carbon dioxide in ionic liquids: [emim][Acetate], [emim][trifluoroacetate], and [emim][Acetate] + [emim][trifluoroacetate] mixtures. *J. Chem. Eng. Data* **2009**, *54*, 108−114.

(175) Carvalho, P. J.; Alvarez, V. H.; Schroder, B.; Gil, A. M.; Marrucho, I. M.; Aznar, M.; Santos, L. M. N. B. F.; Coutinho, J. A. P. Specific solvation interactions of CO2 on acetate and trifluoroacetate imidazolium based ionic liquids at high pressures. *J. Phys. Chem. B* **2009**, *113*, 6803−6812.

(176) Gurau, G.; Rodriguez, H.; Kelley, S. P.; Janiczek, P.; Kalb, R. S.; Rogers, R. D. Demonstration of chemisorption of carbon dioxide in 1,3-dialkylimidazolium acetate ionic liquids. *Angew. Chem., Int. Ed.* **2011**, *50*, 12024−12026.

(177) Besnard, M.; Cabaco, M. I.; Chavez, F. V.; Pinaud, N.; Sebastiao, P. J.; Coutinho, J. A. P.; Danten, Y. On the spontaneous carboxylation of 1-butyl-3-methylimidazolium acetate by carbon dioxide. *Chem. Commun.* **2012**, *48*, 1245–1247.

(178) Gurkan, B. E.; Goodrich, B. F.; Mindrup, E. M.; Ficke, L. E.; Massle, M.; Seo, S.; Senftle, T. P.; Wu, H.; Glaser, M. F.; Shah, J. K.; Maginn, E. J.; Brennecke, J. F.; Schneider, W. F. Molecular design of high capacity, low viscosity, chemically tunable ionic liquids for CO_2 capture. *J. Phys. Chem. Lett.* **2010**, *1*, 3494–3499.

(179) Wang, C.; Luo, H.; Jiang, D.; Li, H.; Dai, S. Carbon dioxide capture by superbase-derived protic ionic liquids. *Angew. Chem., Int. Ed.* **2010**, *49*, 5978–5981.

(180) Wang, C.; Mahurin, S. M.; Luo, H.; Baker, G. A.; Li, H.; Dai, S. Reversible and robust CO_2 capture by equimolar task-specific ionic liquid-superbase mixtures. *Green Chem.* **2010**, *12*, 870–874.

(181) Wang, C.; Luo, H.; Luo, X.; Li, H.; Dai, S. Equimolar CO_2 capture by imidazolium-based ionic liquids and superbase systems. *Green Chem.* **2010**, *12*, 2019–2023.

(182) Wang, C.; Luo, X.; Luo, H.; Jiang, D.; Li, H.; Dai, S. Tuning the basicity of ionic liquids for equimolar CO_2 capture. *Angew. Chem., Int. Ed.* **2011**, *50*, 4918–4922.

(183) Jessop, P. G.; Heldebrant, D. J.; Li, X.; Eckert, C. A.; Liotta, C. L. Reversible nonpolar-to-polar solvent. *Nature* **2005**, *436*, 1102.

(184) Hart, R.; Jessop, P. G.; Thomas, C. A.; Eckert, C. A.; Liotta, C. L. The reaction of 1,8-diazabicyclo[5.4.0]undec-7-ene (DBU) with carbon dioxide. *J. Org. Chem.* **2005**, *70*, 5335–5338.

(185) Liu, Y.; Jessop, P. G.; Cunningham, M.; Eckert, C. A.; Liotta, C. L. Switchable surfactants. *Science* **2006**, *313*, 558–560.

(186) Phan, L.; Chiu, D.; Heldebrant, D. J.; Huttenhower, H.; John, E.; Li, X.; Pollet, P.; Wang, R.; Eckert, C. A.; Liotta, C. L.; Jessop, P. G. Switchable solvents consisting of amide/alcohol or guanidine/alcohol mixtures. *Ind. Eng. Chem. Res.* **2008**, *47*, 539–545.

(187) Heldebrant, D. J.; Yonker, C. R.; Jessop, P. G.; Phan, L. Organic liquid CO_2 capture agents with high gravimetric CO_2 capacity. *Energy Environ. Sci.* **2008**, *1*, 487–493.

(188) Blasucci, V. M.; Hart, R.; Pollet, P.; Liotta, C. L.; Eckert, C. A. Reversible ionic liquids designed for facile separations. *Fluid Phase Equilib.* **2010**, *294*, 1–6.

(189) Blasucci, V. M.; Hart, R.; Mestre, V. L.; Hahne, D. J.; Burlager, M.; Huttenhower, H.; Thio, B. J. R.; Pollet, P.; Liotta, C. L.; Eckert, C. A. Single component, reversible ionic liquids for energy applications. *Fuel* **2010**, *89*, 1315–1319.

(190) Jessop, P. G.; Mercer, S. M.; Heldebrant, D. J. CO_2-triggered switchable solvents, surfactants, and other materials. *Energy Environ. Sci.* **2012**, DOI: 10.1039/c2ee02912j.

(191) Shannon, M. S.; Bara, J. E. Reactive and reversible ionic liquids for CO_2 capture and acid gas removal. *Sep. Sci. Technol.* **2012**, *47*, 178–188.

(192) Reddy, S.; Johnson, D.; Gilmartin, J. Fluor's Econamine FG Plus technology for CO_2 capture at coal-fired power plants. *Power Plant Air Pollut. Control "Mega" Symp.* **2008**, 1–17.

(193) Nguyen, T.; Hilliard, M.; Rochelle, G. T. Amine volatility in CO_2 capture. *Int. J. Greenhouse Gas Control* **2010**, *4*, 707–715.

(194) Nguyen, T.; Hilliard, M.; Rochelle, G. T. Volatility of aqueous amines in CO_2 capture. *Energy Proc.* **2011**, *4*, 1624–1630.

(195) Goff, G. S.; Rochelle, G. T. Monoethanolamine degradation: O_2 mass transfer effects under CO_2 capture conditions. *Ind. Eng. Chem. Res.* **2004**, *43*, 6400–6408.

(196) Davis, J.; Rochelle, G. T. Thermal degradation of monoethanolamine at stripper conditions. *Energy Proc.* **2009**, *1*, 327–333.

(197) Reddy, S.; Scherffius, J.; Freguia, S.; Roberts, C. Fluor's Econamine FG Plus technology; An Enhanced amine-based CO_2 capture process. *2nd Natl. Conf. Carbon Sequestr.* **2003**, 1–11.

(198) Arenas, M. F.; Reddy, R. G. Corrosion of steel in ionic liquids. *J. Miner. Met.* **2003**, *39*, 81–91.

(199) Baranyai, J.; Deacon, G. B.; MacFarlane, D. R.; Pringle, J. M.; Scott, J. L. Thermal degradation of ionic liquids at elevated temperatures. *Aust. J. Chem.* **2004**, *57*, 145–147.

(200) Perissi, I.; Bardi, U.; Caporali, S.; Lavacchi, A. High temperature corrosion properties of ionic liquids. *Corros. Sci.* **2006**, *48*, 2349–2362.

(201) Perissi, I.; Caporali, S.; Fossati, A.; Lavacchi, A. Corrosion resistance of metallic materials in ionic liquids. *Adv. Chem. Res.* **2011**, *6*, 315–322.

(202) Pisarova, L.; Gabler, C.; Dorr, N.; Pittenauer, E.; Allmaier, G. Thermo-oxidative stability and corrosion properties of ammonium based ionic liquids. *Tribol. Int.* **2012**, *46*, 73–83.

(203) Tolstoguzov, A. B.; Bardi, U.; Chenakin, S. P. Study of the corrosion of metal alloys interacting with an ionic liquid. *Bull. Russ. Acad. Sci.: Phys.* **2008**, *72*, 605–608.

(204) Uerdingen, M.; Treber, C.; Balser, M.; Schmitt, G.; Werner, C. Corrosion behaviour of ionic liquids. *Green Chem.* **2005**, *7*, 321–325.

(205) Gabler, C.; Tomastik, C.; Pisarova, L.; Doerr, N.; Allmaier, G. Corrosion properties of ammonium based ionic liquids evaluated by SEM-EDX, XPS, and ICP–OES. *Green Chem.* **2011**, *13*, 2869–2877.

(206) Predel, T.; Schlucker, E.; Wasserscheid, P.; Gerhard, D.; Arlt, W. Ionic liquids as operating fluids in high pressure applications. *Chem. Eng. Technol.* **2007**, *30*, 1475–1480.

(207) https://www.cytec.com/specialty-chemicals/anticorrosion.htm (access date: 21 May 2012).

(208) Shukla, S. K.; Murulana, L. C.; Ebenso, E. E. Inhibitive effect of imidazolium based aprotic ionic liquids on mild steel corrosion in hydrochloric acid medium. *Int. J. Electrochem. Sci.* **2011**, *6*, 4286–4295.

(209) Scovazzo, P.; Kieft, J.; Finan, D. A.; Koval, C.; Dubois, D.; Noble, R. Gas separations using non-hexafluorophosphate [PF6]-anion supported ionic liquid membranes. *J. Membr. Sci.* **2004**, *238*, 57–63.

(210) Scovazzo, P.; Havard, D.; McShea, M.; Mixon, S.; Morgan, D. Long-term, continuous mixed-gas dry fed CO_2/CH_4 and CO_2/N_2 separation performance and selectivities for room temperature ionic liquid membranes. *J. Membr. Sci.* **2009**, *327*, 41–48.

(211) San Roman, M. F.; Bringas, E.; Ibanez, R.; Ortiz, I. Liquid membrane technology: Fundamentals and review of its applications. *J. Chem. Technol. Biotechnol.* **2010**, *85*, 2–10.

(212) Kocherginsky, N. N.; Yang, Q.; Seelam, L. Recent advances in supported liquid membrane technology. *Sep. Purif. Technol.* **2007**, *53*, 171–177.

(213) Noble, R. D.; Gin, D. L. Perspective on ionic liquids and ionic liquid membranes. *J. Membr. Sci.* **2011**, *369*, 1–4.

(214) Ilconich, J.; Myers, C.; Pennline, H.; Luebke, D. Experimental investigation of the permeability and selectivity of supported ionic liquid membranes for CO_2/He separation at temperatures up to 125 °C. *J. Membr. Sci.* **2007**, *298*, 41–47.

(215) Hanioka, S.; Maruyama, T.; Sotani, T.; Teramoto, M.; Matsuyama, H.; Nakashima, K.; Hanaki, M.; Kubota, F.; Goto, M. CO_2 separation facilitated by task-specific ionic liquids using a supported liquid membrane. *J. Membr. Sci.* **2008**, *314*, 1–4.

(216) Myers, C.; Pennline, H.; Luebke, D.; Ilconich, J.; Dixon, J. K.; Maginn, E. J.; Brennecke, J. F. High temperature separation of carbon dioxide/hydrogen mixtures using facilitated supported ionic liquid membranes. *J. Membr. Sci.* **2008**, *322*, 28–31.

(217) Yoo, S.; Won, J.; Kang, S. W.; Kang, Y.; Nagase, S. CO_2 separation membranes using ionic liquids in a Nafion matrix. *J. Membr. Sci.* **2010**, *363*, 72–79.

(218) Neves, L. A.; Crespo, J. G.; Coelhoso, I. M. Gas permeation studies in supported ionic liquid membranes. *J. Membr. Sci.* **2010**, *357*, 160–170.

(219) Iarikov, D. D.; Hacarlioglu, P.; Oyama, S. T. Supported room temperature ionic liquid membranes for CO_2/CH_4 separation. *Chem. Eng. J.* **2011**, *166*, 401–406.

(220) Bara, J. E.; Carlisle, T. K.; Gabriel, C. J.; Camper, D.; Finotello, A.; Gin, D. L.; Noble, R. D. Guide to CO_2 separations in imidazolium-based room-temperature ionic liquids. *Ind. Eng. Chem. Res.* **2009**, *48*, 2739–2751.

(221) Scovazzo, P. Determination of the upper limits, benchmarks, and critical properties for gas separations using stabilized room

temperature ionic liquid membranes (SILMs) for the purpose of guiding future research. *J. Membr. Sci.* **2009**, 343, 199−211.

(222) Kilaru, P. K.; Scovazzo, P. Correlations of low-pressure carbon dioxide and hydrocarbon solubilities in imidazolium-, phosphonium-, and ammonium-based room-temperature ionic liquids. Part 2. Using activation energy of viscosity. *Ind. Eng. Chem. Res.* **2008**, 47, 910−919.

(223) Bara, J. E.; Gabriel, C. J.; Carlisle, T. K.; Camper, D. E.; Finotello, A.; Gin, D. L.; Noble, R. D. Gas separations in fluoroalkyl-functionalized room-temperature ionic liquids using supported liquid membranes. *Chem. Eng. J.* **2009**, 147, 43−50.

(224) Cserjesi, P.; Nemestothy, N.; Belafi-Bako, K. Gas separation properties of supported liquid membranes prepared with unconventional ionic liquids. *J. Membr. Sci.* **2010**, 349, 6−11.

(225) Lazano, L. J.; Godinez, C.; de los Rios, A. P.; Hernandez-Fernandez, F. J.; Sanchez-Segado, S.; Alguacil, F. J. Recent advances in supported ionic liquid membrane technology. *J. Membr. Sci.* **2011**, 376, 1−14.

(226) Anastas, P. T.; Kirchhoff, M. M. Origins, current status, and future challenges of green chemistry. *Acc. Chem. Res.* **2002**, 35, 686−694.

(227) Sanderson, K. It's not easy being green. *Nature* **2011**, 469, 19−20.

(228) Scammells, P. J.; Scott, J. L.; Singer, R. D. Ionic liquids: The neglected issues. *Aust. J. Chem.* **2005**, 58, 155−169.

(229) http://ec.europa.eu/environment/chemicals/reach/ reach_intro.htm (access date: 21 May 2012).

(230) Matzke, M.; Stolte, S.; Thiele, K.; Juffernholz, T.; Arning, J.; Ranke, J.; Welz-Biermann, U.; Jastorff, B. The influence of anion species on the toxicity of 1-alkyl-3-methylimidazolium ionic liquids observed in an (eco)toxicological test battery. *Green Chem.* **2007**, 9, 1198−1207.

(231) Gathergood, N.; Garcia, M. T.; Scammells, P. J. Biodegradable ionic liquids: Part 1. Concept, preliminary targets and evaluation. *Green Chem.* **2004**, 6, 166−175.

(232) Joglekar, H. G.; Rahman, I.; Kulkarni, B. D. The path ahead for ionic liquids. *Chem. Eng. Technol.* **2007**, 30, 819−828.

(233) Boethling, R. S.; Sommer, E.; DiFiore, D. Designing small molecules for biodegradability. *Chem. Rev.* **2007**, 107, 2207−2227.

(234) Gathergood, N.; Scammells, P. J. Design and preparation of room-temperature ionic liquids containing biodegradable side chains. *Aus. J. Chem.* **2002**, 55, 557−560.

(235) Coleman, D.; Gathergood, N. Biodegradation studies of ionic liquids. *Chem. Soc. Rev.* **2010**, 39, 600−637.

(236) Garcia, M. T.; Gathergood, N.; Scammells, P. J. Biodegradable ionic liquids Part II. Effect of the anion and toxicology. *Green Chem* **2005**, 7, 9−14.

(237) Gathergood, N.; Scammells, P. J.; Garcia, M. T. Biodegradable ionic liquids Part III. The first readily biodegradable ionic liquids. *Green Chem.* **2006**, 8, 156−160.

(238) Morrissey, S.; Pegot, B.; Coleman, D.; adn D. Ferguson, M. T. G.; Quilty, B.; Gathergood, N. Biodegradable, non-bactericidal oxygen-functionalised imidazolium esters: A step towards 'greener' ionic liquids. *Green, Chem.* **2009**, 11, 475−483.

(239) Farrell, J. R. H. J.; Garcia, M. T.; Singer, R. D.; Scammells, P. J. Further investigation of the biodegradability of imidazolium ionic liquids. *Green Chem.* **2009**, 11, 821−829.

(240) Docherty, K. M.; Dixon, J. K.; Kulpa, C. F., Jr Biodegradability of imidazolium and pyridinium ionic liquids by an activated sludge microbial community. *Biodegradation* **2007**, 18, 481−493.

(241) Zhang, C.; Wang, H.; Malhotra, S. V.; Dodge, C. J.; Francis, A. J. Biodegradation of pyridinium-based ionic liquids by an axenic culture of soil Corynebacteria. *Green Chem.* **2010**, 12, 851−858.

(242) Harjani, J. R.; Singer, R. D.; Garcia, M. T.; Scammells, P. J. Biodegradable pyridinium ionic liquids: Design, synthesis and evaluation. *Green Chem.* **2009**, 11, 83−90.

(243) Ford, L.; Harjani, J. R.; Atefi, F.; Garcia, M. T.; Singer, R. D.; Scammells, P. J. Further studies on the biodegradation of ionic liquids. *Green Chem.* **2010**, 12, 1783−1789.

(244) Wells, A. S.; Coombe, V. T. On the freshwater ecotoxicity and biodegradation properties of some common ionic liquids. *Org. Process Res. Dev.* **2006**, 10, 794−798.

(245) Yu, Y.; Lu, X.; Zhou, Q.; Dong, K.; Yao, H.; Zhang, S. Biodegradable naphthenic acid ionic liquids: Synthesis, characterization, and quantitative structure-biodegradation relationship. *Chem.—Eur. J.* **2008**, 14, 11174−11182.

(246) Pavlovica, S.; Zicmanis, A.; Gzibovska, E.; Klavins, M.; Mekss, P. (2-Hydroxyethyl)ammonium lactates—Highly biodegradable and essentially non-toxic ionic liquids. *Green Sus. Chem.* **2011**, 1, 103−110.

(247) Atefi, F.; Garcia, M. T.; Singer, R. D.; Scammells, P. J. Phosphonium ionic liquids: design, synthesis and evaluation of biodegradability. *Green Chem.* **2009**, 11, 1595−1604.

(248) Zhao, D.; Liao, Y.; Zhang, Z. Toxicity of ionic liquids. *Clean* **2007**, 35, 42−48.

(249) Ranke, J.; Stolte, S.; Störmann, R.; Arning, J.; Jastorff, B. Design of sustainable chemical products—The example of ionic liquids. *Chem. Rev.* **2017**, 107, 2183−2206.

(250) Pham, T. P. T.; Cho, C.; Yun, Y. Environmental fate and toxicity of ionic liquids: A review. *Water Res.* **2010**, 44, 352−372.

(251) Frade, R. F. M.; Afonso, C. A. M. Impact of ionic liquids in environment and humans: An overview. *Hum. Exp. Toxicol.* **2010**, May, 1−17.

(252) Petkovic, M.; Seddon, K. R.; Rebelo, L. P. N.; Pereira, C. S. Ionic liquids: A pathway to environmental acceptability. *Chem. Soc. Rev.* **2011**, 40, 1383−1403.

(253) Couling, D. J.; Bernot, R. J.; Docherty, K. M.; Dixon, J. K.; Maginn, E. J. Assessing the factors responsible for ionic liquid toxicity to aquatic organisms via quantitative structure-property relationship modeling. *Green Chem.* **2006**, 8, 82−90.

(254) Romero, A.; Santos, A.; Tojo, J.; Rodríguez, A. Toxicity and biodegradability of imidazolium ionic liquids. *J. Hazardous Mater.* **2008**, 151, 268−273.

(255) Pretti, C.; Chiappe, C.; Pieraccini, D.; Gregori, M.; Abramo, F.; Monni, G.; Intorre, L. Acute toxicity of ionic liquids to the zebrafish (Danio rerio). *Green Chem.* **2006**, 8, 238−240.

(256) Papaiconomou, N.; Estager, J.; Traore, Y.; Bauduin, P.; Bas, C.; Legeai, S.; Viboud, S.; Draye, M. Synthesis, physicochemical properties, and toxicity data of new hydrophobic ionic liquids containing dimethylpyridinium and trimethylpyridinium cations. *J. Chem. Eng. Data* **2010**, 55, 1971−1979.

(257) Salminen, J.; Papaiconomou, N.; Kumar, R. A.; Lee, J.; Kerr, J.; Newman, J.; Prausnitz, J. M. Physicochemical properties and toxicities of hydrophobic piperidinium and pyrrolidinium ionic liquids. *Fluid Phase Equilib.* **2007**, 261, 421−426.

(258) Stolte, S.; Matzke, M.; Arning, J.; Böschen, A.; Pitner, W.; Welz-Biermann, U.; Jastorff, B.; Ranke, J. Effects of different head groups and functionalised side chains on the aquatic toxicity of ionic liquids. *Green Chem.* **2007**, 9, 1170−1179.

(259) Latala, A.; Nedzi, M.; Stepnowski, P. Toxicity of imidazolium and pyridinium based ionic liquids towards algae. *Chlorella vulgaris*, *Oocystis submarina* (green algae) and *Cyclotella meneghiniana*, *Skeletonema marinoi* (diatoms). *Green Chem.* **2009**, 11, 580−588.

(260) Pretti, C.; Chiappe, C.; Brunini, I. B. S.; Monni, G.; Intorre, L. Acute toxicity of ionic liquids for three freshwater organisms: *Pseudokirchneriella subcapitata, Daphnia magna* and *Danio rerio*. *Ecotoxicol. Environ. Saf.* **2009**, 72, 1170−1176.

(261) Frade, R. F. M.; Rosatella, A. A.; Marques, C. S.; Branco, L. C.; Kulkarni, P. S.; Mateus, N. M. M.; Afonso, C. A. M.; Duarte, C. M. M. Toxicological evaluation on human colon carcinoma cell line (CaCo-2) of ionic liquids based on imidazolium, guanidinium, ammonium, phosphonium, pyridinium and pyrrolidinium cations. *Green Chem.* **2009**, 11, 1660−1665.

(262) *Cost and Performance Baseline for Fossil Energy Plants, Volume 1: Bituminous Coal and Natural Gas to Electricity*; DOE-NETL: Pittsburgh, PA, 2007

(263) Rojey, A.; Jaffret, C.; Cornot-Gandolphe, S.; Durand, B.; Jullian, S.; Valais, M. *Natural Gas Production Processing Transport*; Editions Technip: Paris, 1994.

(264) Henni, A.; Hromek, J. J.; Tontiwachwuthikul, P.; Chakma, A. Volumetric properties and viscosities for aqueous diisopropanolamine solutions from 25 °C to 70 °C. *J. Chem. Eng. Data* **2003**, *48*, 1062–1067.

(265) Bucklin, R. W.; Schendel, R. L. Comparison of Fluor Solvent and Selexol Processes. *Energy Prog.* **1984**, *4*, 137–142.

(266) Kohl, A. L.; Nielsen, R. B. *Gas Purification*, (5th ed.); Gulf Publishing Company: Houston, TX, 1997.

(267) Shannon, M. S.; Tedstone, J. M.; Danielsen, S. P. O.; Bara, J. E. Evaluation of alkylimidazoles as physical solvents for CO$_2$/CH$_4$ separation. *Ind. Eng. Chem. Res.* **2012**, *51*, 515–522.

(268) Burr, B.; Lyddon, L. A comparison of physical solvents for acid gas removal. *87th Annu. Conv. Proc.* **2008**, 100–113.

(269) Zhang, S.; Sun, N.; He, X.; lu, X.; Zhang, X. Physical properties of ionic liquids: Database and evaluation. *J. Phys. Chem. Ref. Data* **2006**, *35*, 1475–1517.

(270) Filburn, T.; Helble, J. J.; Weiss, R. A. Development of supported ethanolamines and modified ethanolamines for CO$_2$ capture. *Ind. Eng. Chem. Res.* **2005**, *44*, 1542–1546.

(271) Fulem, M.; Ruzicka, K.; Ruzicka, M. Recommended vapor pressures for thiophene, sulfolane, and dimethyl sulfoxide. *Fluid Phase Equilib.* **2011**, *303*, 205–216.

(272) Hochgesand, G. Rectisol and Purisol. *Ind. Eng. Chem.* **1970**, *62*, 37–43.

(273) Isaacs, E. E.; Otto, F. D.; Mather, A. E. Solubility of hydrogen sulfide and carbon dioxide in an aqueous diisopropanolamine solution. *J. Chem. Eng. Data* **1977**, *22*, 71–73.

(274) Isaacs, E. E.; Otto, F. D.; Mather, A. E. The solubility of mixtures of carbon dioxide and hydrogen sulphide in an aqueous DIPA solution. *Can. J. Chem. Eng.* **1977**, *55*, 210–212.

(275) Isaacs, E. E.; Otto, F. D.; Mather, A. E. Solubility of hydrogen sulfide and carbon dioxide in a sulfinol solution. *J. Chem. Eng. Data* **1977**, *22*, 317–319.

(276) Jou, F.; Mather, A. E.; Otto, F. D. The solubility of CO$_2$ in a 30 mass percent monoethanolamine solution. *Can. J. Chem. Eng.* **1995**, *73*, 140–147.

(277) Lee, J. I.; Otto, F. D.; Mather, A. E. The solubility of H$_2$S and CO$_2$ in aqueous monoethanolamine solutions. *Can. J. Chem. Eng.* **1974**, *52*, 803–805.

(278) Mandal, B. P.; Kundu, M.; Bandyopadhyay, S. S. Density and viscosity of aqueous solutions of (N-methyldiethanolamine + monoethanolamine), (N-methyldiethanolamine + diethanolamine), (2-amino-2-methyl-1-propanol + monoethanolamine), and (2-amino-2-methyl-1-propanol + diethanolamine). *J. Chem. Eng. Data* **2003**, *48*, 703–707.

(279) Murrieta-Guevara, F.; Romero-Martinez, A.; Trejo, A. Solubilities of carbon dioxide and hydrogen sulfide in propylene carbonate, N-methylpyrrolidone and sulfolane. *Fluid Phase Equilib.* **1998**, *44*, 105–115.

(280) Nichols, G.; Orf, J.; Reiter, S. M.; Chickos, J.; Gokel, G. W. The vaporization enthalpies of some crown and polyethers by correlation gas chromatography. *Thermochim. Acta* **2000**, *346*, 15–28.

(281) Verevkin, S. P.; Toktonov, A. V.; Chernyak, Y.; Schaffner, B.; Borner, A. Vapour pressure and enthalpy of vaporization of cyclic alkylene carbonates. *Fluid Phase Equilib.* **2008**, *268*, 1–6.

(282) Xu, Y.; Schutte, R. P.; Hepler, L. G. Solubilities of carbon dioxide, hydrogen sulfide and sulfur dioxide in physical solvents. *Can. J. Chem. Eng.* **1992**, *70*, 569–573.

(283) http://www.vattenfall.com/en/ccs/capture-of-co2.htm (access date: 21 May 2012).

(284) Ng, H.; Robinson, D. B. Equilibrium phase properties of the toluene–carbon dioxide system. *J. Chem. Eng. Data* **1978**, *23*, 325–327.

(285) Li, Y.; Dillard, K. H.; Robinson, R. L. Vapor–liquid phase equilibrium for carbon dioxide-n-hexane at 40, 80, and 120 °C. *J. Chem. Eng. Data* **1981**, *26*, 53–55.

(286) Shariati, A.; Peters, C. J. High-pressure phase behavior of systems with ionic liquids: II. The binary system carbon dioxide+1-

ethyl-3-methylimidazolium hexafluorophosphate. *J. Supercrit. Fluids* **2004**, *29*, 43–48.

(287) Carvalho, P. J.; Alvarez, V. H.; Machado, J. J. B.; Pauly, J.; Daridon, J.; Marrucho, I. M.; Aznar, M.; Coutinho, J. A. P. High pressure phase behavior of carbon dioxide in 1-alkyl-3-methylimidazolium bis(trifluoromethylsulfonyl)imide ionic liquids. *J. Supercrit. Fluids* **2009**, *48*, 99–107.

(288) Daneshvar, M.; Kim, S.; Gulari, E. High-pressure phase equilibria of ploy(ethylene glycol)–carbon dioxide systems. *J. Phys. Chem.* **1990**, *94*, 2124–2128.

(289) Muldoon, M. J.; Aki, S. N. V. K.; Anderson, J. L.; Dixon, J. K.; Brennecke, J. F. Improving carbon dioxide solubility in ionic liquids. *J. Phys. Chem. B* **2007**, *111*, 9001–9009.

(290) Kumelan, J.; Perez-Salado Kamps, A.; Tuma, D.; Maurer, G. Solubility of CO$_2$ in the ionic liquids [bmim][CH$_3$SO$_4$] and [bmim][PF$_6$]. *J. Chem. Eng. Data* **2006**, *51*, 1802–1807.

(291) Carvalho, P. J.; Alvarez, V. H.; Marrucho, I. M.; Aznar, M.; Coutinho, J. A. P. High carbon dioxide solubilities in trihexylte-tradecylphosphonium-based ionic liquids. *J. Supercrit. Fluids* **2010**, *52*, 258–265.

(292) Schilderman, A. M.; Raeissi, S.; Peters, C. J. Solubility of carbon dioxide in the ionic liquid 1-ethyl-3-methylimidazolium bis(trifluoromethylsulfonyl)imide. *Fluid Phase Equilib.* **2007**, *260*, 19–22.

(293) Yim, J.; Song, H. N.; Yoo, K.; Lim, J. S. Measurement of CO$_2$ solubility in ionic liquids: [BMP][Tf2N] and [BMP][MeSO$_4$] by measuring bubble-point pressure. *J. Chem. Eng. Data* **2011**, *56*, 1197–1203.

(294) Song, H. N.; Lee, B.; Lim, J. S. Measurement of CO$_2$ solubility in ionic liquids: [BMP][TfO] and [P14,6,6,6][Tf2N] by measuring bubble-point pressure. *J. Chem. Eng. Data* **2010**, *55*, 891–896.

(295) Revelli, A.; Mutelet, F.; Jaubert, J. High carbon dioxide solubilities in imidazolium-based ionic liquids and in poly(ethylene glycol) dimethyl ether. *J. Phys. Chem. B* **2010**, *114*, 12908–12913.

(296) Carvalho, P. J.; Alvarez, V. H.; Marrucho, I. M.; Aznar, M.; Coutinho, J. A. P. High pressure phase behavior of carbon dioxide in 1-butyl-3-methylimidazolium bis(trifluoromethylsulfonyl)imide and 1-butyl-3-methylimidazolium dicyanamide ionic liquids. *J. Supercrit. Fluids* **2009**, *50*, 105–111.

(297) Costantini, M.; Toussaint, V. A.; Shariati, A.; Peters, C. J.; Kikic, I. High-pressure phase behavior of systems with ionic liquids: Part IV. binary system carbon dioxide + 1-hexyl-3-methylimidazolium tetrafluoroborate. *J. Chem. Eng. Data* **2005**, *50*, 52–55.

(298) Shariati, A.; Peters, C. J. High-pressure phase behavior of systems with ionic liquids: III. The binary system carbon dioxide+1-hexyl-3-methylimidazolium hexafluorophosphate. *J. Supercrit. Fluids* **2004**, *30*, 139–144.

(299) Gutkowski, K. I.; Shariati, A.; Peters, C. J. High-pressure phase behavior of the binary ionic liquid system 1-octyl-3-methylimidazolium tetrafluoroborate + carbon dioxide. *J. Supercrit. Fluids* **2006**, *39*, 187–191.

(300) Soriano, A. N.; Doma, B. T., Jr; Li, M. Carbon dioxide solubility in some ionic liquids at moderate pressures. *J. Taiwan Inst. Chem. Eng.* **2009**, *40*, 387–393.

(301) Mattedi, S.; Carvalho, P. J.; Coutinho, J. A. P.; Alvarez, V. H.; Iglesias, M. High pressure CO$_2$ solubility in N-methyl-2-hydroxyethy-lammonium protic ionic liquids. *J. Supercrit. Fluids* **2011**, *56*, 224–230.

(302) Crosthwaite, C. P. F. J. M.; Hert, D. G.; Aki, S. N. V. K.; Brennecke, J. F. Thermophysical properties of imidazolium-based ionic liquids. *J. Chem. Eng. Data* **2004**, *49*, 954–964.

(303) Domanska, U.; Krolikowska, M. Density and viscosity of binary mixtures of 1-butyl-3-methylimidazolium thiocyanate + 1-heptanol, 1-octanol, 1-nonanol, or 1-decanol. *J. Chem. Eng. Data* **2010**, *55*, 2994–3004.

(304) Mokhtarani, B.; Sharifi, A.; Mortaheb, H. R.; Mirzaei, M.; Mafi, M.; Sadeghian, F. Density and viscosity of pyridinium-based ionic liquids and their binary mixtures with water at several temperatures. *J. Chem. Thermodyn.* **2009**, *41*, 323–329.

(305) Tariq, M.; Forte, P. A. S.; Costa Gomes, M. F.; Canongia Lopes, J. N.; Rebelo, L. P. N. Densities and refractive indices of imidazolium- and phosphonium-based ionic liquids: Effect of temperature, alkyl chain length, and anion. *J. Chem. Thermodyn.* **2009**, *41*, 790−798.

(306) Goncalves, F. A. M. M.; Costa, C. S. M. F.; Ferreira, C. E.; Bernardo, J. C. S.; Johnson, I.; Fonseca, I. M. A.; Ferreira, A. G. M. Pressure-volume-temperature measurements of phosphonium-based ionic liquids and analysis with simple equations of state. *J. Chem. Thermodynamics* **2011**, *43*, 914−929.

(307) Galan Sanchez, L.; Espel, J. R.; Onink, F.; Meindersma, G. W.; de Haan, A. B. Density, viscosity, and surface tension of synthesis grade imidazolium, pyridinium, and pyrrolidinium based room temperature ionic liquids. *J. Chem. Eng. Data* **2009**, *54*, 2803−2812.

(308) Seoane, R. G.; Corderi, S.; Gomez, E.; Calvar, N.; Gonzalez, E. J.; Macedo, E. A.; Dominguez, A. Temperature dependence and structural influence on the thermophysical properties of eleven commercial ionic liquids. *Ind. Eng. Chem. Res.* **2012**, *51*, 2492−2504.

(309) Taguchi, R.; Machida, H.; Sato, Y.; Smith, R. L., Jr. High-pressure densities of 1-alkyl-3-methylimidazolium hexafluorophosphates and 1-alkyl-3-methylimidazolium tetrafluoroborates at temperatures from (313 to 473) K and at pressures up to 200 MPa. *J. Chem. Eng. Data* **2009**, *54*, 22−27.

(310) Esperanca, J. M. S. S.; Visak, Z. P.; Plechkova, N. V.; Seddon, K. R.; Guedes, H. J. R.; Rebelo, L. P. N. Density, speed of sound, and derived thermodynamic properties of ionic liquids over an extended pressure range. 4. [C3mim][NTf2] and [C5mim][NTf2]. *J. Chem. Eng. Data* **2006**, *51*, 2009−2015.

(311) Anderson, J. L.; Dixon, J. K.; Maginn, E. J.; Brennecke, J. F. Measurement of SO_2 solubility in ionic liquids. *J. Phys. Chem. B* **2006**, *110*, 15059−15062.

(312) Gardas, R. L.; Ge, R.; Goodrich, P.; Hardcare, C.; Hussain, A.; Rooney, D. W. Thermophysical properties of amino acid-based ionic liquids. *J. Chem. Eng. Data* **2010**, *55*, 1505−1515.

(313) Crosthwaite, J. M.; Muldoon, M. J.; Dixon, J. K.; Anderson, J. L.; Brennecke, J. F. Phase transition and decomposition temperatures, heat capacities and viscosities of pyridinium ionic liquids. *J. Chem. Thermodyn.* **2005**, *37*, 559−568.

(314) Jin, H.; O' Hare, B.; Dong, J.; Arzhantsev, S.; Baker, G. A.; Wishart, J. F.; Benesi, A. J.; Maroncelli, M. Physical properties of ionic liquids consisting of the 1-butyl-3-methylimidazolium cation with various anions and the bis(trifluoromethylsulfonyl)imide anion with various cations. *J. Phys. Chem. B* **2008**, *112*, 81−92.

(315) Tsunashima, K.; Sugiya, M. Physical and electrochemical properties of low-viscosity phosphonium ionic liquids as potential electrolytes. *Electrochem. Commun.* **2007**, *9*, 2353−2358.

(316) Ge, M.; Zhao, R.; Yi, Y.; Zhang, Q.; Wang, L. Densities and viscosities of 1-butyl-3-methylimidazolium trifluoromethanesulfonate + H_2O binary mixtures at T (303.15 to 343.15) K. *J. Chem. Eng. Data* **2008**, *53*, 2408−2411.

(317) Fernandez, A.; Garcia, J.; Torrecilla, J. S.; Oliet, M.; Rodriguez, F. volumetric, transport and surface properties of [bmim][MeSO4] and [emim][EtSO4] ionic liquids as a function of temperature. *J. Chem. Eng. Data* **2008**, *53*, 1518−1522.

(318) Ahosseini, A.; Scurto, A. M. Viscosity of imidazolium-based ionic liquids at elevated pressures: Cation and anion effects. *Int. J. Thermophys.* **2008**, *29*, 1222−1243.

(319) Andreatta, A. E.; Arce, A.; Rodil, E.; Soto, A. Physical properties of binary and ternary mixtures of ethyl acetate, ethanol, and 1-octyl-3-methyl-imidazolium bis(trifluoromethylsulfonyl)imide at 298.15 K. *J. Chem. Eng. Data* **2009**, *54*, 1022−1028.

(320) Camper, D.; Becker, C.; Koval, C.; Noble, R. Diffusion and solubility measurements in room temperature ionic liquids. *Ind. Eng. Chem. Res.* **2006**, *45*, 445−450.

(321) Hayduk, W.; Malik, V. K. Density, viscosity, and carbon dioxide solubility and diffusivity in aqueous ethylene glycol solutions. *J. Chem. Eng. Data* **1971**, *16*, 143−146.

(322) Won, Y. S.; Chung, D. K.; Mills, A. F. Density, viscosity, surface tension, and carbon dioxide solubility and diffusivity of methanol, ethanol, aqueous propanol, and aqueous ethylene glycol at 25 °C. *J. Chem. Eng. Data* **1981**, *26*, 141−144.

(323) Dim, A.; Gardner, G. R.; Ponter, A. B.; Wood, T. Diffusion of carbon dioxide into primary alcohols and methyl cellulose ether solutions. *J. Chem. Eng. Jpn.* **1971**, *4*, 92−95.

(324) Robeson, L. M. The upper bound revisited. *J. Membr. Sci.* **2008**, *320*, 390−400.

(325) Stern, S. A. Polymers for gas separations: The next decade. *J. Membr. Sci.* **1994**, *94*, 1−65.

8177

dx.doi.org/10.1021/ie3003705 | *Ind. Eng. Chem. Res.* **2012**, *51*, 8149−8177